Studies of Amide Acyl Transfer Reactions.

By

Ahmed M. Aman

A thesis submitted to the Department of Chemistry in conformity with the requirements for the degree of Doctor of Philosophy

Queen's University

Kingston, Ontario, Canada

December, 1998

ABSTRACT

Part 1: The rate and equilibrium constants for formation and hydrolysis of formanilide, acetanilide, *p*-nitroformanilide and *p*-methoxyformanilide have been determined under dilute aqueous acidic conditions. The reactions were followed from both directions (formation and hydrolysis) under identical conditions. The results demonstrate that the reactive species for the formation of anilides are non-ionized acids and unprotonated amines and equilibrium position for formanilides shifts more towards formation with increasing basicity of the constituent amine. The equilibrium constant, K'_{eq}, based on the concentration of non-ionized acid and unprotonated amine, follows the equation $K'_{eq} = -0.95 + 0.57\ pK_a$. Under comparable conditions, the rate of attainment of equilibrium is 249 times slower for acetanilide relative to formanilide, while K'_{eq} decreases only 3.7 times. At pH 3.6, (μ = 1.0), 0.5 M phosphate increases the attainment of equilibria for formanilide by 1.6 times without changing the equilibrium position. Addition of ethanol to the solvent system increased the rate of attainment of equilibrium and shifted the equilibrium towards formation of formanilide.

Part 2: The reaction of distorted amide **1** with thioglycolic acid (**29**) has been studied at 25 °C. From high to low pH, the pH rate profile increases with decreasing pH until the second pK_a of **29** (10.22), and then it shows a plateau until pH 2 with a minor inflection at the first pK_a of **29** (3.55). Below pH 3.5, the reaction mechanism involves an attack of the monoanionic **29** on the protonated amide (**1**-H^+). At pH > 3.5, an additional efficient mechanism involving attack of **29**-S^- on neutral **1** is operative. In the latter mechanism, the reaction proceeds via an initial attack by **29**-S^- on **1** to produce an unstable tetrahedral

intermediate which is subsequently trapped by an intramolecular proton transfer from the pendant COOH, thereby preventing reversal to the starting materials.

The synthesis of 4-nitrobenzoate esters of ethyl 2-mercaptoacetate, thioglycolic acid, 2-(*N*,*N*-dimethylamino)ethanethiol, and 2-(*N*,*N*,*N*-trimethylammonium)ethanethiol iodide (**34-37**) have been carried out and their rates of hydrolysis at 50 °C studied as a function of pH. Thiol esters **35** and **36** exhibit a plateau in their pH vs log k_{obs} profiles due to the participation of pendant carboxylate and dimethylamino groups. Thiol esters **34** and **37** have linear pH vs log k_{obs} profiles which are indicative of an exclusive specific base attack of ^{-}OH.

ACKNOWLEDGEMENTS

I gratefully acknowledge the supervision and guidance of Professor R. S. Brown throughout the course of this work, and especially in the preparation of this manuscript.

My sincere thanks to Vimal Balakrishnan, Kirsten Exall and James Wojtyk for proofreading this manuscript.

Finally, I would like to thank my wife Salma Shirin for her help and encouragement. I am indebted to her for her love and support.

To My Wife, Salma Shirin

Claims to originality:

To the best of the author's knowledge, the original work presented in this thesis includes the following:

1. Equilibrium studies of formanilide, acetanilide, *p*-nitroformanilide and *p*-methoxyformanilide under dilute aqueous acidic conditions.
2. Studies of acid catalyzed formation of anilides starting with constituent acid and amine without any condensing agent or tandem reactions.
3. Determination of the solvent deuterium kinetic isotope effects on the formation equilibrium constant of formanilide.
4. Determination of second order rate constants for phosphate catalysis on formation and hydrolysis of formanilide at pH 3.2 and 3.6, 79 ± 1 °C and μ = 1.0 (KCl).
5. Determination of the effect of temperature on the formation equilibrium constant of formanilide.
6. Determination of the effects of added ethanol to the solvent system on both rate of attainment of equilibrium and equilibrium position of formanilide.
7. Determination of second order rate constants for the attack of thioglycolic acid (**29**) on the strained amide **1** at pH 2.0 – 3.5 and 9.7 – 10.5.
8. Synthesis of 4-nitrobenzoate esters of ethyl 2-mercaptoacetate, thioglycolic acid, 2-dimethylaminoethanethiol, and 2-(*N,N,N*-trimethylammonium)ethanethiol iodide (**34-37**).
9. Studies of rate of hydrolysis of compounds **34 – 37** as a function of pH at 50 °C.

TABLE OF CONTENTS

LIST OF TABLES

Part 1.

Part 2.

LIST OF FIGURES

Part 1.

Part 2.

LIST OF ABBREVIATIONS

Asp	aspartate
CD	cyclodextrin
Cys	cysteine
DTNB	5,5'-dithiobis(2-nitrobenzoic acid)
EM	effective molarities
Glu	glutamine
His	histidine
HIV	human immunodeficiency virus
HPLC	high performance liquid chromatography
Im	imidazole
k_f	pseudo-first order rate constant for formation
k_{obs}	observed pseudo-first order rate constant
k_r	pseudo-first order rate constant for hydrolysis
K'	conditional equilibrium constant
K'_{eq}	corrected equilibrium constant
μ	ionic strength
NLLSQ	non-linear least squares
Ser	serine
SKIE	solvent kinetic isotope effect
T	tetrahedral intermediate
T^0	neutral tetrahedral intermediate
T_{2O}^-	dioxyanionic tetrahedral intermediate

T_N^-	N-protonated tetrahedral intermediate
T_O^-	oxyanionic tetrahedral intermediate
TS	transition state
ZW	zwitterionic species

Part 1: Studies of Equilibria of Formation and Hydrolysis of Anilides in Aqueous Media.

CHAPTER 1: INTRODUCTION

Amide bonds are important because they form the backbone of proteins. It is generally believed that peptide (amide) bond formation in aqueous solution is an unfavourable reaction both from a thermodynamic and from a kinetic viewpoint, and the large excess of water favours the hydrolysis[1] process, eq 1.

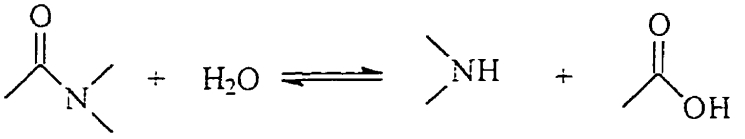

(1)

The formation of amide bonds in aqueous media in the absence of enzymes is also of importance since this formation is implicated in the origin of life.[2-7] Various attempts have been made to form peptides from amines and acids, or by coupling of amino acids, under conditions that resemble those of primitive earth. In studies simulating prebiotic conditions, linear and cyclic polyphosphates,[3] cyanamide,[4] metal ions,[5] silica, alumina, and clay[6] were used as catalysts for amide bond formations. However, it is well known that different catalysts will only increase the rate at which the equilibrium is attained without changing the equilibrium position. Unfortunately, this aspect has not been addressed in prebiotic studies. One should remember that unlike the normal time-scale of laboratory experiments, Nature had ample time to attain equilibrium under its prebiotic conditions.

Proteases are important classes of enzymes which hydrolyze amide (peptide) bonds. However, proteases can also resynthesize amides from their constituent carboxylic acids and amines under certain circumstances. While many mechanistic studies of the hydrolytic pathways have been performed, fewer investigations concerning the amide reformation are available.[1] These latter studies did, however, highlight the biological

importance of the equilibrium conditions of amide bond formations. Knowledge of the equilibria involved in hydrolysis and formation of amides (peptides) is fundamental to understanding biochemical processes: however, since these reactions are slow in aqueous media, only a few such studies have been reported.[7, 8]

A. Amide bond formation simulating prebiotic conditions.

Most studies simulating prebiotic conditions for amide bond formation involve condensing amino acids into (mostly) dipeptides in the presence of a catalyst, otherwise known as a "condensing agent", at elevated temperatures. Polyphosphate was shown to be one of the most successful catalysts used to form oligopeptides. Rabinowitz showed that up to 36 percent diglycine can be formed starting with glycine in the presence of sodium trimetaphosphate at 70 °C under neutral to basic conditions.[3c] The proposed mechanism[3a] of phosphate catalysis under alkaline conditions involves a phosphoramidate intermediate, Scheme 1, which cyclizes intramolecularly to give a five membered cyclic phosphate ester. Attack from another glycine molecule on the carbonyl

Scheme 1

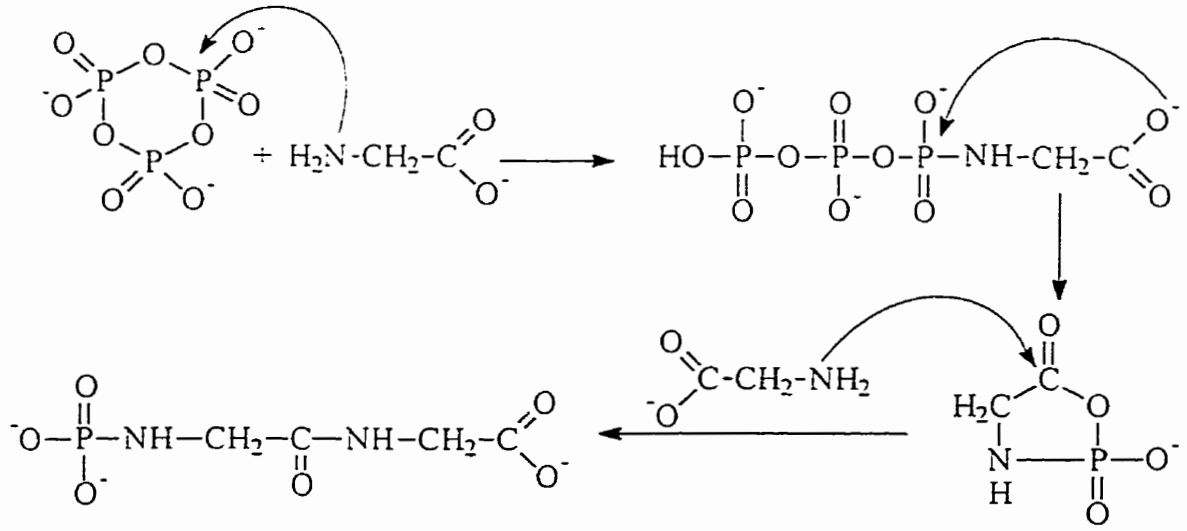

carbon of the cyclic ester leads to the N-phosphylated dipeptide.

More recently, condensation of di and tri-glycine was carried out[3b] to form tetra- and hexa-glycine in the the presence of tri- or tetrametaphosphate at 38 °C under various pH conditions ranging from 4 to 9. Trimetaphosphate was found to be a more effective catalyst than tetrametaphosphate. It was suggested that under neutral to acidic pH, condensation of di- and tri-glycine to form higher oligopeptides in the presence of polyphosphate proceeds through a phosphate ester intermediate, Scheme 2.

Scheme 2

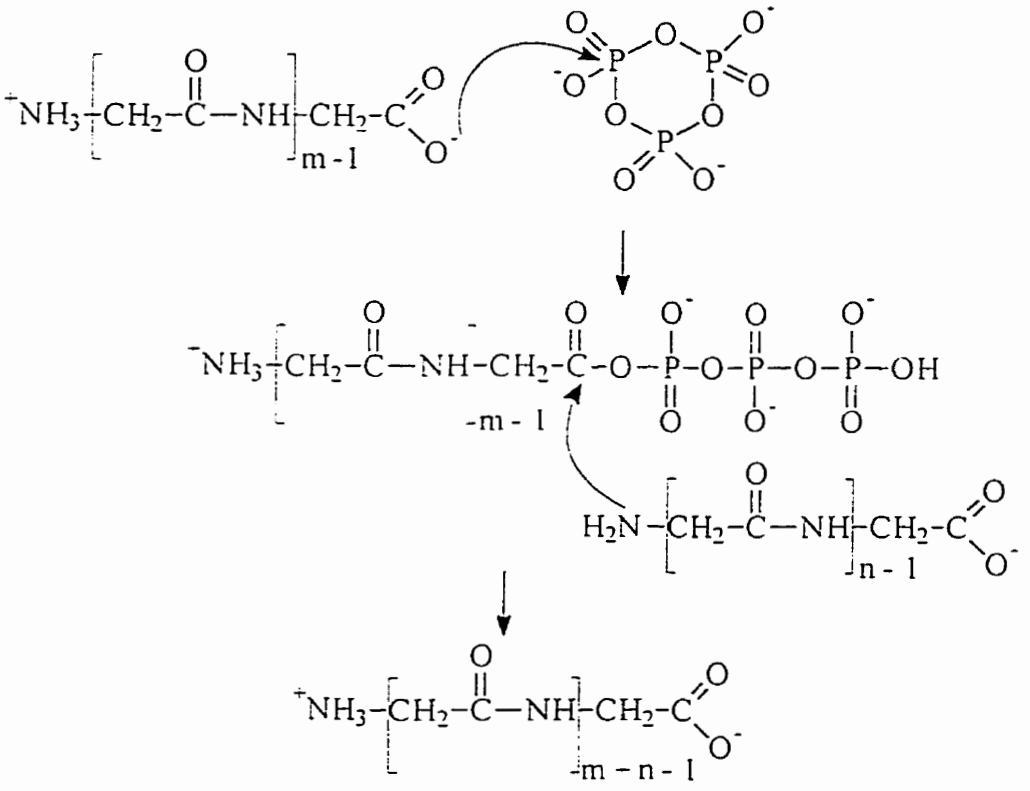

Staimman showed[4a, b] that cyanamide can also act as a condensing agent to form peptide bonds under probable prebiotic conditions. The possible role of silica, alumina and clays as catalysts in the chemical evolution of peptide bonds has also been studied by various groups. In a recent report, Bujdak *et al*[6a] have shown that when condensing

amino acids, up to 1 percent dimer was obtained on alumina, silica or clay at 80 °C. Similar amounts of tripeptide were obtained when condensing an amino acid and a dipeptide under the same experimental conditions. It was found that silica and alumina were better catalysts than clays.

In another study, Schwendinger showed that dipeptides can be formed starting from amino acids at high (5M NaCl) salt concentrations in the presence of Cu(II) ions.[6b] The formation of diglycine and mixed dipeptides of glycine and valine had been observed in a reaction system containing glycine, valine, Cu(II) ions and high concentration of salt.

More recently, it has been suggested[9] that oxidative formation of pyrite from iron sulfide and hydrogen sulfide, eq 2, can provide the driving force for

$$FeS + HS^- \longrightarrow FeS_2 + H^- + 2e^-; \quad E^\circ = -620\ mV \qquad (2)$$

reductive acetylation of amino acids with mercaptoacetic acid ($HSCH_2COOH$). The reactions were carried out at 100 °C and at pH 4.5. In this experiment, aniline, *o*-carboxy aniline and tyrosine were acylated by the above process. It was suggested that the acylation proceeds via thioacetic acid (CH_3COSH), which was aminolyzed to get the N-acylated compounds, eq 3. Under similar conditions, aniline produced the highest amount of amide compared to the other two amines.

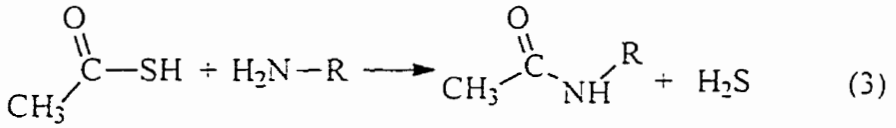

$$(3)$$

B. Enzyme catalyzed formation of amide bonds:

The normal biological role of proteases is to catalyze peptide bond hydrolysis (for an account on enzyme catalyzed hydrolysis, see Part 2 of this thesis). Nevertheless, it has

long been known that *in vitro*, many proteases catalyze[1] the microscopic reverse reaction, namely the resynthesis of peptide bonds. Recently, proteases have been used to synthesize oligopeptides. In one such example human insulin was obtained from coupling of deoctapeptide-(B23-B30)-insulin with an octapeptide using trypsin in a semisynthetic process.[10]

In the earlier enzymatic studies[1, 11] of amide bond synthesis starting with amino acids, it was realized that at physiological pH values (i.e. pH 7), removal of a proton from

$$RCOO^- + {}^+NH_3R' \rightleftharpoons RCOOH + NH_2R' \rightleftharpoons RCONHR' + H_2O \qquad (4)$$

a positively charged amine group and the addition of a proton to negatively charged carboxylate group (eq 4) was considerably endothermic. Part of the overall free energy change involved in the formation of amide bonds at a given pH may therefore be attributed to the neutralization of these groups. For comparison of free energy (ΔG^o) changes involved only in the hydrolysis (or formation) of similar types of bonds in various compounds, Carpenter proposed[11] the "non ionized compound" convention. This convention is expressed as follows[11]: "ΔG^o refers to the free-energy change involved in the hydrolysis of non-ionized reactant at unit activity in water by water in the liquid state to yield non-ionized products at unit activity in water."

In 1952, Fruton and co-workers determined[12] the chymotrypsin catalyzed equilibrium for the formation and hydrolysis of benzoyl-L-tyrosylglycinamide, starting with benzoyl-L-tyrosine, ^{15}N-labelled glycine and the dipeptide. To determine the equilibrium constant, a tracer technique and calorimetric procedure were used. The authors found that the apparent extent of hydrolysis of benzoyl-L-tyrosylglycinamide as a function of pH followed eq 5.

$$K'_{app} = \frac{([RCOOH] + [RCOO^-])([H_3\bar{N}R'] + [H_2NR'])}{[RCONHR']} = \left(1 + \frac{a_H}{K'_A} + \frac{K'_B}{a_H}\right) K'_{hyd} \qquad (5)$$

where K'_A and K'_B are the ionization constants of RCOOH and H_3N^+R' respectively, a_H is the hydrogen ion activity, K'_{app} and K'_{hyd} are the apparent and the corrected equilibrium constants. This relationship indicates that maximum synthesis or minimum hydrolysis. ($K'_{syn} = 1/K'_{hyd}$) would occur at pH values intermediate between the pK_as, expressed as $a_H = \sqrt{K'_A K'_B}$. More recently, Laskowski *et al* showed[13] that eq 5 could be applied to the resynthesis of peptide bonds in ribonuclease-S by the enzyme subtilisin.

Laskowski and co-workers also studied the effect of organic co-solvents on chymotrypsin catalyzed synthesis of a dipeptide.[14] Six different polyhydroxy compounds were used as co-solvents. All these co-solvents shifted the equilibrium position towards synthesis as the percentage of co-solvent was increased. Solvents such as ethanol, acetonitrile and acetone were not used because the enzyme activity was decreased in these co-solvents. The best co-solvent was found to be 1,4-butanediol, and at 85% (v/v) K'_{syn} increased to 38 M^{-1} from 0.45 M^{-1} in aqueous medium. Co-solvent concentration could not be increased beyond 85% because the enzyme activity decreased. The shift of the equilibrium position towards synthesis due to the addition of organic co-solvents was attributed to the shift of the apparent pK_as of RCOOH and $R'N^+H_3$ of the amino acid substrates.

Using chymotrypsin as the catalyst, N-benzoyl-L-tyrosylglycylanilide, a dipeptide, was synthesized from N-benzoyl-L-tyrosine (**1**) and glycylanilide (**2**).[15] The rate constants

showed a Michaelis-Menten dependency (saturation) on the concentration of N-benzoyl-L-tyrosine (amine protected amino acid). On the other hand, with glycylanilide, the rate

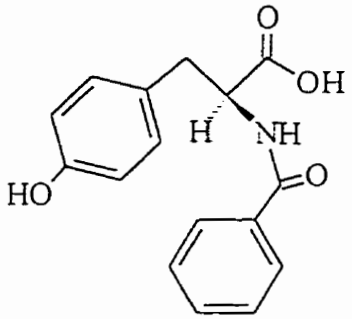

1

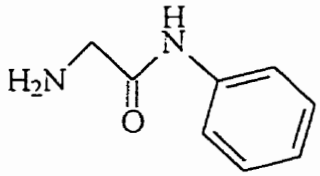

2

constants varied linearly with concentration. These findings suggested that the tyrosine derivative formed a complex with the enzyme and that this complex reacted with the amino group of glycylanilide to form the dipeptide and regenerated the enzyme as depicted in Scheme 3.

Scheme 3

$$\mathrm{RCOOH + EH \rightleftharpoons RCOE + H_2O}$$

$$\mathrm{RCOE \xrightarrow{-R'NH_2} RCONHR' + EH}$$

Hence, the authors suggested that the process of chymotrypsin catalyzed synthesis of peptide bonds was the microscopic reverse of the hydrolysis process, since both the formation and hydrolysis of amide bonds proceeded via acyl enzyme intermediates.

Many other proteases, such as papain,[16] pepsin,[17] and thermolysin[18] have been shown to catalyze peptide bond synthesis. Most enzyme mediated amide bond syntheses involve an N-protected amino acid and another amino acid with a protected carboxylic acid. Organic co-solvent is frequently used to increase the solubility of the starting

materials. Another aspect of enzymatic synthesis of amide bonds is the specificity of enzymes in forming the bonds, which is beyond the scope of this thesis.

C. Non enzymatic hydrolysis of amide bonds.

Amide bonds are highly stable towards hydrolysis, which allows the construction of robust polypeptides from relatively simple amino acids. Non enzymatic acyl transfer reactions of unactivated amides are extremely slow[19] which is generally rationalized using resonance theory, where canonical form **II** is an important contributor to the

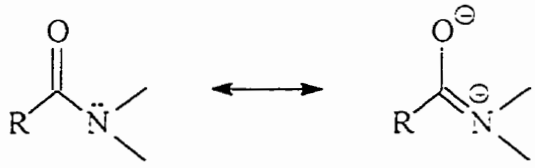

I **II**

stability. Most of the properties of amide bonds such as the short N-C(=O) bond length, the barrier to N-(C=O) bond rotation, the C=O infrared stretching frequencies, and resistance toward nucleophilic attack (and hydrolysis) can be explained by the above resonance forms.[20] Due to the inherent stability of the amide linkage, elevated temperature and highly acidic or basic conditions are required for hydrolysis. As a result, nonenzymatic hydrolysis processes were rather ill defined, until recently.[21] However, recent experiments[22, 23] have contributed significantly towards the mechanistic understanding of amide hydrolysis. As depicted in eq 6 amide bond hydrolysis in water or base proceeds through an addition elimination mechanism, in which the nucleophilic oxygen (from H_2O or OH^-) is bound to the acyl carbon to form one (or more) unstable tetrahedral intermediates, **T**.

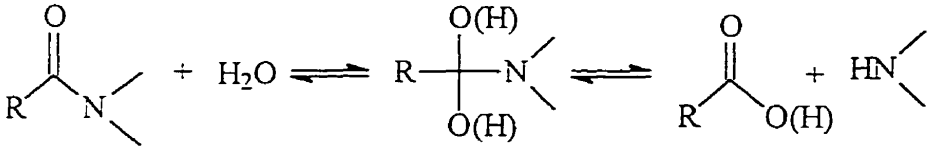

(6)

T

Brown *et al* have outlined three key sets of experiments used to distinguished between possible amides hydrolysis mechanisms.[19] They are: A) measurement of the kinetics as a function of $[H_3O^+]$ or $[^-OH]$ to determine the stoichiometry of the rate determining transition states (TS); B) the kinetics of carbonyl ^{18}O-exchange in unreacted amide recovered from partly hydrolyzed reaction mixtures as a function of $[H_3O^+]$ or $[^-OH]$, which provides information about the reversibility of the steps leading to the tetrahedral intermediates; and C) solvent deuterium kinetic isotope effects (SKIE) on the hydrolysis and ^{18}O-exchange. These provide information about the proton transfers in the respective rate limiting transition states. A brief account on the mechanisms of specific acid , specific base and water catalyzed amide hydrolysis is given here.

Specific acid catalyzed hydrolysis:

The generally excepted mechanism for H_3O^+ catalyzed amide hydrolysis is detailed in Scheme 4. The mechanism involves protonation of the carbonyl O in a pre-equilibrium step followed by nucleophilic attack on the carbonyl carbon by one H_2O assisted by a second H_2O molecule yielding the tetrahedral intermediate $\mathbf{T}^0$ and H_3O^+. Generally, the plots of log k_{hyd} vs pH have slopes of -1 indicating that the rate limiting TS for hydrolysis contains one proton and the amide. At high $[H_3O^+]$, however, these plots level off and then curve downward. These observations are consistent with substantial

Scheme 4

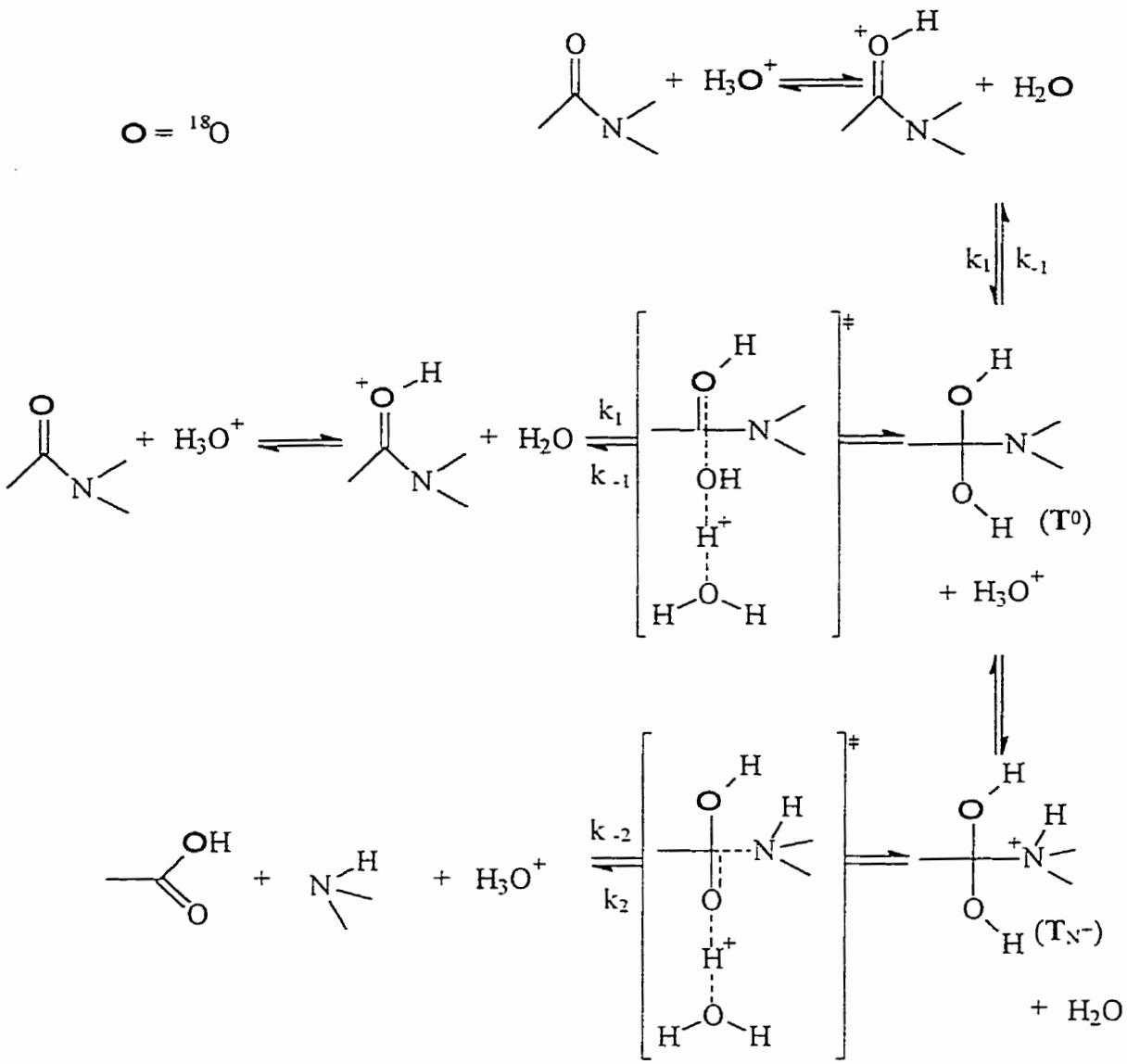

equilibrium O-protonation (pK_a -0 to -3[24]) and a reduction in H_2O activity in concentrated acid media.

In earlier studies[25] no significant loss of ^{18}O was observed during acid promoted amide hydrolysis. However, in later experiments[26] small, but significant, loss of ^{18}O was detected. The hydrolysis and exchange rate constants (k_{hyd} and k_{ex}) can be expressed in

terms of k_1, k_{-1}, and k_2 (Scheme 4), where k_1 and k_2 are redefined to incorporate the protonations of C=O, and the nitrogen of $\mathbf{T}^0$.

$$k_{hyd} = k_1k_2/(k_{-1} + k_2) \qquad (7a)$$

$$k_{ex} = k_1k_{-1}/2(k_{-1} + k_2) \qquad (7b)$$

$$k_{ex}/k_{hyd} = k_{-1}/2k_2 \qquad (7c)$$

The partitioning of $\mathbf{T}^0$ can be obtained from eq 7c. The factor of 2 in the denominators of eq 7b and 7c is due to the fact that only half of reversal of the step leading to $\mathbf{T}^0$ will give ^{18}O exchange in the starting materials since the two oxygens are equivalent.

Brown *et al* reported[23b] significant ^{18}O exchange in amides like N-2,4-trimethyl acetanilide during acidic hydrolysis, with an observed k_{ex}/k_{hyd} of about 0.2. They also observed that both exchange and hydrolysis were first order in $[H_3O^+]$ and the SKIE on both were close to unity. From these observations, it follows that there must be an intermediate which is partitioned between exchange and hydrolysis. Because the exchange was smaller than hydrolysis, it was suggested that k_1 was the predominantly rate limiting step. Both the exchange and hydrolysis TS must contain one proton since they were both first order in $[H_3O^+]$, hence ruling out a neutral or zwitterionic TS. The observed unit SKIE for hydrolysis and exchange was explained by the fact that the inverse equilibrium isotope effect of carbonyl O-protonation was being compensated for by the normal kinetic effect for H_2O promoted delivery of water. Subsequent studies showed that the k_{ex}/k_{hyd} ratio varied as a function of amine basicity. The amount of O^{18}-exchange was observed to increase as the basicity of the ammonium ion decreased since more reversal from $\mathbf{T}^0$ takes place as it becomes increasingly difficult to install a proton on N to form $\mathbf{T}_N^+$.

Specific base catalyzed hydrolysis:

Specific base catalyzed hydrolysis of amide bonds proceeds as shown in Scheme 5. The steps in this hydrolytic mechanism involve attack of ^{-}OH on the neutral amide to

Scheme 5

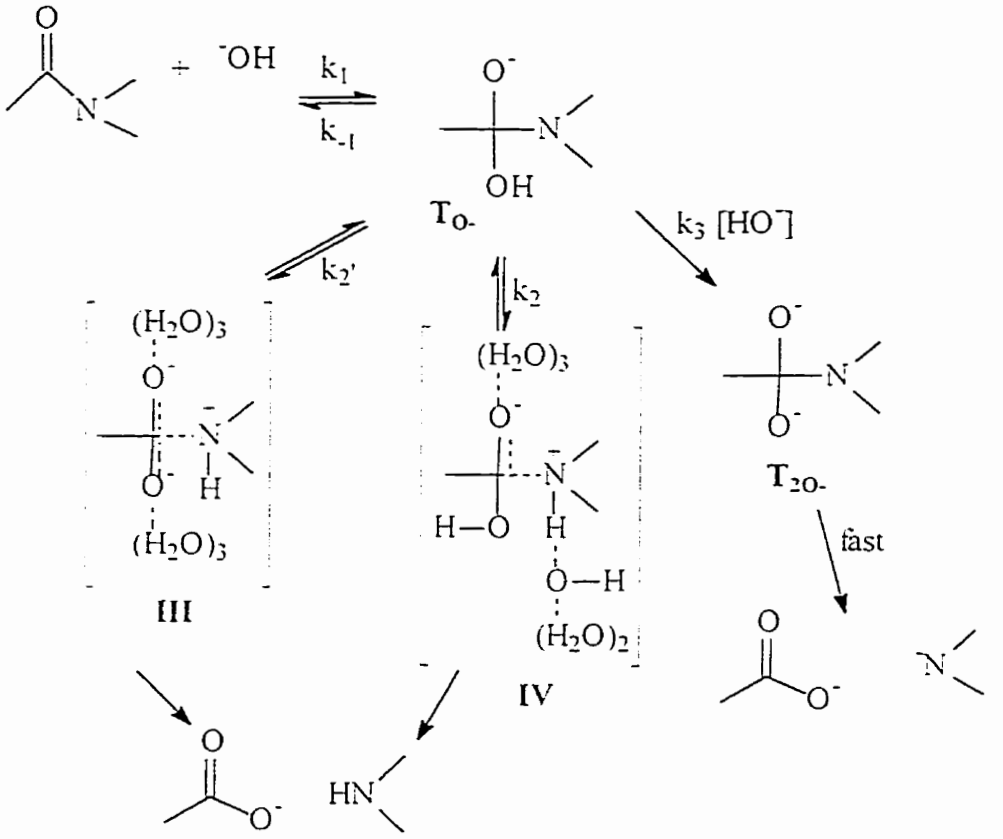

form the anionic tetrahedral intermediate T_{O-}, which may revert back to starting materials or can break down to products with (k_3) or without ($k_2 + k_{2'}$) assistance from a second ^{-}OH. Second order dependence in [^{-}OH] has been observed for the hydrolysis of several amides.[27] and is explained by a process where a second ^{-}OH deprotonates T_{O-} to give the dianionic intermediate T_{2O-} which subsequently gives carboxylate and amide ions. At high [^{-}OH], this process becomes predominant, so as soon as T_{O-} is formed it is trapped by another ^{-}OH to produce T_{2O-}, thereby preventing the reversal, and making the

formation of $\mathbf{T_{O^-}}$ (k_1) the rate limiting step. Accordingly, such amides show large ^{18}O exchange at low [OH^-], and little or none at high [OH^-].

There are many amides[28] which do not show a second order term in [^-OH]. For these amides, $\mathbf{T_{O^-}}$ is reactive enough that it can break down to products (k_2) with the simple assistance of water (solvent). For this process, the dominant factor controlling the partitioning of $\mathbf{T_{O^-}}$ (to reactants (k_{-1}) and products (k_2)) is amine basicity. If the amine is highly basic, N protonation becomes thermodynamically favourable and consequently k_2 becomes faster than k_{-1} so that little or no ^{18}O-exchange is observed for these amides. On the other hand, for amides containing less basic amines, the breakdown (k_2) of the tetrahedral intermediate to product will become the rate-limiting step. SKIE studies suggested that in the water catalyzed breakdown (k_2) step a proton is completely installed on N prior to C-N cleavage which occurs by **III** or **IV**.

Water catalyzed hydrolysis:

Water catalyzed hydrolysis of amide bonds is an extremely slow process.[20] Most of the studies involving water catalysis were performed on amides which were activated in some way. In a recent study, Brown and co-workers studied[29] the water catalyzed hydrolysis of trifluoroacetanilide (**3a**) and *p*-nitrotrifluoroacetanilide (**3b**). The water hydrolysis of both compounds exhibited a large negative entropy of activation, indicating an ordered TS involving more than one water molecule. No ^{18}O-exchange was observed in the ^{18}O- labelled *p*-nitrotrifluoroacetanilide recovered after partial hydrolysis. From these observations, it was suggested that the formation of a diol ($\mathbf{T_O}$) in a concerted or

nearly concerted fashion was the rate limiting step for the reaction. followed by rapid cleavage of the C-N bond in preference to OH expulsion. Scheme 6.

Scheme 6

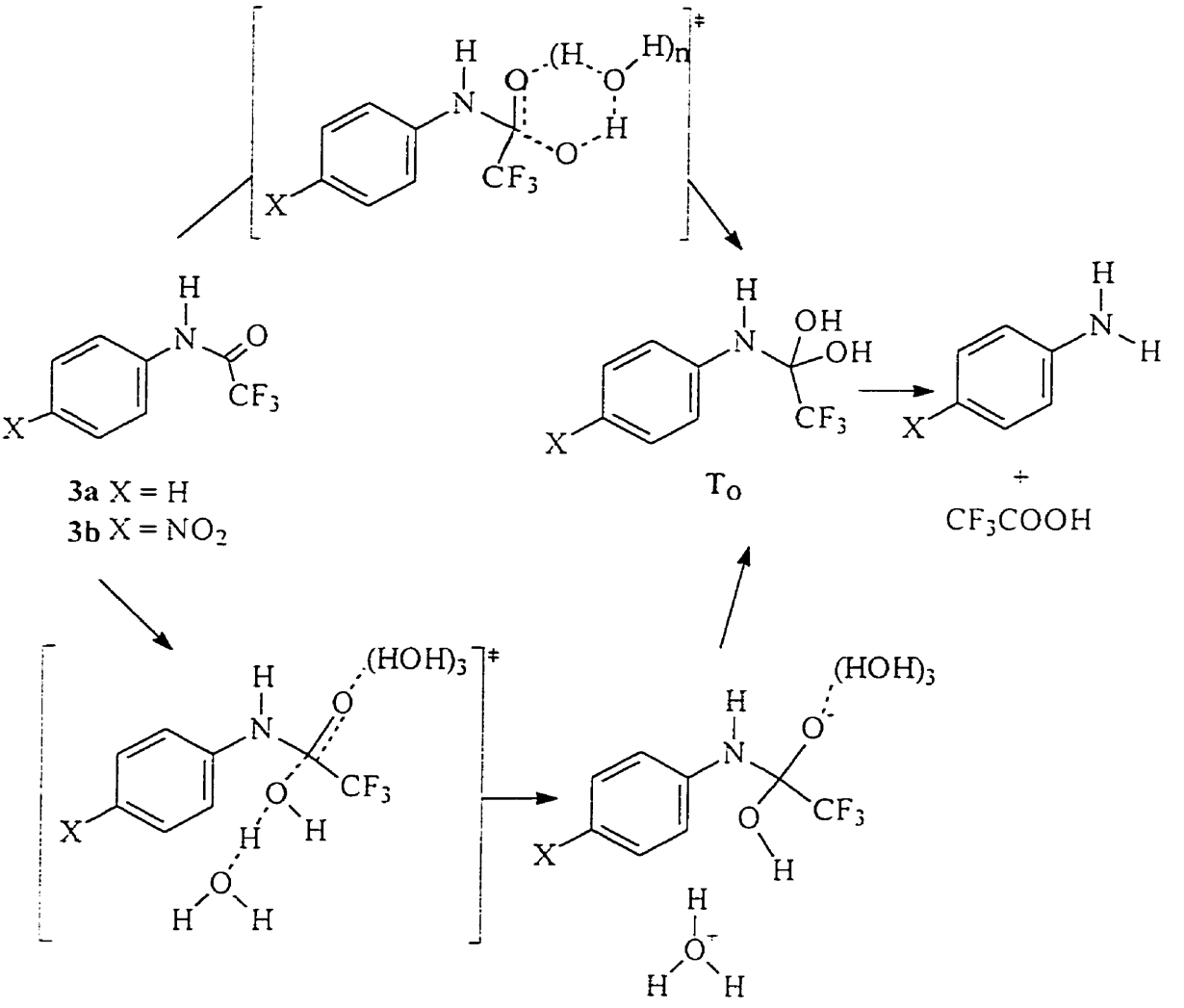

D. Non enzymatic formation of amide bonds.

Small molecule mimics of proteases have been extensively studied in this laboratory and the reactions of a series of amine alcohols **4** - **6**[30] with **7** were investigated as possible models for serine proteases. The reactions of bicyclic amide **7** with small

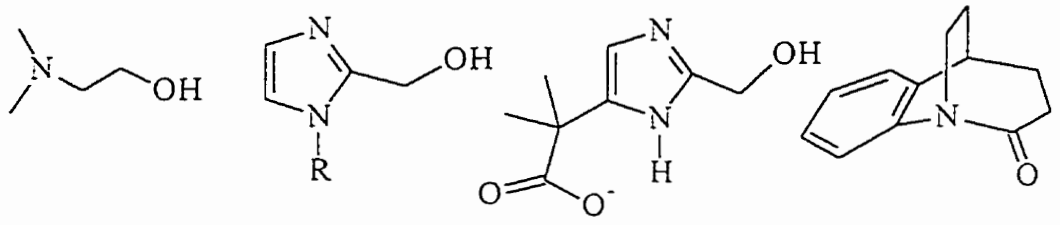

4 **5a** R = H, **b** R = CH_3 **6** **7**

molecules containing thiols **8-11**[31-36] have been studied as models of cysteine proteases.

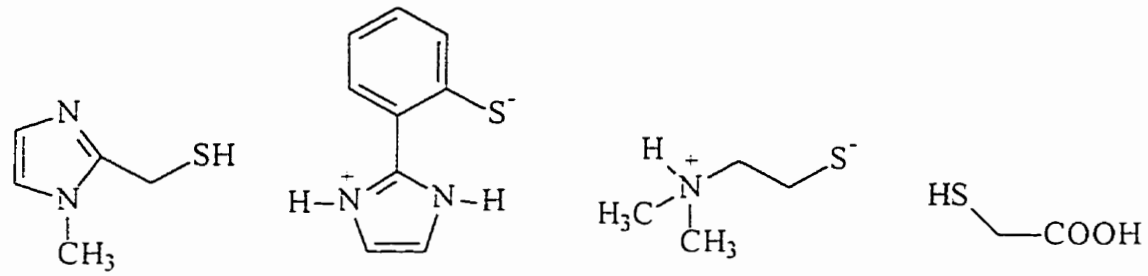

8 **9** **10** **11**

while a series of dicarboxylic acids **12-14**[37] have been used to mimic the chemistry believed to occur in the active sites of aspartate proteases. For a brief account on amide bond hydrolysis using these models, see Part 2 of this thesis.

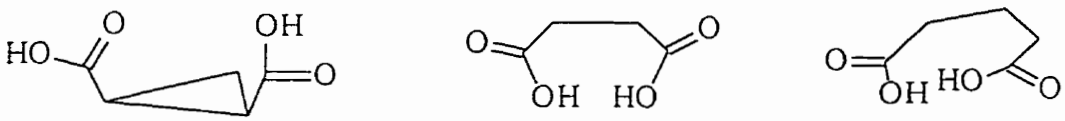

12 **13** **14**

Among the aforementioned small molecule protease models, **8** has been shown to catalyze the reformation of amide bonds,[35a] Scheme 7. The catalytic mechanism of **8** mediated formation and hydrolysis of amide bonds proceeds via a common thiol ester intermediate **8a**.

Scheme 7

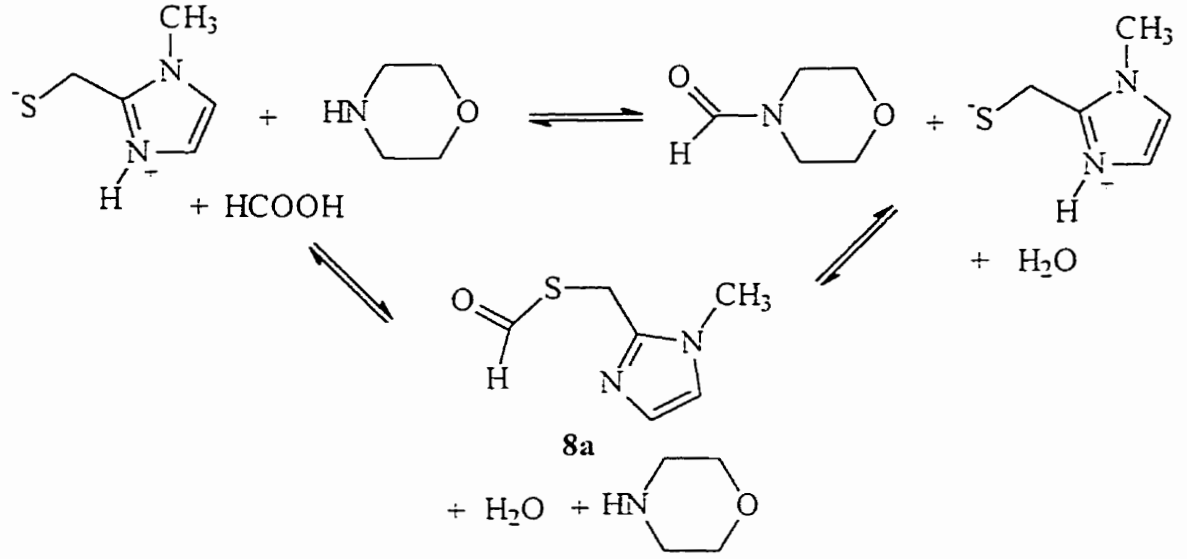

8a

Hence, the equilibrium position between the hydrolysed products and the amide would depend on the partitioning of this intermediate between hydrolysis or aminolysis. The apparent equilibrium constant,[35b]

$$K'' = [\text{amide}]/[\text{amine}]_{\text{total}}[\text{acid}]_{\text{total}}$$

for N-formylmorpholine was found to be 1.2 M^{-1} at pD 8.0 and 98 °C. The formation and hydrolysis of N-formylmorpholine was also observed to be catalyzed by phosphate buffer under the same conditions.

Kirby *et al* showed that cyclic amides (lactams) could be made from intramolecular aminolysis of ester **15**[38a] and from the intramolecular cyclization of amino acids **16a-d.**[38b]

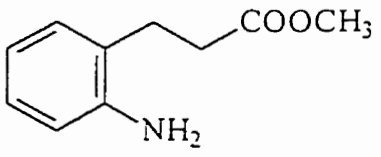

15

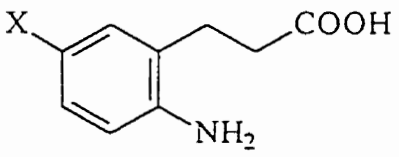

16a; X = H
b; X = CH_3O
c; X = CH_3
d; X = Cl

The effects of various buffers on the cyclization of **15** were studied and it was found that the cyclization process is susceptible to both general base and general acid catalysis. Buffers with pK_a values higher than 6.6 acted as general bases while buffers with pK_a values lower than 6.6 acted as general acids. It was also suggested that phosphate and carbonate acted as bifunctional catalysts.

The pH-rate profile for cyclization of **16a-b** showed[38b] a plateau region at lower pH (below ca. pH 4) while at higher pH, the log k_{obs} decreased linearly with increasing pH. It was concluded from this observation that the intramolecular condensation of amine and carboxylic acid **16a-b** proceeded from the protonated form of the compound at lower pH and from the neutral compound at higher pH, Scheme 8 (only **16a** is shown). The neutral amino group acted as a nucleophile to attack the protonated or undissociated carboxylic group in **16a**-H^+, or **16a** to subsequently form the neutral tetrahedral intermediate which

Scheme 8

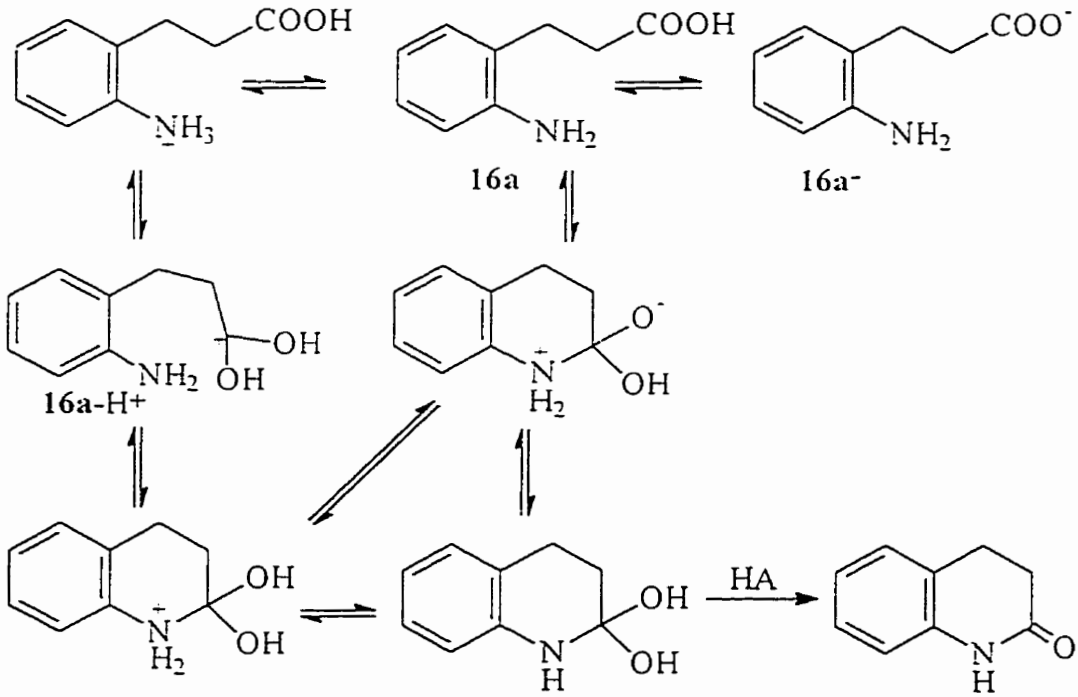

breaks down in the rate limiting step to the cyclic amide product. The anionic form of the compound (**16a**$^-$) was not reactive. Buffer catalysis was studied for the cyclization of **16a**, and it was suggested that the rate enhancement due to the buffers came from the general acid catalyzed breakdown of the neutral tetrahedral intermediate. A Brønsted α value of 0.49 was obtained for this process, and the log of the second order rate constant due to phosphate catalysis was above the Brønsted line, indicating the possible bifunctional role of phosphate.

Fife and coworkers studied[39] the intramolecular cyclization of **17** which produces a five membered cyclic amide, eq 8.

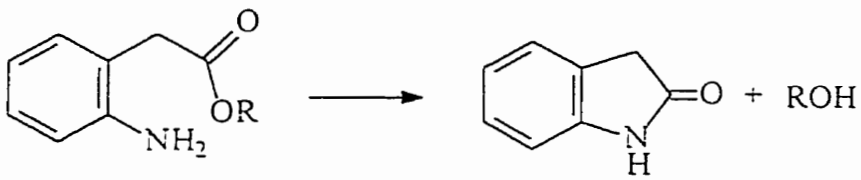

(8)

17 a; R = CH_3
b; R = CH_2CF_3

Unlike cyclization of **15**, these reactions exhibited specific base catalysis. It was suggested that intramolecular aminolysis of aliphatic esters proceeded through multi-step mechanisms with various rate-limiting steps. Three key features controlling these aminolysis reactions have been identified: A) the pK_a of the amine nucleophile; B) steric fit of the nucleophile to the carbonyl carbon; and, C) the ease of C-O bond breakage in the decomposition of a tetrahedral intermediate to form products.

Blackburn and Jencks studied[40] the mechanism of the aminolysis of methyl formate using morpholine, n-propylamine, methoxyethylamine, hydrazine, glycinamide and glycylglycine as the amine nucleophile. In aqueous media, the reaction proceeded predominantly by the attack of a free amine on the carbonyl carbon with general base

assistance from a second molecule of amine. Given that the rate decreased with decreasing pH at a constant free amine concentration, the authors suggested that the rate limiting step for the reaction of morpholine with methyl formate was the attack of the amine to give a tetrahedral intermediate at high pH, versus the breakdown of the said intermediate at low pH. This argument was further strengthened by the finding that when N-(methoxymethylene) morpholinium methosulphate (a compound producing the same tetrahedral intermediate as is formed during aminolysis of methyl formate by morpholine but by a in a different route) was hydrolyzed under basic conditions, the amide resulted. However, under acidic conditions, the ester was formed, Scheme 9.

Scheme 9

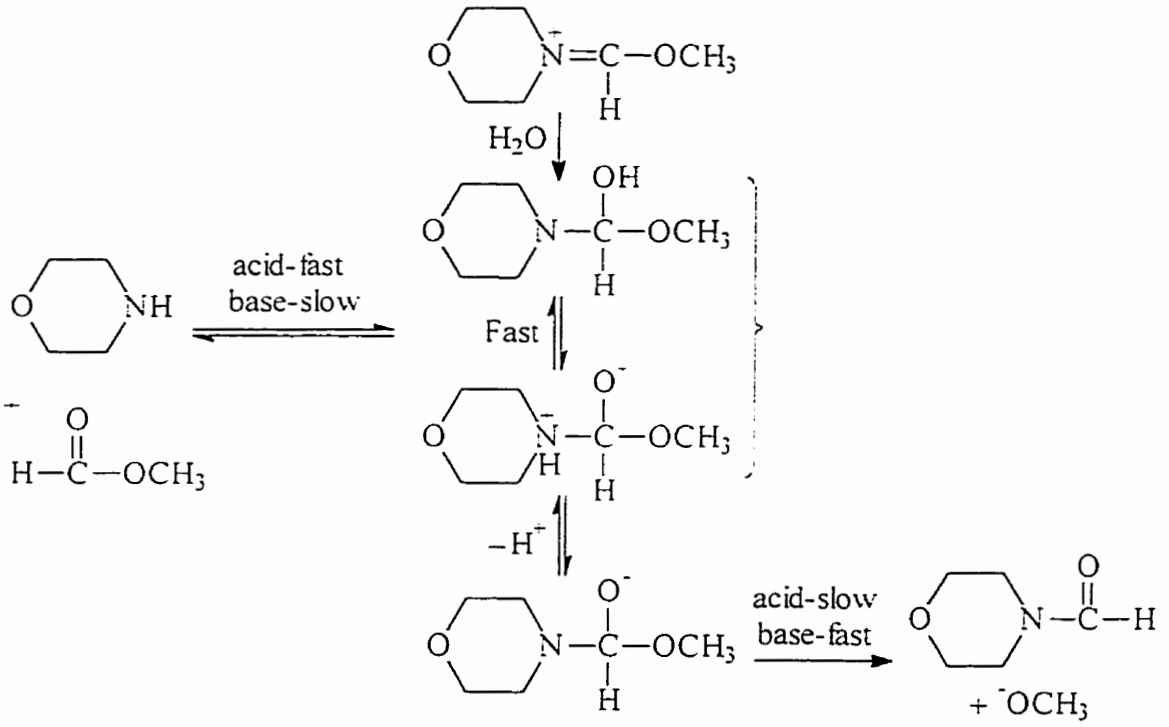

In another study by Jencks *et al*, the equilibrium constants for the formation of hydroxamic acids from carboxylic acids plus hydroxylamine were obtained.[41]

Equilibrium had been obtained from the direction of both formation and hydrolysis, starting with hydroxylamine and the appropriate acid or the hydroxamic acid, respectively, eq 9. The equilibrium constant of the acetohydroxamic acid was determined

$$RCOOH + H_2NOH \rightleftharpoons RCONHOH + H_2O \qquad (9)$$

in dilute, aqueous acidic conditions at 25 °C. For hydrolysis of hexanohydroxamic and octanohydroxamic acids the determination was performed using liver esterase whereas chymotrypsin was used for the determination of equilibrium constants at neutral pH for the hydrolysis of N-acetyl-L-tyrosine hydroxamic acid. The value of the apparent equilibrium constants at pH 7, K'_{pH7}, eq 10a, taking $[H_2O] = 1$ M, for all the hydroxamic acids were close to 1, except for that of N-acetyl-L- -tyrosine hydroxamic acid which

$$K'_{pH7} = \frac{[RCONHOH][H_2O]}{[RCOOH]_{total}[NH_2OH]_{total}} \qquad (10a)$$

was 0.042. However, when the equilibrium constants, K_I (eq 10b) were corrected for respective acid and amine pK_as to get the uncharged species and taking $[H_2O] = 1$, the values were very close to each other, at 402, 422, 372 and 362 for acetohydroxamic,

$$K_I = \frac{[RCONHOH][H_2O]}{[RCOOH][NH_2OH]} \qquad (10b)$$

hexanohydroxamic, octanohydroxamic and N-acetyl-L-tyrosine hydroxamic acid, respectively.

The formation of formamide from ammonia and formic acid, given in eq 11a, has been studied using semiempirical and *ab initio* methods.[2] It was concluded[2a] that in the gas phase, the stepwise and concerted mechanisms for amide bond formation are

$$NH_3 + HCOOH \rightleftharpoons H_2NCHO + H_2O \qquad (11a)$$

equally competitive. Nevertheless, the stepwise mechanism, involving a tetrahedral intermediate, was found to be more favourable than the concerted mechanism in a subsequent study[2b] where two molecules of ammonia were considered in the model reaction (eq 11b), with the second molecule of ammonia acting as a catalyst. It was also

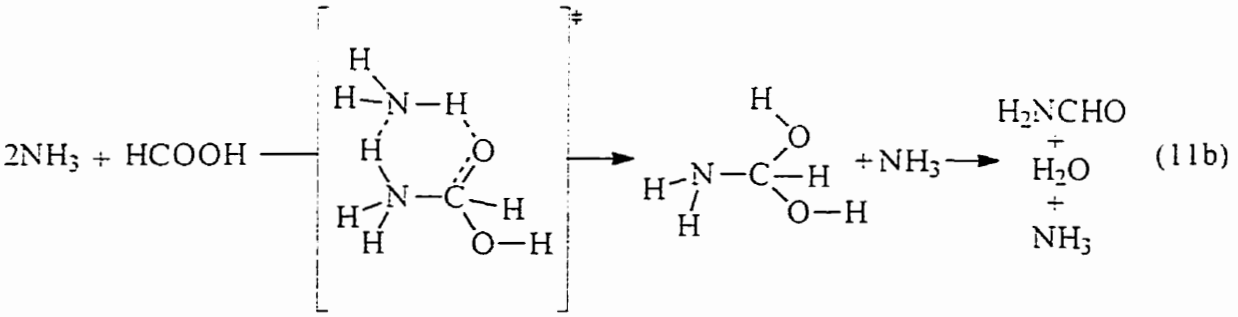

(11b)

found that for the two step mechanism, the first step was rate determining.

Guthrie has previously calculated the thermochemical data for equilibrium formation of formanilide and acetanilide from their constituent acids and amines.[24] More recently, he has calculated the corrected equilibrium constants (K'_{eq}, see Results) and heats of formation of *N,N*-dimethyl amides of substituted benzoic acids, eq 12.[42]

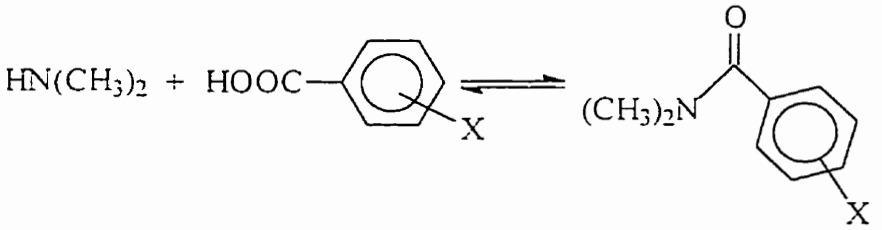

(12)

Fersht and Requena have reported the equilibrium constants for a series of formamide formations using indirect methods for a series of primary and secondary amines.[8] To attain the equilibrium position the reaction of hydroxylamine and formic acid was used to form methanohydroxamic acid, which would subsequently be aminolysed to give the amide, Scheme 10.[8] The equilibrium constants were calculated based on the concentration of non-ionized reagents and taking the activity of water as unity. The

authors showed that the log of the equilibrium constant is linearly dependent on the pK_a of the ammonium ion of the amine (eq 13). However, the corrected equilibrium constant (K'_{eq}) corresponding to aniline did not fall on the line.

$$\log K'_{eq} = 0.50 + 0.51 \log pK_a. \qquad (13)$$

Scheme 10

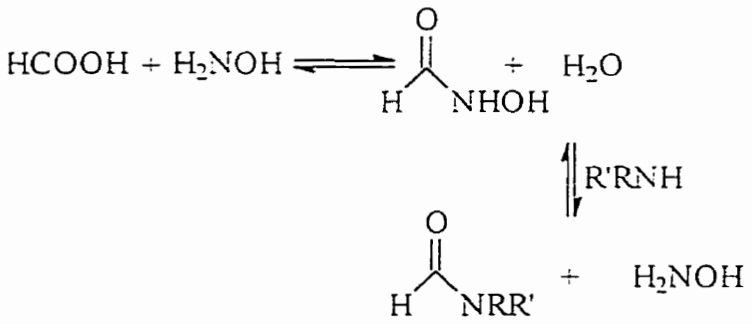

In an earlier study by Morawetz and Otaki, the equilibrium constants for amide formation were determined under aqueous basic conditions for a series of amines and carboxylates as described in eq 14.[7] The equilibrium constants were determined from the ratios of the rate constants of formation (k_1) and hydrolysis (k_2). It was observed that there was very little effect on the equilibrium constants due to the change in the acyl part of the amide.

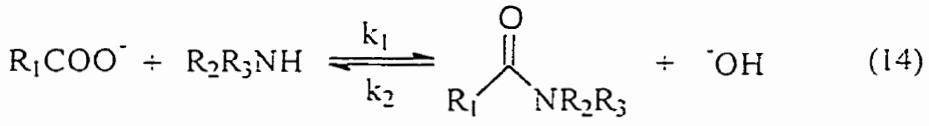

(14)

E. Purpose of this study.

As pointed out[8] by Fersht, "the most rigorous method of determining equilibrium constants is to approach the equilibrium from both sides and measure the equilibrium concentrations of reagents". Amide bond reformation from the constituent acid and amine without the use of condensing agents would be of practical use in large scale (industrial) synthesis, owing both to the reduction in the number of steps required and due to its cost effectiveness. Although in previous studies Morawetz and Otaki have reported[7] amide reformation taking place in basic media, equilibrium constants for the non-enzymatic formation of amides have not yet been obtained directly starting with the constituent acids and amines in dilute aqueous acidic media. While acid catalysis accelerates hydrolysis of amide bonds, it should also increase the rate of amide reformation, and since in acid the concentration of free amine will decrease, the apparent formation equilibrium constant also decreases. This work is aimed at: A) understanding factors important for attaining equilibrium directly without recourse to tandem reactions like those used by Fersht;[8] B) determining ways to catalyze attainment of equilibrium by buffers; and C) examining the effect of ethanol as an additive that may alter pKas, thus yielding greater amounts of the required neutral acid and amine, which in turn should alter the apparent equilibrium constant.

In the present study, equilibrium constants for formation/hydrolysis have been obtained for formanilide, acetanilide, *p*-nitroformanilide and *p*-methoxyformanilide by approaching the equilibrium position from both sides under dilute aqueous acidic (pH 2.8-4.2) conditions. The rate constants for the attainment of equilibrium have also been determined. All the reactions were carried out under pseudo-first order conditions, where

formic acid or acetic acid was used in excess, and the reactions were carried out under various conditions of pH and substrate concentration to determine how these affected the rate and equilibrium constant. The effect of temperature on the rate and equilibrium constants of formanilide formation and hydrolysis was also studied. Since previous studies have shown that phosphate can act as a bifunctional catalyst for both formation and hydrolysis of amide bonds, the effect of varying phosphate concentration was studied for formation and hydrolysis of formanilide. Previously, for the enzymatic formation of amide bonds, it was observed that organic co-solvents increased the extent of amide formation.[14] Accordingly, we have studied the effect of added ethanol on the formation and hydrolysis of formanilide. To calculate the concentration of non-ionized amine and acids, the ionization equilibrium constants, K_a, were determined or computed under the reaction conditions for all reactants. Finally to determine the solvent deuterium kinetic isotope effects on both the equilibrium position and the rate of formanilide formation and hydrolysis, reactions were also carried out in D_2O. The following presents our findings.

CHAPTER 2: EXPERIMENTAL

A. Materials and General Methods.

Aniline, formic acid and *p*-nitroaniline were obtained from BDH. Acetanilide, formanilide, acetic anhydride and *p*-methoxyaniline were purchased from Aldrich and used as supplied. Glacial acetic acid was obtained from Fisher Scientific. Methanol (HPLC grade) was obtained from EM Science. Aniline and acetic acid were distilled prior to use. All HPLC solvents were filtered through a 0.45 μm filter before use. All melting points were obtained using Fisher-Johns melting point apparatus and are uncorrected.

All buffers were prepared using purified deoxygenated water from an Osmonic Aries water purification system. The pH was measured using a Radiometer Vit 90 video titrator equipped with a GK2321 C combination electrode, standardized by Fisher Certified pH 2, 4, 7 and 10 buffers.

B. Synthesis.

p-Nitroformanilide and *p*-methoxyformanilide were synthesized from *p*-nitroaniline and *p*-methoxyaniline respectively, using formic acetic anhydride, as described[43] by Krishnamurthy. *p*-Nitroformanilide was recrystallized 2 times from ethyl acetate before use and had a melting point of 196-197 °C (lit.[44] mp, 196-198 °C). *p*-Methoxyformanilide was purified by recrystallizing 3 times from chloroform-hexane mixture (hexane was added dropwise to chloroform solution until some cloudiness was observed). The pure product had a melting point of 79-80 °C (lit.[45] mp, 78-80 °C).

C. HPLC Conditions.

For HPLC analysis a Hewlett-Packard 1050 series HPLC system, fitted with variable wavelength UV-Vis detector and autoinjector, was used. For separation, an μ-Bonda-Pak C_{18} (Waters) cartridge column was used. A gradient mixture of 0.005 M potassium phosphate buffer (pH 7.2) and methanol was used to separate aniline from formanilide. For each injection the initial solvent composition was 20% methanol: 80% phosphate buffer which after 15 min. was modified to 30% methanol: 70% phosphate buffer until 21 min. whereupon 100% methanol was used to wash the column for 9 minutes before next injection. For separation of aniline and acetanilide, an isocratic mixture of 25% methanol: 75% phosphate buffer (0.005 M, pH 7.2) was used. In both cases the flow rate was 1.2 mL/min. and the detector was set at λ = 231 nm. Aniline eluted before the anilides. Figure 1.

D. Kinetics by HPLC.

For kinetics studies at 98 ± 2 °C, (5.0 - 5.3) x 10^{-3} M formanilide or aniline solutions were made in 10-20 mL of formate buffer (pH 3.2 - 4.2, $[buffer]_{total}$ = 0.1-1.0 M, μ = 1.0 M (KCl)) and were degassed by passing Ar through them for 30 min. These solutions were then divided into 10-20 autosampler-vials which were sealed with teflon lined septa. The vials were heated in a boiler containing boiling water, and at certain intervals were withdrawn from the boiler, cooled immediately in ice water and analyzed by HPLC. The pseudo-first order rate constants for appearance and disappearance of aniline and formanilide were obtained by NLLSQ fitting of peak area vs time data to a standard exponential model (*vide supra*). The response factor for formanilide and aniline

Figure 1. Typical HPLC elution traces. **(a)** 5 x 10^{-3} M aniline in formate buffer, $[buffer]_{total}$ = 0.1 M, pH 4.20, μ = 1.0 (KCl), analyzed after heating at 98 ± 2 °C for 29 hr. **(b)** 5 x 10^{-3} M acetanilide and 1.0 M acetic acid in HCl buffer, pH 1.95, μ = 1.0 (KCl), analyzed after heating at 98 ± 2 °C for 12 hr.

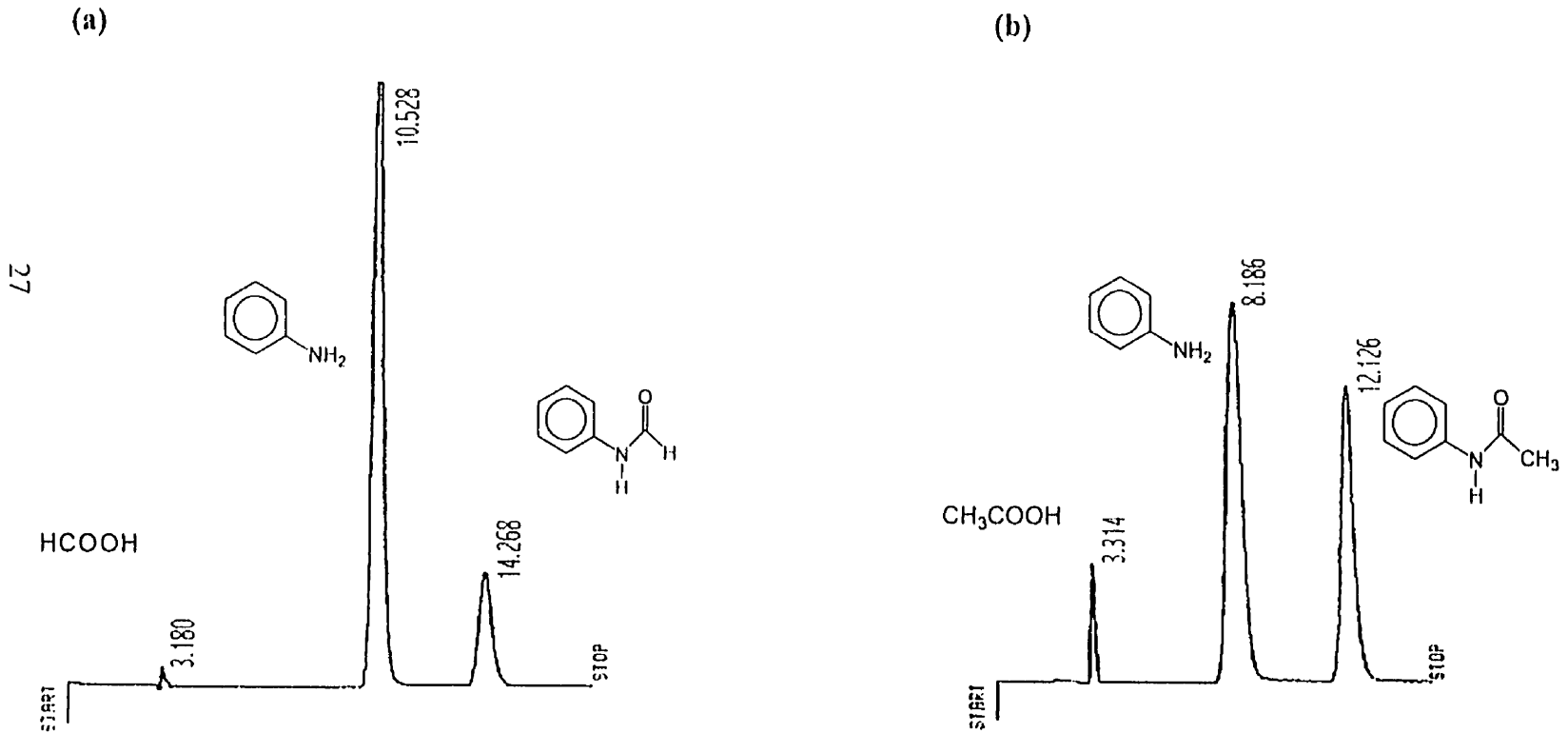

under the experimental conditions were obtained by injecting, and determining the peak areas of, a 1:1 formanilide and aniline mixture. For each run two rate constants could be obtained (for example for hydrolysis of formanilides the pseudo-first order rate constants of disappearance of the formanilide as well as the appearance of aniline were obtained).

Kinetic data for formation and hydrolysis of acetanilide were obtained similarly at the same temperature at pH 1.95 ± 0.03 and at pH 3.72 ± 0.03 with (5.2-5.4) x 10^{-3} M solutions of acetanilide or aniline. At lower pH, HCl comprised the buffer and 1.0 M acetic acid was added to the solutions. At higher pH acetate buffer was used with the total buffer concentration being 1.0 M. The ionic strength of all the runs was maintained at 1.0 (KCl).

E. Kinetics by UV-vis spectrophotometry.

The rates of formation and hydrolysis of formanilide, *p*-nitroformanilide and *p*-methoxyformanilide were observed at 79 ± 1 °C, using a Cary-219 UV-vis spectrophotometer interfaced with an IBM 486 PC equipped with Olis software (Online Instrument Systems, Jefferson Ga., 1992). The temperature was kept constant by using a Poly Science 1160A circulating water bath. Kinetic data were obtained by observing the rate of change in absorbance (increase for formation and decrease for hydrolysis) of formanilide at 246 nm and *p*-methoxyformanilide at 260 nm. For *p*-nitroformanilide, rates of formation and hydrolysis were obtained by following the rates of disappearance and appearance of *p*-nitroaniline, respectively, at 429 nm.

Runs were initiated by injecting 5 μL of a stock solution in DME (5.0-6.9 x 10^{-2} M) of either (*p*-H or *p*-NO_2 or *p*-OCH_3)-aniline or (*p*-H or *p*-NO_2 or *p*-OCH_3)-

formanilide into 3mL of formate buffer (pH 2.80 - 4.20. $[buffer]_{total}$ = 0.001-1.0 M. μ = 1.0 (KCl)). which had been thermally equilibrated at 79 ± 1 °C in the instrument cell holder for 30 min. The final pH of each of the runs was measured and shown to agree with the initial pH. A typical kinetic trace for hydrolysis and formation of formanilide at pH 3.60 at different $[buffer]_{total}$ is shown in Figure 2. The pseudo-first order rate constants were obtained by NLLSQ fitting of absorbance (A) vs time (t) data to a standard exponential model ($A_t = A_\infty + (A_0 - A_\infty) \exp(-kt)$).

The acid catalysed hydrolysis of formanilide was followed at 79 ± 1 °C using 9.86 x 10^{-3} M HCl. μ = 1.0 (KCl). with runs being initiated as above. All the runs were followed for at least 5 half-lives.

F. D_2O studies.

The rate of formation and hydrolysis of formanilide at 79 ± 1 °C was determined in formate buffer ($[buffer]_{total}$ = 0.25-1.0 M) at pD 3.60 ± 0.03 where. $pD = pH_{measured} + 0.40$.[46] The rate of hydrolysis of formanilide was also obtained in 1.10 x 10^{-2} M DCl. μ = 1.0 (KCl). The kinetic data were obtained as above.

G. Studies in the presence of phosphate.

The rate of formation and hydrolysis of formanilide was determined similarly at 79 ± 1 °C in the presence of phosphate (0.10-0.50 M) in 1.0M formate buffer at pH 3.20 ± 0.03 and pH 3.60 ± 0.03. with the ionic strength again being maintained at 1.0 (KCl).

Figure 2. Typical kinetic traces for formanilide equilibration at pH 3.60 at different $[formate]_{total}$, 0.10-1.00 M, μ = 1.0 (KCl), T = 79 ± 1 °C. The lines are obtained from NLLSQ fitting of data to ($A_t = A_\infty + (A_0 - A_\infty) \exp(-k_1)$).

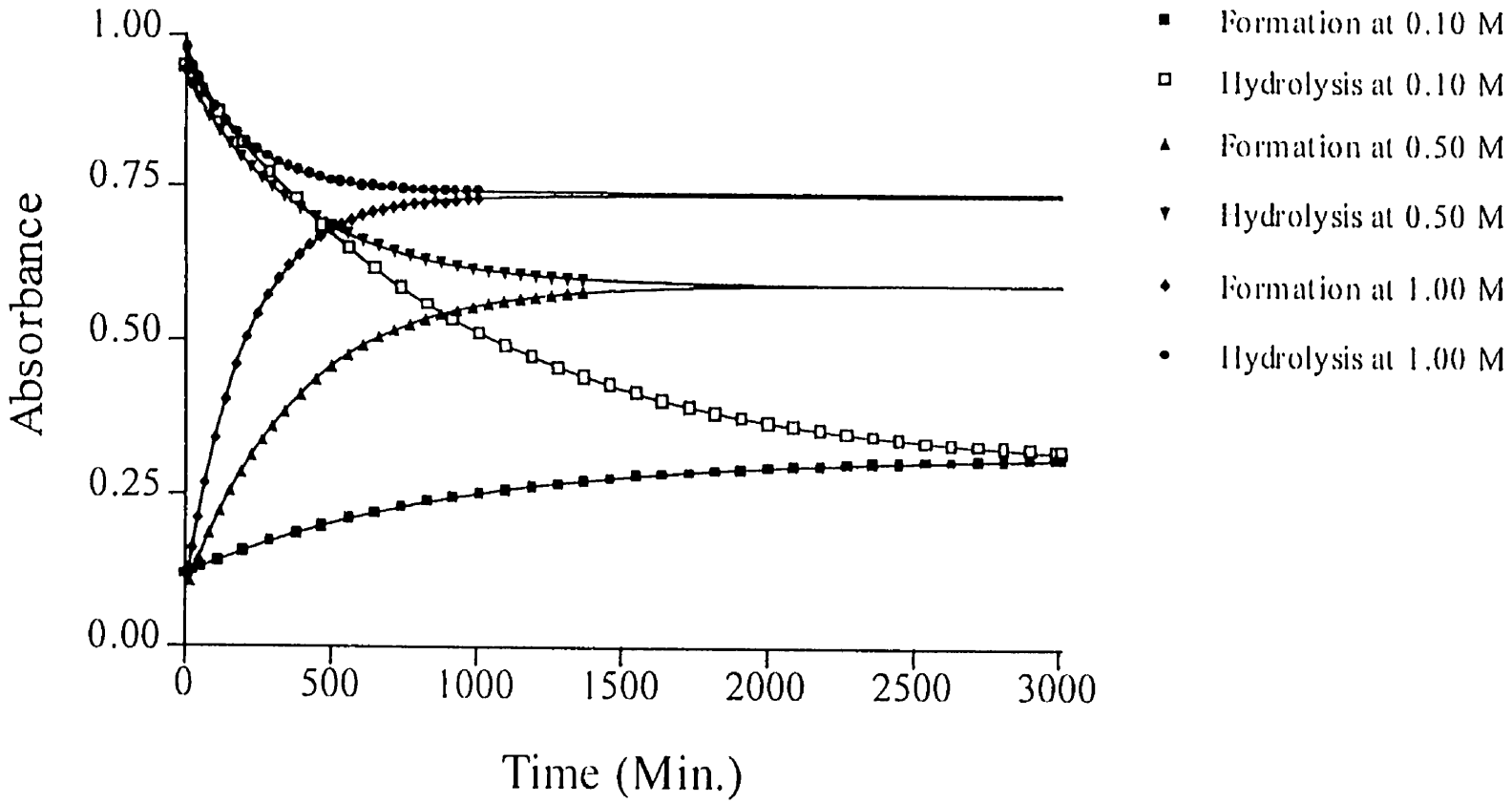

H. Studies in aqueous ethanol.

The rate of formation and hydrolysis of formanilide was obtained in 1.0 M formate buffer in 20% ethanol and 80% water, pH 3.59 μ = 1.0(KCl). The kinetic data were obtained as above at 60 ± 0.3 °C. Kinetic data were also obtained in 80% ethanol and 20% water in 1.0 M formate at pH 3.60 and 4.92 (pH was adjusted by adding a suitable amount of concentrated NaOH or HCl and measured before and after the reaction) at the same temperature. The ionic strength in 80% ethanol-20%water was not corrected. The rate of formation and hydrolysis of formanilide was also obtained at 60 °C in 1.0 M aqueous formate buffer pH 3.60, μ = 1.0 (KCl).

I. Determination of pK_a.

The pK_as of aniline and formic acid were determined by titration at 24 ± 1 °C. For each determination, 0.048-0.051 mmol of aniline or formic acid was used in a 5 mL solution. In the case of aniline enough HCl was added to convert all of it to anilinium ion. The pH was measured using a Radiometer Vit 90 video titrator equipped with a GK2321C combination electrode and interfaced with an IBM pc. The pH was recorded as a function of added 0.0105 M NaOH, which was delivered by a Radiometer ABU 91 auto-burette. The ionic strength of all the solutions was maintained at 1.0 using KCl. Data were analyzed by a computer version of Simms method.[47] The pK_a values reported are an average of three determinations.

CHAPTER 3: RESULTS

A. Rate and equilibrium constants of formanilide formation and hydrolysis at 98 °C.

The pseudo-first order rate constants rate constants, k_{obs}, for the attainment of equilibrium of the formation of formanilide were obtained starting with (5.0-5.3) x 10^{-3} M aniline in formate buffer at various pH and $[formate]_{total}$ at 98 ± 2 °C, μ = 1.0 (KCl). The runs were followed by HPLC. For each run, k_{obs} for appearance of formanilide and the disappearance of aniline were obtained and are given in Appendix 1, Table 1S (various pH) and Table 2S (various [formate]). The conditional equilibrium constant K', defined as the ratio of concentration of formanilide to aniline at equilibrium (eq 15), was obtained directly by HPLC analysis of the products of reaction, and is also given for each run in the aforementioned tables. As described in the experimental section, the response factors under the experimental conditions in the HPLC analysis for formanilide and aniline were determined using a 1:1 mixture of known concentrations of formanilide and aniline.

$$K' = [formanilide]^{eq}_{total} / [aniline]^{eq}_{total} \qquad (15)$$

Similarly, k_{obs} and K' were obtained from the hydrolysis direction starting with (5.0-5.3) x 10^{-3} M formanilide under identical conditions to those described above. Here, the rate constants were obtained for the appearance of aniline and the disappearance of formanilide, and are also given in Table 1S and Table 2S. The data in Table 1S show that at low formate concentrations buffer catalysis is small and log k_{obs} is linear with pH over the investigated range of 3.18 to 4.17. It can also be seen from the data in Table 1S that the value of K' attains a maximum value at about pH 3.60 and then drops at higher and lower pH.

Under pseudo-first order conditions where the total concentration of formate is much higher than the concentration of aniline or anilide, k_{obs} can be written as the sum of the pseudo-first order rate constants, k_r and k_f, (eq 16) for the hydrolysis and formation of anilides as shown in Scheme 11, and K' can expressed as eq 17.

$$k_{obs} = k_f + k_r \qquad (16)$$

$$K' = k_f/k_r \qquad (17)$$

Scheme 11

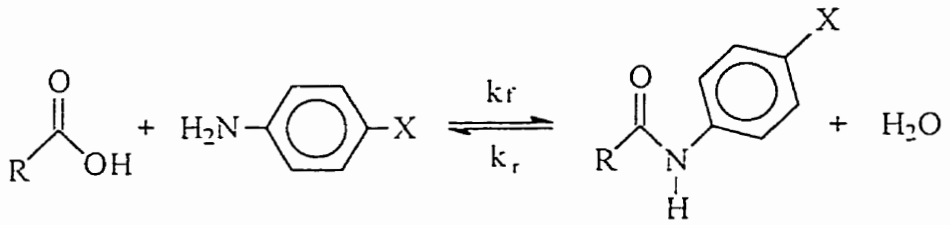

R = H, CH_3 X = H, NO_2, OCH_3

The k_r and k_f values were calculated from k_{obs} and K' using eq 16 and 17, and are listed in Table 1. A corrected equilibrium constant K'_{eq} has also been included in Table 1 which is based on the concentration of non-ionized aniline and formic acid (according to Scheme 12) with the concentration of water being treated as unity, eq 18.[11] The changes in pK_as due to change in temperature and ionic strength have been considered in calculating the concentration of non-ionized species (*vide supra*). After such correction, under the experimental conditions the average K'_{eq} is 12.6 M^{-1}, while K' (defined in eq 17) is 0.2 -2.6 depending on the conditions and $[formate]_{total}$.

$$K'_{eq} = \frac{[formanilide]}{[aniline]\ [formic\ acid]} \qquad (18)$$

Table 1. The pseudo-first order rate constants[a] for formation (k_f) and hydrolysis (k_r) of formanilide at 98 ± 2 °C and the equilibrium constants[b] (K'_{eq}) obtained by HPLC at various pH and buffer concentration in aqueous formate buffer.

pH	[formate]$^{c}_{total}$ (M)	k_r (s^{-1})	k_f (s^{-1})	K'_{eq} (M^{-1})
4.17 ± 0.03	0.10	$(1.22\pm 0.03)*10^{-5}$	$(0.23\pm 0.01)*10^{-5}$	12.3 ± 0.2
3.60 ± 0.03	0.10	$(4.15\pm 0.02)*10^{-5}$	$(1.13\pm 0.04)*10^{-5}$	13.1 ± 0.6
3.18 ± 0.03	0.10	$(1.29\pm 0.06)*10^{-4}$	$(2.56\pm 0.11)*10^{-5}$	12.9 ± 0.2
3.57 ± 0.03	0.50	$(9.72\pm 0.30)*10^{-5}$	$(1.20\pm 0.01)*10^{-4}$	11.9 ± 0.4
3.57 ± 0.03	1.00	$(1.27\pm 0.04)*10^{-4}$	$(3.36\pm 0.08)*10^{-4}$	12.7 ± 0.2

[a]Calculated from the pseudo-first order rate constants (k_{obs}) for establishment of equilibrium, using $k_{obs} = k_r + k_f$ and $K' = k_f/k_r$. Errors are deviation from the mean for duplicate values and standard deviations for triplicate values.

[b]Calculated using the non-ionized of concentrations at equilibrium (eq 18), taking concentration of water as unity and accounting for changes in the pK_as due to temperature and ionic strength variations.

[c]μ=1.0 (KCl).

Scheme 12

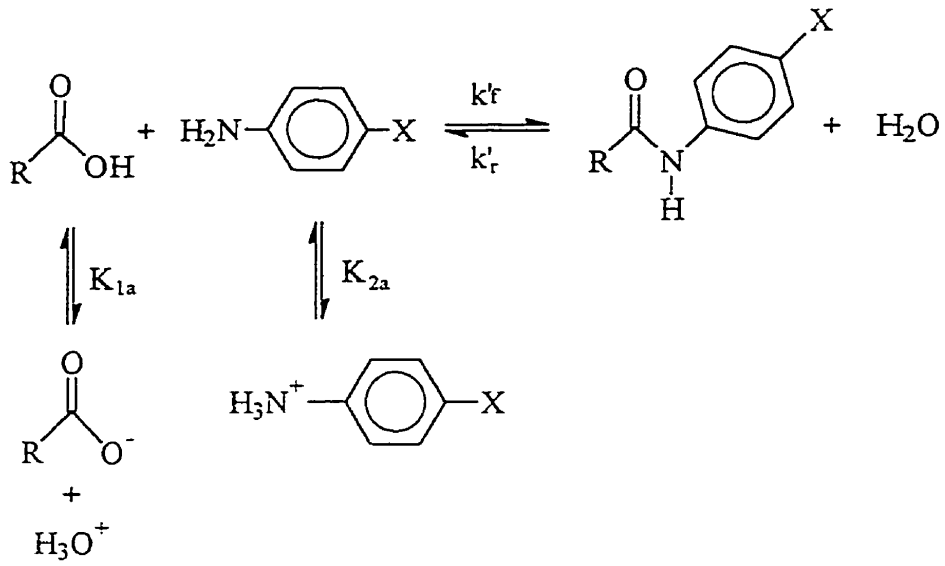

To obtain the rate constants for buffer catalysis of the hydrolysis and the formation of formanilide, k_r and k_f were plotted against $[formate]_{total}$ at a constant pH (3.60). The k_r values plotted in Figure 3 are fit to a linear equation (eq 19),

$$k_r = k_{0r} + k_{1r}\,[HCOOH]_{total} \qquad (19)$$

where k_{0r}, the intercept, is the rate constant for the hydrolysis at pH 3.60 without buffer catalysis. The k_{0r} represents the combination of acid catalysed hydrolysis, $k_{(H_3O^+)}$ and water catalysed hydrolysis, $k_{(H_2O)}$ (if any), $k_{0r} = k_{(H_3O^+)}[H_3O^+] + k_{(H_2O)}$. The second order rate constant for formic acid catalyzed formanilide hydrolysis (k_{1r}) can be obtained from the slope of the line.

The k_f values were fit to a non-linear equation (eq 20), Figure 3.

$$k_f = k_{1f}[HCOOH]_{total} + k_{2f}[HCOOH]^2_{total} \qquad (20)$$

The rate constant k_{1f} is the second order rate constant of formation of formanilide at a given pH (here 3.6) where one molecule of both formic acid and aniline are involved. For

Figure 3. The pseudo first order rate constants of formation (k_f) and hydrolysis (k_r) of formanilide vs $[formate]_{total}$ at 98 ± 2 °C (pH = 3.60 and μ=1.0 (KCl)). The lines were obtained from the fits to eq 19 and 20.

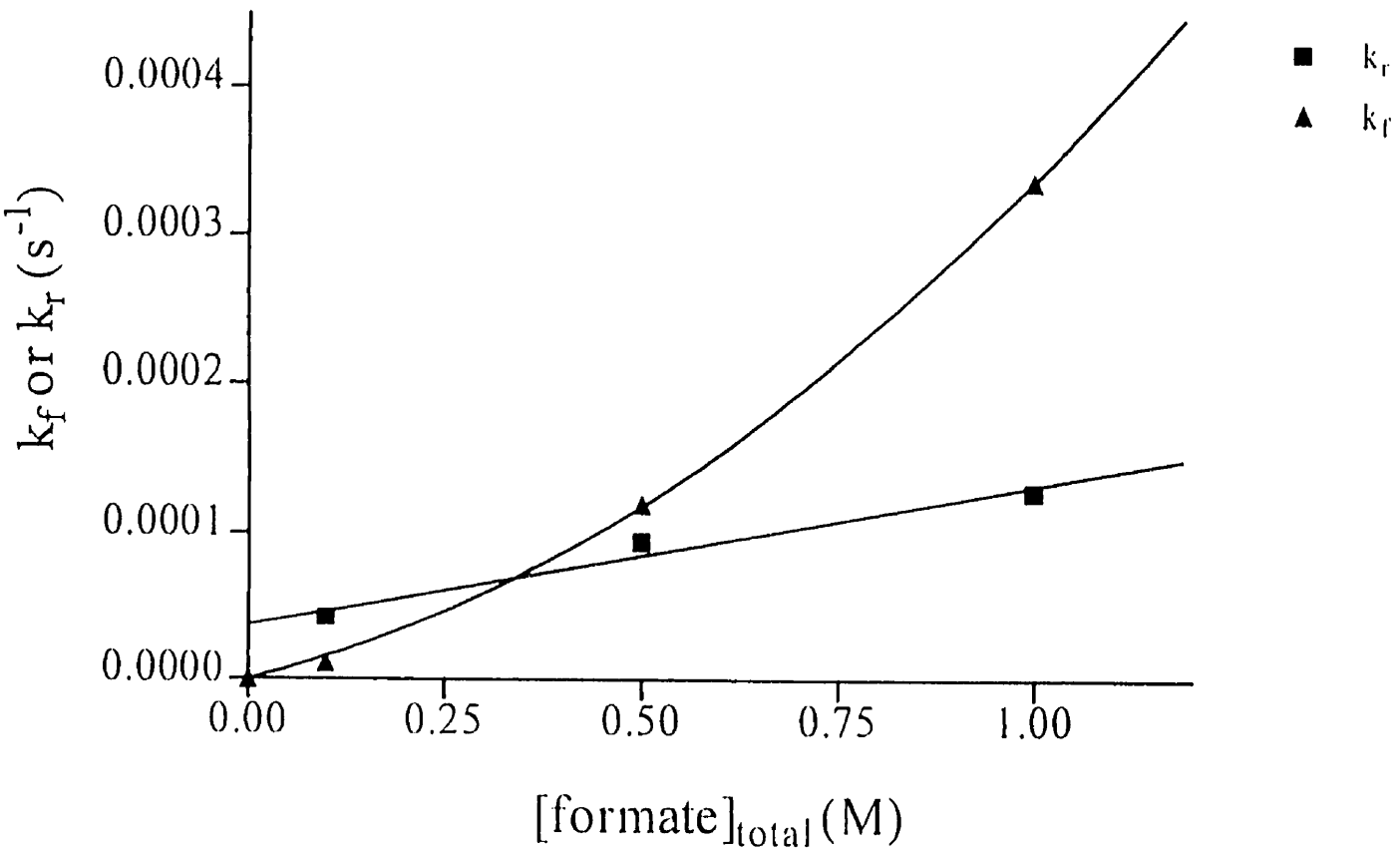

k_{2f} two molecules of formic acid/formate and one molecule of aniline are involved. The second molecule of formic acid acts as the catalyst so overall k_{2f} is a third order rate constant. The values of k_{0r}, k_{1r}, k_{1f} and k_{2f} are given in Table 2.

B. Rate and equilibrium constants of acetanilide formation and hydrolysis at 98 °C.

The pseudo-first order rate constants (k_{obs}) for establishment of equilibrium during formation and hydrolysis of acetanilide at various pH values in the presence of 1.0 M acetate and 98 ± 2 °C are given in Appendix 1, Table 3S. These data were obtained using HPLC. The k_r and the k_f values have been calculated from k_{obs} using eq 16 and 17, and are provided in Table 3. Based on the concentration of non-ionized forms of acetic acid and aniline a corrected equilibrium constant K'_{eq} has also been included in the table. At lower pH (1.95) k_r is about 17 times larger than k_f, but k_f is slightly higher than k_r at pH 3.75 and 1.0 M acetate. The average K'_{eq} for acetanilide is 3.4 M^{-1}.

Under the same conditions of temperature, pH, and $[RCOOH]_{total}$ as described for formanilide, k_{obs} for acetanilide is 240 times lower at pH 3.75 than that of formanilide at pH 3.60. However, K'_{eq} under the same conditions is only 3.7 times smaller than that of formanilide. Thus the effect on the equilibrium position due to the acyl group is small but the effect on the rate for establishing equilibrium is larger.

Table 2. Pseudo-first order rate constants for the acid catalysed hydrolysis. k_{0r} (s^{-1})[a] of formanilide at a given pH or pD. second order rate constants. k_{1r} (M^{-1} s^{-1})[a] of formate (buffer) catalysis on hydrolysis. second and third order rate constants. k_{1f} (M^{-1} s^{-1})[a] and k_{2f} (M^{-2} s^{-1})[a] of formate (buffer) catalysis on formation of formanilide from aniline and formic acid at various temperatures and pH or pD.

Temp. °C	pH or pD	$k_{0r} \times 10^5$ (s^{-1})	$k_{1r} \times 10^6$ (M^{-1} s^{-1})	$k_{1f} \times 10^5$ (M^{-1} s^{-1})	$k_{2f} \times 10^5$ (M^{-2} s^{-1})
79± 1	2.80	7.02± 0.21	8.50± 3.50[b]	7.84± 0.09	1.45± 0.11
79± 1	3.20	3.24± 0.01	8.45± 0.01	6.24± 0.05	1.95± 0.06
79± 1	3.60	1.35± 0.01	8.01± 0.14	4.45± 0.14	1.47± 0.15
79± 1	4.00	0.54± 0.01	5.19± 0.13	2.02± 0.08	0.93± 0.08
79± 1	3.60[c, d]	1.38± 0.08	8.31± 1.10	3.04± 0.10	0.91± 0.10
79± 1	2.00[d]	43.8± 0.01	-	-	-
79± 1	1.96[c]	53.2± 0.01	-	-	-
98± 2	3.60	3.72± 0.56	95.0± 18.0	13.7± 0.10	19.9± 0.20

[a]The errors calculated from the standard deviation of the fit of k_r vs $[formate]_{total}$ and k_f vs $[formate]_{total}$ to eq 19 and 20. respectively at the given pH or pD.

[b]At this pH the acid catalyzed hydrolysis. k_{0r} is much higher than the buffer catalyzed hydrolysis. k_{1r} (less than 11% at highest buffer concentration).

[c]pD

[d]HCl or DCl was used as buffer; no formate added, μ = 1.0 (KCl).

Table 3. The pseudo-first order rate constants[a] for formation (k_f) and hydrolysis (k_r) of acetanilide at 98 ± 2 °C and the equilibrium constants[b] (K'_{eq}) at various pH values in aqueous HCl or acetate buffer.

pH	Buffer	k_r (s^{-1})	k_f (s^{-1})	K'_{eq} (M^{-1})
1.95 ± 0.05	HCl[c, e]	$(3.47\pm 0.04)*10^{-5}$	$(0.19\pm 0.02)*10^{-5}$	3.6 ± 0.3
3.75 ± 0.05	Acetate[d, e]	$(0.81\pm 0.02)*10^{-6}$	$(1.07\pm 0.02)*10^{-6}$	3.2 ± 0.3

[a]Calculated from the pseudo-first order rate constants (k_{obs}) for establishment of equilibrium, using $k_{obs} = k_r + k_f$ and $K' = k_f/k_r$. Errors are deviation from the mean for duplicate values and standard deviations for triplicate values.

[b]Calculated using the non-ionized concentrations at equilibrium, taking concentration of water as unity and accounting for changes in the pK_as due to temperature and ionic strength variations.

[c]1.0 M acetate added.

[d]$[buffer]_{total}$ = 1.0 M

[e]μ=1.0 (KCl).

C. Rate and equilibrium constants of formanilide formation and hydrolysis at 79 ±1 °C.

The k_{obs} values for formation and hydrolysis of formanilide at 79 ± 1 °C were obtained using UV-vis spectrophotometry, starting with either aniline or formanilide in formate buffer at a given pH. The initial concentration of aniline or formanilide was (8.3-8.6) x 10^{-5} M. Here the conditional equilibrium constants, K', have been calculated from the ratio of change in absorbance for formation (ΔA_f) and change in absorbance for hydrolysis (ΔA_r) under identical conditions, see Figure 2. Data were obtained at four different pHs ranging from 2.8-4.0 with at least three different concentrations of formate buffer used at each pH. The k_{obs} and the K' values are given in Appendix 1, Table 4S-7S. Similar experiments for formation and hydrolysis of formanilide were studied at the same temperature in D_2O at pD = 3.60 with varying concentrations of formate buffer (0.001-1.0 M). The k_{obs} and K' values are reported in Appendix 1, Table 8S. The values of k_r and k_f were calculated using eq 16 and 17, as described above and are reported in Table 4. The equilibrium constant K'_{eq}, calculated as described before has also been included in the table. The average value of K'_{eq} is 20.0 M^{-1}. The values of k_{0r}, k_{1r}, k_{1f} and k_{2f} are given in Table 2. As expected the k_{obs} at 80 °C is smaller than the k_{obs} at 100 °C. However, there is little effect on K' of the temperature change when $[formate]_{total}$ is the same (e.g. at pH 3.6 and 1 M $[formate]_{total}$, K' is 2.77 at 80 °C and 2.66 at 100 °C, also see Table 2S and 6S). As seen in Tables 4S to 7S both the k_{obs} and the extent of formation of formanilide (K') increases with increasing concentration of formate at each pH. Under comparable conditions there is very little (or no) solvent kinetic isotope effect (SKIE) on

Table 4. The pseudo-first order rate constants[a] for formation (k_f) and hydrolysis (k_r) of formanilide at 79 ± 1 °C and the equilibrium constants[b] (K'_{eq}) at various pH or pD and at various buffer concentration in aqueous formate buffer.

pH or pD	[formate]$^{d}_{total}$ (M)	k_r (s^{-1})	k_f (s^{-1})	K'_{eq}(M^{-1})
2.80± 0.03	0.10	(7.02± 0.05)*10^{-5}	(0.77± 0.01)*10^{-5}	20.6
2.79± 0.03	0.50	(7.60± 0.10)*10^{-5}	(4.29± 0.05)*10^{-5}	22.7
2.81± 0.03	0.90	(7.69± 0.02)*10^{-5}	(8.22± 0.02)*10^{-5}	20.7
3.18± 0.03	0.10	(3.32± 0.05)*10^{-5}	(0.66± 0.02)*10^{-5}	19.1
3.20± 0.03	0.50	(3.66± 0.05)*10^{-5}	(3.60± 0.05)*10^{-5}	18.2
3.20± 0.03	1.00	(4.09± 0.03)*10^{-5}	(8.20± 0.02)*10^{-5}	18.6
3.56± 0.03	0.001	(1.36± 0.02)*10^{-5}	-	-
3.60± 0.03	0.10	(1.42± 0.02)*10^{-5}	(0.42± 0.01)*10^{-5}	20.4
3.61± 0.03	0.50	(1.76± 0.03)*10^{-5}	(2.64± 0.02)*10^{-5}	20.9
3.59± 0.03	1.00	(2.15± 0.03)*10^{-5}	(5.97± 0.04)*10^{-5}	19.5
4.01± 0.03	0.10	(5.93± 0.02)*10^{-6}	(1.83± 0.01)*10^{-6}	20.9
4.02± 0.03	0.50	(7.90± 0.01)*10^{-6}	(1.25± 0.01)*10^{-5}	21.7
4.03± 0.03	1.00	(1.06± 0.01)*10^{-5}	(2.94± 0.01)*10^{-5}	19.0
3.60± 0.03[c]	0.001	(1.34± 0.03)*10^{-5}	-	-
3.58± 0.03[c]	0.50	(1.93± 0.09)*10^{-5}	(1.77± 0.10)*10^{-5}	22.3
3.61± 0.03[c]	0.75	(2.01± 0.12)*10^{-5}	(2.76± 0.30)*10^{-5}	21.9
3.60± 0.03[c]	1.00	(2.18± 0.03)*10^{-5}	(3.96± 0.06)*10^{-5}	21.6

[a]Calculated from the pseudo-first order rate constants (k_{obs}) for establishment of equilibrium, using $k_{obs} = k_r + k_f$ and $K' = k_f/k_r$. Errors are deviation from the mean for duplicate values and standard deviations for triplicate values.

[b]Calculated using the non-ionized concentrations at equilibrium and taking concentration of water as unity. Changes in the pK_as due to temperature, ionic strength and solvent isotope effects have been considered.

[c]pD

[d]μ=1.0 (KCl).

k_{obs}. Although the apparent equilibrium constant K' appeared to be smaller in D_2O than that in H_2O under comparable conditions, the K'_{eq}, after correcting for the changes in pK_a due to the D_2O medium was the same as in H_2O.

The buffer catalyses on k_r and k_f for each pH have been obtained using eq 19 and 20 and the trends can be seen from the plots in Figure 4 (k_r) and Figure 5 (k_f). The computed rate constants k_{0r}, k_{1r}, k_{1f} and k_{2f} are given in Table 2. It is observed that the hydrolysis at zero formate buffer, k_{0r}, increases linearly with increasing concentration of H_3O^+, the slope of a log k_{0r} vs pH plot being -1 (Figure 6) as expected for a specific acid catalyzed hydrolysis. The k_{0r} points obtained with HCl (hydrolysis only) also fall on this line. Hence, under these experimental conditions there is no significant water catalyzed hydrolysis. Buffer catalysis increases with decreasing pH until pH 3.6, which is the pK_a of formic acid. Below pH 3.6 rate constant for buffer catalysis attains a saturation value, remaining constant despite further lowering of the pH. This signifies that either the undissociated acid, or a hydronium ion and a formate ion, are the catalytic species. However, these two processes are kinetically indistinguishable (see the discussion for possible mechanisms). It should be noted that $k_{1r} = k_{HA}\,\alpha$, where k_{HA} is the maximal rate constant for formic acid catalysis and α is the fraction of undissociated acid. A plot of k_{1r} vs α should be linear. However, when plotted, the data in Table 2 showed deviation from linearity at lower pH, probably because the error in the buffer catalysis at these pHs is large since less than 10% of the total reaction is buffer catalyzed at lower pHs (also see footnote in Table 2). No significant SKIE was observed for acid catalysed hydrolysis, k_{0r}, of formanilide, when the data were compared at pH/pD 3.60 and 2.0. The SKIE on buffer catalysis for hydrolysis at pH/pD 3.6, ($k_{1r}^{H2O}/k_{1r}^{D2O}$), is 0.96±0.13, while the SKIE for

Figure 4. The plot of k_r vs $[\text{formate}]_{total}$ at various pHs, μ = 1.0 (KCl), T = 79 ± 1 °C. The lines were obtained from the fit to eq 19.

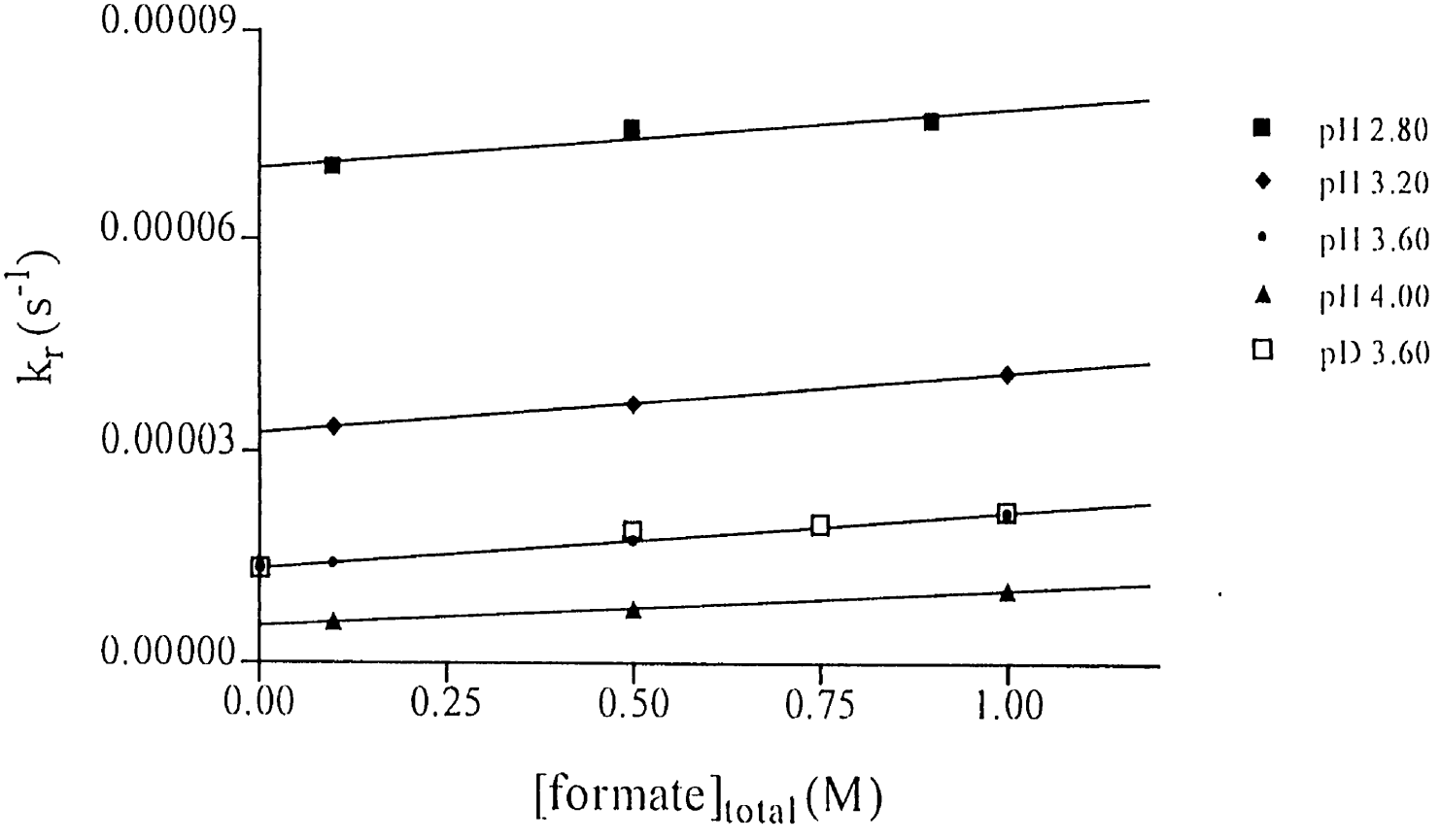

Figure 5. The plot of k_f vs $[formate]_{total}$ at various pHs, μ = 1.0 (KCl), T = 79 ± 1 °C. The lines were obtained from NLLSQ fit to eq 20.

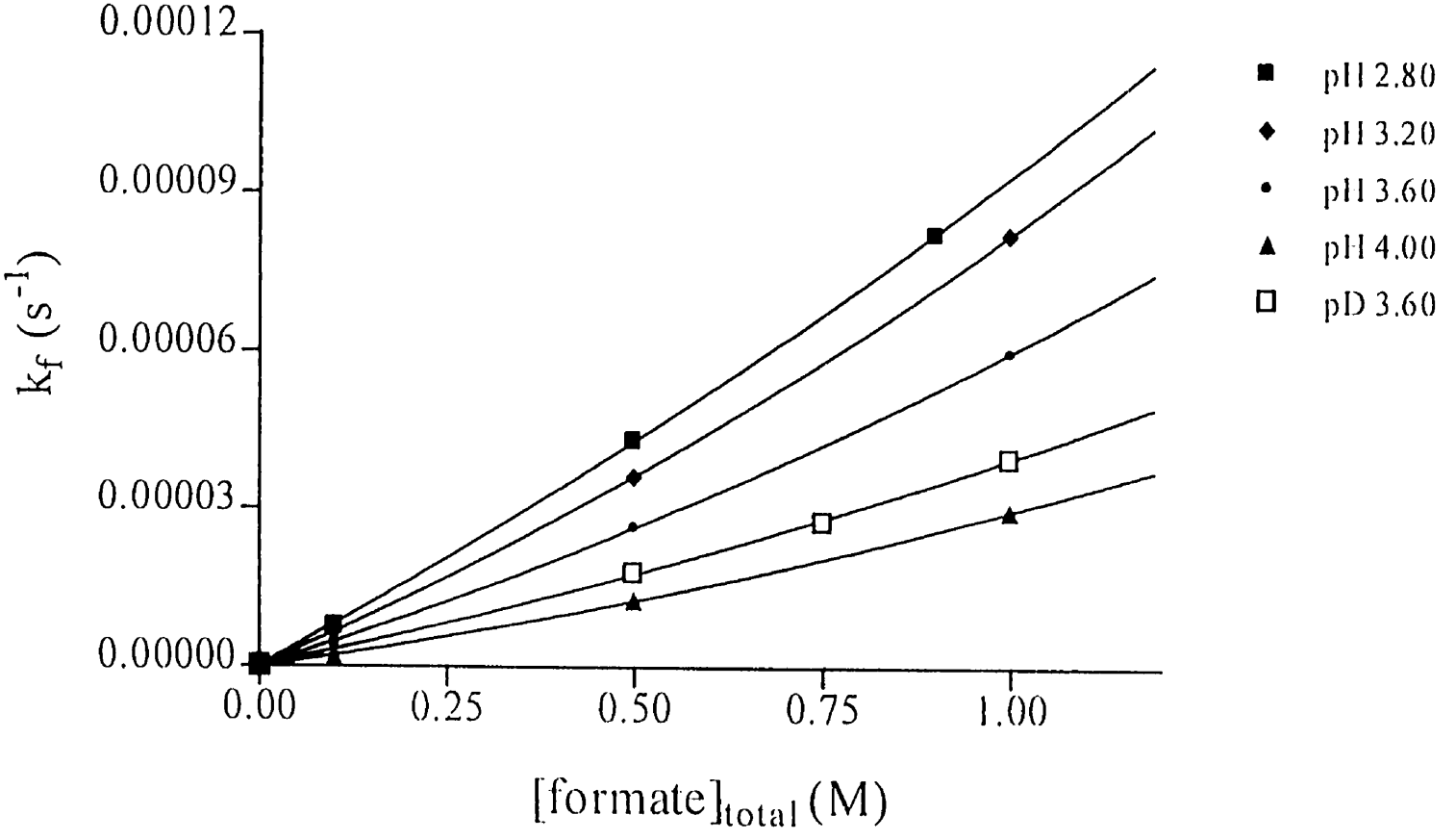

Figure 6. The log of pseudo-first order rate constants of acid catalysed hydrolysis (k_{0r}) of formanilide vs pH at 79 ± 1 °C.

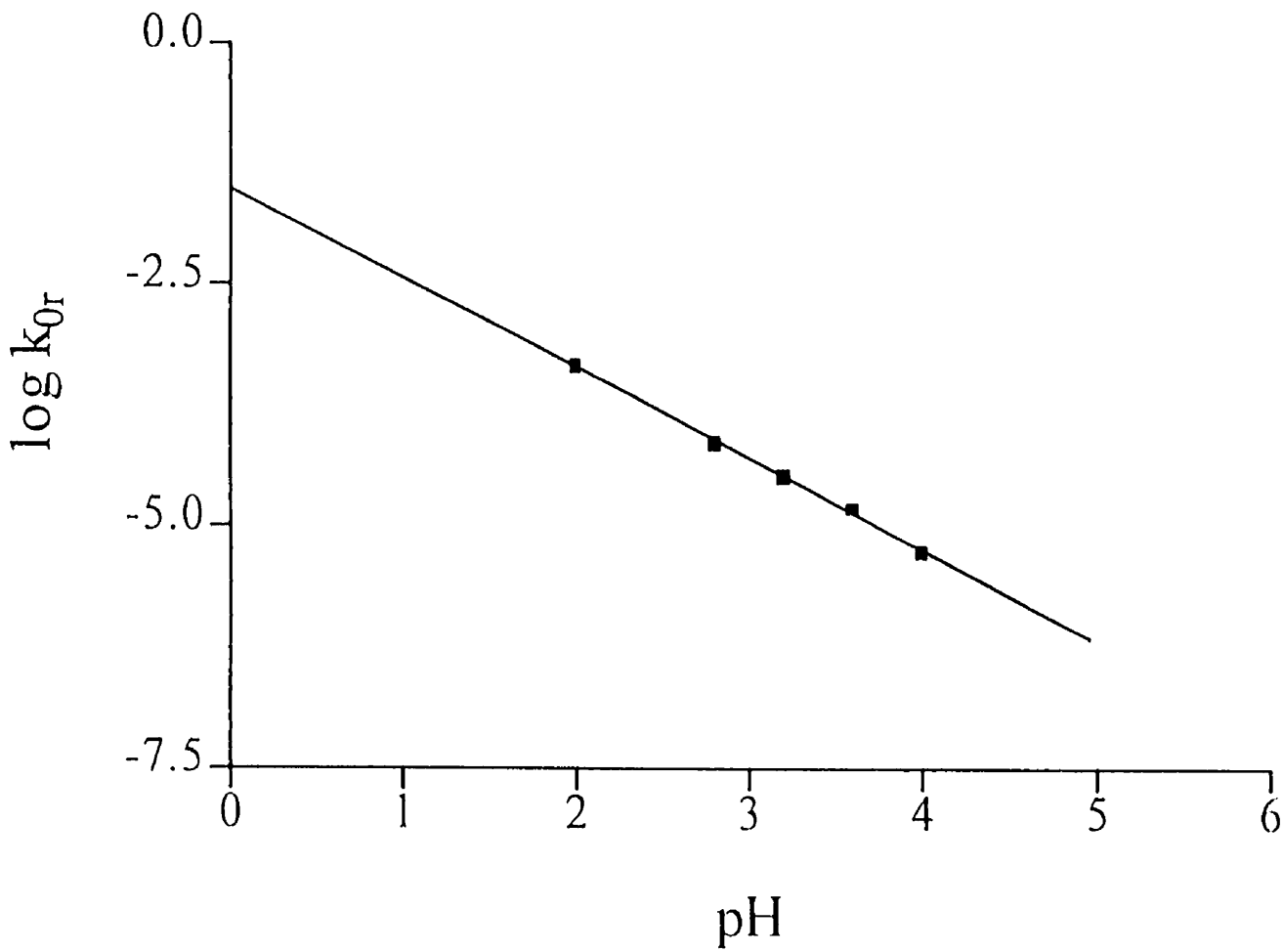

formation are ($k_{1f}^{H2O}/k_{1f}^{D2O}$) = 1.46±0.10, and ($k_{2f}^{H2O}/k_{2f}^{D2O}$) = 1.61±0.31. The k_{0r} and k_{2f} values each increased by factor of three for formanilide when the temperature was raised from 80 °C to 100 °C with all the other conditions remaining the same. The effect of this temperature change on each of k_{1r} and k_{2f} was one order of magnitude.

D. Rate and equilibrium constants of *p*-nitroformanilide formation and hydrolysis.

The kinetics of formation and hydrolysis of *p*-nitroformanilide were obtained at three different pHs ranging from 2.8-3.6 in formate buffer, μ = 1.0 (KCl). The starting concentration of *p*-NO_2-aniline or anilide was (1.84-1.86) x 10^{-4} M. To determine the buffer catalysis, the concentration of formate/formic acid was varied from 0.10 M to 1.0 M at pH 3.20. The k_{obs} and K' are reported in Appendix 1, Table 9S. The overall k_{obs} for *p*-nitroformanilide is larger than that of formanilide at all comparable pH and buffer concentrations, however, the K' values at a given [formate] are considerably smaller. The k_r, k_f and K'_{eq} values are given in Table 5. One notes that the k_r values for *p*-nitroformanilide are larger than those for formanilide, as *p*-nitroaniline is a stronger electron attractor than aniline. This will encourage more rapid nucleophilic attack on the carbonyl carbon of *p*-nitroformanilide compared to formanilide. On the other hand, k_f is lower because *p*-nitroaniline is the weaker of the two nucleophiles. Accordingly, the average K'_{eq} for *p*-nitroformanilide is 0.27 M^{-1}, which is 75 times smaller than the K'_{eq} for formanilide. To obtain the values of k_{0r}, k_{1r}, k_{1f} and k_{2f}, the k_r and k_f were plotted against total buffer concentration (see Figure 7), and the best fit values for the former constants (from eq 19 and 20) are given in Table 6. Both k_{0r} and k_{1r} are three-fold larger for *p*-nitroformanilide than formanilide at pH 3.20. However, under the same conditions, the

k_{1f} and k_{2f} are 3 times and 14 times smaller respectively. It is noted that the value of k_{2f} is very small compared to k_{1f}; hence the plot of k_f vs $[formate]_{total}$ is almost linear (Figure 7), suggesting that there is very little buffer catalysis on formation of *p*-nitroformanilide from formic acid and *p*-nitroaniline.

E. Rate and equilibrium constants of *p*-methoxyformanilide formation and hydrolysis.

Starting with a (1.14-1.15) x 10^{-4} M solution of *p*-methoxyformanilide or *p*-methoxyaniline, the kinetics for hydrolysis and formation were obtained at pH 2.8 and 3.2 in 1.0 M formate buffer, μ = 1.0 (KCl). The k_{obs} and K' values are reported in Appendix 1, Table 10S. The k_{obs} values are less than those for both *p*-nitroformanilide and formanilide, while the K' value is higher than that of *p*-nitroformanilide and slightly lower than that of formanilide under comparable conditions. The k_r, k_f and K'_{eq} are given in Table 7. The k_r values are lower for *p*- methoxyformanilide than those of both *p*-nitroformanilide and formanilide at both pHs. However, k_f is larger at pH 3.20 but smaller at pH 2.80 than the respective values for *p*-nitroformanilide. At both pHs, k_f is smaller than those obtained for formanilide. The average K'_{eq} is 39.9 M^{-1}, which is twice as large as that for formanilide and 146 times larger than the K'_{eq} of *p*-nitroformanilide.

Table 5. The pseudo-first order rate constants[a] for formation (k_f) and hydrolysis (k_r) of *p*-nitroformanilide at 79 ± 1 °C and the equilibrium constants[b] (K'_{eq}) at various pH and [buffer] in aqueous formate buffer.

pH	[formate]$^{c}_{total}$ (M)	k_r (s^{-1})	k_f (s^{-1})	K'_{eq}(M^{-1})
2.80± 0.03	1.00	(2.33± 0.05)*10^{-4}	(5.34± 0.04)*10^{-5}	0.26
3.18± 0.03	0.10	(9.86± 0.02)*10^{-5}	(2.16 ±0.20)*10^{-6}	0.29
3.20± 0.03	0.50	(1.12± 0.03)*10^{-4}	(1.17± 0.05)*10^{-5}	0.27
3.20± 0.03	1.00	(1.28± 0.03)*10^{-4}	(2.40± 0.06)*10^{-5}	0.26
3.60± 0.03	1.00	(7.22± 0.07)*10^{-5}	(9.33 ±0.60)*10^{-6}	0.25

[a]Calculated from the pseudo-first order rate constants (k_{obs}) for establishment of equilibrium, using $k_{obs} = k_r + k_f$ and $K' = k_f/k_r$. Errors are deviation from the mean for duplicate values and standard deviations for triplicate values.

[b]Calculated using the non-ionized of concentrations at equilibrium and taking concentration of water as unity. Changes in the pK_as due to temperature have been considered. For formic acid, the change in pK_a due to ionic strength variation has also been considered. However, the effect of ionic strength on the pK_a of *p*-nitroanilinium ion was not considered since at these pHs, a change of ± 0.35 in pK_a unit will have less than 2% effect on the K'_{eq}.

[c]μ=1.0 (KCl).

Figure 7. The pseudo-first order rate constants of formation (k_f) and hydrolysis (k_r) of *p*-nitroformanilide vs $[formate]_{total}$ at 79 ± 1 °C, pH = 3.20 and μ=1.0 (KCl). The lines were obtained from fits of the data to eq 19 and 20.

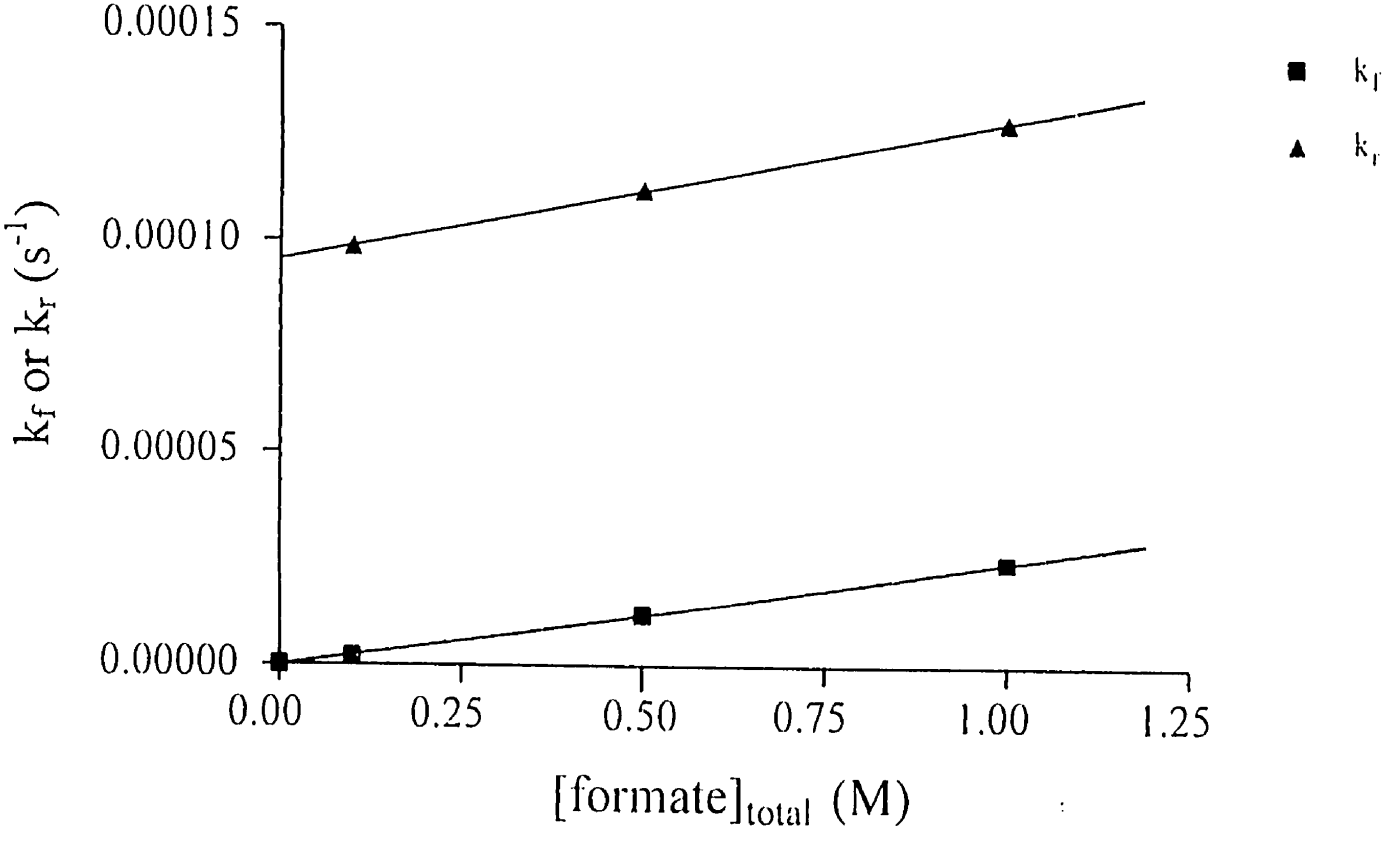

Table 6. Rate constants[a] for the acid catalysed hydrolysis and formate (buffer) catalysis of hydolysis and formation of *p*-nitroformanilide at a given pH[b] and at 79 ± 1 °C.

k_{0r} (s^{-1})[c]	k_{1r} (M^{-1} s^{-1})[d]	k_{1f} (M^{-1} s^{-1})[e]	k_{2f} (M^{-2} s^{-1})[f]
$(9.54\pm 0.02)\times10^{-5}$	$(3.26\pm 0.04)\times10^{-5}$	$(2.26\pm 0.03)\times10^{-5}$	$(1.39\pm 0.36)\times10^{-6}$

[a]The errors calculated from the standard deviation of the fit of k_r vs $[formate]_{total}$ and k_f vs $[formate]_{total}$ to eq 19 and 20 respectively at the given pH.

[b]at pH 3.20

[c]k_{0r}. pseudo-first order rate constant for the acid catalysed hydrolysis.

[d]k_{1r} second order rate constant for hydrolysis.

[e]k_{1f} second order rate constant for formation.

[f]k_{2f} third order rate constant for formation. The value of k_{2f} is very small compared to k_{1f} giving rise to almost linear fit of k_f vs $[formate]_{total}$ plot (see text).

Table 7. The pseudo-first order rate constants[a] for formation (k_f) and hydrolysis (k_r) of *p*-methoxyformanilide at 79 ± 1 °C and the equilibrium constants[b] (K'_{eq}) at pH 2.80 and 3.20 in aqueous formate buffer.

pH[c]	k_r (s^{-1})	k_f (s^{-1})	K'_{eq} (M^{-1})
2.82± 0.03	(4.08± 0.05)x10^{-5}	(4.01± 0.04)x10^{-5}	41.0
3.18± 0.03	(2.13± 0.03)x10^{-5}	(4.11± 0.06)x10^{-5}	38.9

[a]Calculated from the pseudo-first order rate constants (k_{obs}) for establishment of equilibrium, using $k_{obs} = k_r + k_f$ and $K' = k_f/k_r$. Errors are deviation from the mean for duplicate values and standard deviations for triplicate values.

[b]Calculated using the non-ionized of concentrations at equilibrium and taking concentration of water as unity and accounting for changes in the pK_as due to temperature and ionic strength.

[c]$[buffer]_{total}$ = 1.0, μ=1.0 (KCl).

F. Phosphate catalyzed formation and hydrolysis of formanilide.

Formation and hydrolysis of formanilide was followed at 79 ± 1 °C in 1.0 M formate buffer at pH 3.20 and 3.60 with added KH_2PO_4 (0.1-0.5 M). At these pH values KH_2PO_4 exists mostly as the monoanionic species. In all cases, the total ionic strength was kept constant by the addition of KCl. The k_{obs} and K' are reported in Appendix 1, Table 11S. Although k_{obs} increases with increasing KH_2PO_4 concentration, the value of K' remains unchanged. The values of k_f and k_r are plotted against the concentration of KH_2PO_4 to obtain a straight line, Figure 8, the slope of which represents the second order rate constant for phosphate catalysis $k_r^{phos.}$ on hydrolysis and $k_f^{phos.}$ on formation. The values of k_f, k_r, $k^r_{phos.}$, k^f_{phos} and K'_{eq} are given in Table 8. The values of both k_f and k_r increased with increasing phosphate concentrations at both pHs.

G. Formation and hydrolysis of formanilide in aqueous ethanol.

A 1 M formate buffer solution was made in 20% aqueous ethanol, pH 3.59 and μ =1.0 (KCl). The rate constants for formation and hydrolysis of formanilide were obtained using this ethanolic buffer at 60.0 ± 0.3 °C. Data were also obtained in 1 M formate buffer in 80% ethanol-water of measured pH 3.60 and 4.92, μ uncontrolled. Formation and hydrolysis were also performed in 100% aqueous buffer, pH = 3.60, [formate] = 1.0 M, μ = 1.0 (KCl) at this temperature. The k_{obs} and K' are reported in Appendix 1, Table 12S. Under comparable conditions both k_{obs} and K' increase with increasing percentage of ethanol in the solution, at 80% ethanol the increment being about 3.5 times compared to the aqueous values. The values of k_f, k_r and K'_{eq} are given in Table 9.

Figure 8. Effect of added phosphate on hydrolysis (k_r) and formation (k_f) of formanilide.

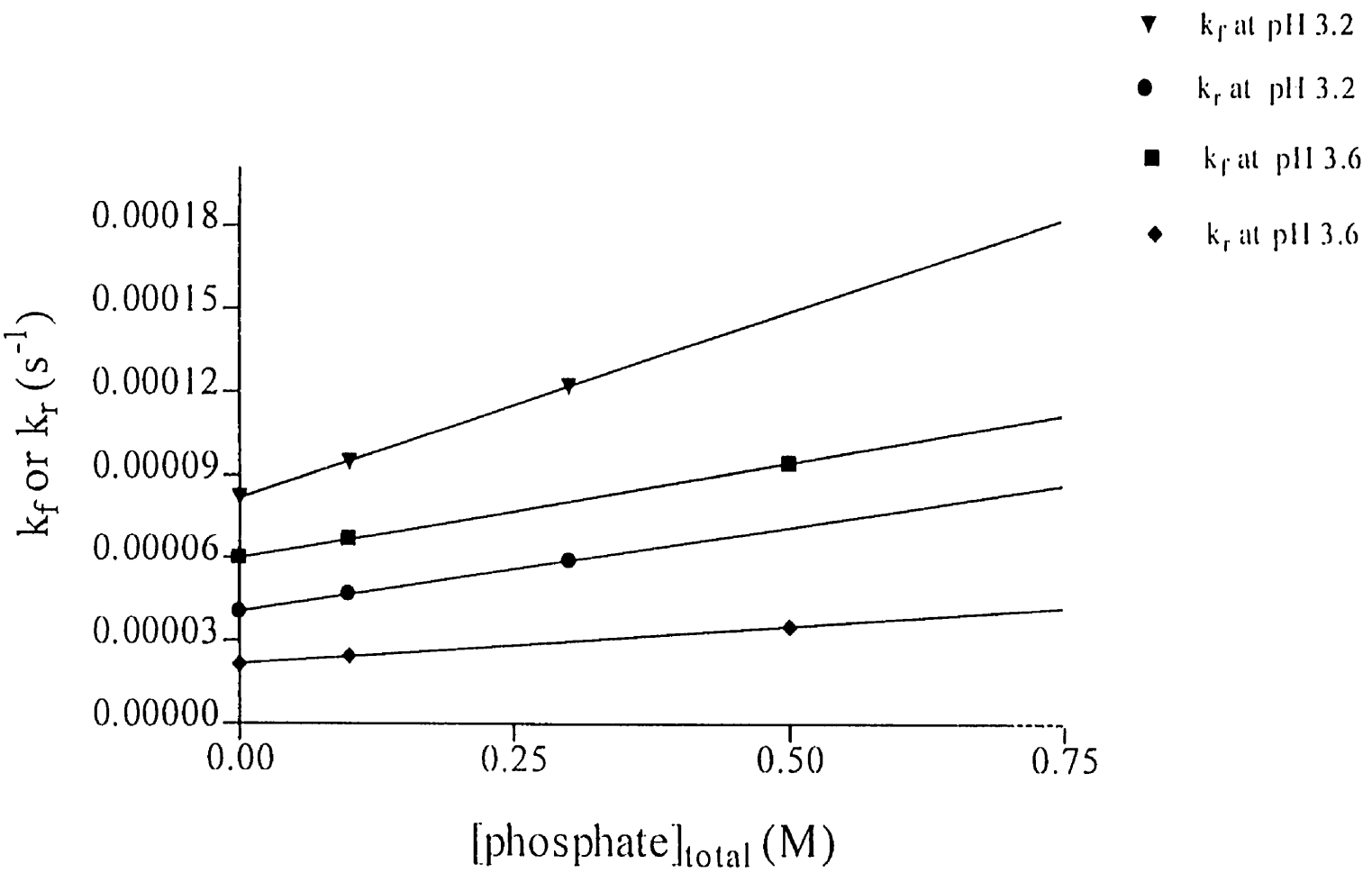

Table 8. The pseudo-first order rate constants of formation (k_f) and hydrolysis (k_r) of formanilide and the equilibrium constants (K'_{eq}) in the presence of phosphate at 79 ± 1 °C in aqueous formate buffer and the second order rate constant for phosphate catalysis on hydrolysis ($k_r^{phos.}$)[b] and formation(k_f^{phos})[b].

pH[a]	$[phos.]_{total}$ (M)	$k_r \times 10^5$ (s^{-1})	$k_f \times 10^5$ (s^{-1})	K'_{eq} (M^{-1})	$k_r^{phos} \times 10^5$ (M^{-1} s^{-1})	$k_f^{phos} \times 10^5$ (M^{-1} s^{-1})
3.21	0.10	(4.66±0.02)	(9.50 ±0.03)	18.5	6.14± 0.05	13.4± 0.10
3.21	0.30	(5.90±0.10)	(12.2 ±0.05)	18.6		
3.58	0.10	(2.47±0.03)	(6.71 ±0.02)	19.1	2.70± 0.09	6.90± 0.09
3.60	0.50	(3.52±0.05)	(9.44 ±0.01)	18.8		

[a]$[buffer]_{total}$ = 1.00 M, μ = 1.0 (KCl)

[b]The errors are calculated from the standard deviation of the fit of k_r vs $[phosphate]_{total}$ and k_f vs $[phosphate]_{total}$ to a linear equation, $k_r = k_r^0 + k_r^{phos}[phosphate]_{total}$ or $k_f = k_f^0 + k_f^{phos}[phosphate]_{total}$ where k_r^0 and k_f^0 are the pseudo-first order rate constants of hydrolysis and formation without added phosphate under the experimental conditions (see Figure 8) at the given pH. The data at zero phosphate concentration were obtained form Table 4.

Table 9. The pseudo-first order rate constants[a] of formation (k_f) and hydrolysis (k_r) of formanilide and the equilibrium constants[b] (K'_{eq}) in aqueous ethanolic . formate buffer. at 60.0 ± 0.3 °C.

pH[c]	% (v/v) ethanol	k_r (s^{-1})	k_f (s^{-1})	K'_{eq} (M^{-1})
3.59± 0.03	20	(5.32± 0.55)*10^{-6}	(3.30±0.02)*10^{-5}	26.1
4.92± 0.05	80	(2.82± 0.03)*10^{-6}	(1.85±0.02)*10^{-5}	14.1[d]
3.60± 0.05	80	(7.01± 0.02)*10^{-6}	(7.14±0.02)*10^{-5}	16.5[d]
3.60± 0.05	0	(5.86± 0.03)*10^{-6}	(1.65±0.02)*10^{-5}	32.7

[a]Calculated from the pseudo-first order rate constants (k_{obs}) for establishment of equilibrium, using $k_{obs} = k_r + k_f$ and $K' = k_f/k_r$. Errors are deviation from the mean for duplicate values and standard deviations for triplicate values.

[b]Calculated using the non-ionized of concentrations at equilibrium and taking concentration of water as unity, accounting for the changes in the pK_as due to percent ethanol present in the solvent and variation of temperature.

[c]$[buffer]_{total}$ = 1.0 M.

[d]μ uncorrected.

H. Changes in pK_as for temperature, ionic strength and solvent polarity change.

Various pK_as relating to the present study are given in Appendix 1, Table 13S. The measured pK_as of formic acid and anilinium ion at 24 ± 1 °C and μ = 1.0 (KCl) are 3.63 ± 0.03 and 4.89 ± 0.05, respectively. These values are very close to the reported[8] values of 3.66 and 4.85 for formic acid and anilinium ion, respectively, under similar conditions. The changes in the pK_a value of anilinium ion with temperature were calculated using known[48] values of $\Delta H_{ionization}$ and $\Delta S_{ionization}$ of ionization (see Appendix 1). The temperature effect produces a change of 1.11 pK_a units from 25 °C to 100 °C. The pK_as of aliphatic acids are less dependent on temperature[49] because the ΔH values are small. Using the reported $\Delta H_{ionization}$ and $\Delta S_{ionization}$ values[48] it was found that the pK_a of formic acid does not change appreciably from 25 °C to 100 °C.

The pK_a of formic acid in D_2O, at 80° C and μ = 1.0 was taken as 4.09. This value was calculated after Bell and Kuhn[50], who reported that ΔpK is 0.46 for formic acid (where $\Delta pK = pK_D - pK_H$). Similarly the pK_a of anilinium ion was taken as 4.50 (4.02 + 0.48 = 4.50: $pK_D = pK_H + \Delta pK$) since the reported[51] ΔpK_a was 0.48.

The pK_a of acetic acid is reported to decrease by 0.14 units from 0 M to 0.2 M ionic strength[49] and at low ionic strength the change in pK_a is almost linear with increasing μ. However, at higher μ the pK_a approaches a limiting value. Using these assumptions, the pK_a of acetic acid was taken to be 4.60 at 25° C and μ = 1.0. However, at the experimental pHs (3.7 and 1.9) even if the assumed pK_a is in error by 0.15 pK_a unit, the effect on K'_{eq} will be less than 1%, because most of the acid will remain

undissociated at these pHs. The pK_a of acetic acid at 100° C was calculated from the available[48] activation parameters as described above, and shown to be insensitive to temperature.

The pK_a of *p*-nitroanilinium ion is reported[52] to be 0.65 at 80° C. For the present study this value was used without correcting for ionic strength, since a change of ± 0.30 pK_a units will have less than a 2% effect on K'_{eq} because the experiments were conducted at pH 2.82 - 3.60 where more than 99% of the aniline will remain un-protonated. For *p*-methoxyanilinium ion, pK_a data are available[51] from 20 °C to 40 °C at μ = 0.10 and the pK_a vs temperature plot follows a linear trend; accordingly the pK_a at 80° C was extrapolated to be 4.35.

Grunwald and Berkowitz have provided the pK_as of different carboxylic acids in ethanol-water systems[53] at 25 °C. From these data pK_a values of 3.97 and 4.88 were obtained for formic acid in 20% and 80% (v/v) ethanol-water, respectively, at 25 °C. Assuming there is no effect on the pK_a of carboxylic acids due to changes in temperature in ethanol water media, these values were used to calculate the K_{eq} a t 60 °C. Similarly, the pK_as of anilinium ion in aqueous ethanol were obtained from reported[54] data, and were 4.42 and 3.86 in 20% and 80% (v/v) ethanol-water, respectively, at 25 °C. Assuming the effect of temperature change on pK_a in the ethanolic media is similar to that of aqueous media, the respective pK_as can be calculated as 3.89 and 3.33 at 60 °C for anilinium ion in these ethanol/water media.

CHAPTER 4: DISCUSSION

The conditional equilibrium constant, K', which is the simple observed ratio of $[anilide]^{c}_{total}/[aniline]^{c}_{total}$ (eq 15) at equilibrium, provides information in practical terms, how far to the right (Scheme 11) the equilibrium will go under various conditions of pH, temperature and $[formate]_{total}$. The K' and the corrected equilibrium constant, K'_{eq}, as defined by eq 18 (page 33) are listed in Table 10 under various conditions. Several features can be noted from this table such as: A) for a given amide, K' increases as $[formate]_{total}$ increases; B) for the series of formanilide, the functional group alters K'_{eq} at a common set of conditions; C) for acetanilide K'_{eq} is 3.7 times lower than that for formanilide, while the rate at which equilibrium is established under a comparable set of conditions is 240 times lower for acetanilide; D) for a given amide, as temperature increases, K'_{eq} decreases while K' remains almost unchanged; E) added phosphate increases the rate of attainment of equilibrium without changing K' or K'_{eq} for formanilide; F) ethanol increases both rate of attainment of equilibrium and K'. In the following sections these features will be discussed in more detail.

A. Mechanism for specific acid catalyzed hydrolysis and formation.

Amide bond formation is microscopically the reverse reaction of the hydrolysis process (see page 9-11) and follows the same steps in the reverse direction. The formation involves H_3O^+-promoted attack of neutral amine on the non-ionized acid to obtain T^0 via T_N^+. The equilibrium position for the processes of formation and hydrolysis relates to the partitioning of the tetrahedral intermediates T^0 and T_N^+. Importantly, the rates for amide formation and hydrolysis under these conditions are first-order in $[H_3O^+]$, see Figure 6.

Table 10. The conditional equilibrium constants (K') and the corrected equilibrium constants (K'_{eq})[a] of formanilide, acetanilide, *p*-nitroformanilide and *p*-methoxyformanilide under various conditions.

Compound	pH	Temp. (°C)	$[RCOOH]_{total}$ (M)	K'	K'_{eq} (M^{-1})
Formanilide	4.17	98	0.10	0.19	12.3
Formanilide	3.60	98	0.10	0.27	13.1
Formanilide	3.18	98	0.10	0.20	12.9
Formanilide	3.60	98	0.50	1.23	11.9
Formanilide	3.60	98	1.00	2.64	12.7
Acetanilide	1.95	98	1.00[b]	0.06	3.60
Acetanilide	3.75	98	1.00[b]	1.34	3.20
Formanilide	2.80	79	0.10	0.11	20.6
Formanilide	2.79	79	0.50	0.57	22.7
Formanilide	2.81	79	0.90	1.07	20.7
Formanilide	3.20	79	0.10	0.21	19.1
Formanilide	3.20	79	0.50	1.00	18.2
Formanilide	3.20	79	1.00	2.05	18.6
Formanilide	3.60	79	0.10	0.29	20.4
Formanilide	3.61	79	0.50	1.49	20.9
Formanilide	3.59	79	1.00	2.77	19.5
Formanilide	4.01	79	0.10	0.30	20.9
Formanilide	3.20	79	0.50	1.58	21.7
Formanilide	3.20	79	1.00	2.78	19.0
Formanilide	3.58[c]	79	0.50	0.93	22.3
Formanilide	3.61[c]	79	0.75	1.37	21.9
Formanilide	3.60[c]	79	1.00	1.80	21.6
p-nitroformanilide	2.82	79	1.00	0.23	0.26
p-nitroformanilide	3.20	79	0.10	0.02	0.29
p-nitroformanilide	3.20	79	0.50	0.10	0.27
p-nitroformanilide	3.21	79	1.00	0.19	0.26
p-nitroformanilide	3.60	79	1.00	0.13	0.25
p-methoxyformanilide	2.82	79	1.00	0.98	41.0
p-methoxyformanilide	3.18	79	1.00	1.88	38.9
Formanilide	3.21	79	1.00[d]	2.04	18.5
Formanilide	3.21	79	1.00[e]	2.04	18.5
Formanilide	3.58	79	1.00[d]	2.72	19.1
Formanilide	3.58	79	1.00[f]	2.70	19.0
Formanilide	3.60	60	1.00	2.82	32.7
Formanilide	3.59	60	1.00[g]	6.21	26.1
Formanilide	3.60	60	1.00[h]	10.2	16.5
Formanilide	4.92	60	1.00[h]	6.54	14.1

[a]Obtained using $K'_{eq} = \frac{[\text{Formanilide}]}{[\text{Aniline}]\ [\text{Formic acid}]}$ and taking activity of water as unity. The concentrations of non-ionized acid and un-protonated amine were calculated using the corrected pK_a under the given conditions.

[b]Acetate

[c]pD

[d]In presence of 0.10 M KH_2PO_4.

[e]In presence of 0.30 M KH_2PO_4.

[f]In presence of 0.50 M KH_2PO_4.

[g]In 20% aqueous ethanol.

[h]In 80% aqueous ethanol.

B. Mechanism for formate/formic acid catalyzed hydrolysis and formation.

As pointed out in the results section (page 35), the observed rate constant for the attainment of equilibrium, k_{obs}, is the sum of the pseudo-first order rate constants k_r and k_f. Both these rate constants are dependent upon [RCOOH], but in different ways. From

$$k_r = k_{0r} + k_{1r}[RCOOH]_{total} \quad (19)$$

$$k_f = k_{1f}[RCOOH]_{total} + k_{2f}[RCOOH]^2_{total} \quad (20)$$

the concentration dependencies, the k_f term must be non-existent at $[RCOOH]_{total} = 0$, but must increase sharply as $[RCOOH]_{total}$ increases. It is this latter effect that allows an equilibrium situation to attained at higher $[RCOOH]_{total}$.

From Table 2, it can be seen that the rate constants for formate catalysis both for hydrolysis (k_{1f}) and formation (k_{2f}) remain constant with increasing pH until pH 3.6 whereupon they decrease. Three possible mechanisms can be proposed for hydrolysis from this observation. The first, *Mechanism I, a general acid mechanism,* involves the non-ionized acid is acting as a general acid to install a proton on the carbonyl oxygen, while a water molecule attacks the carbonyl carbon with concomitant general base assistance from another water molecule yielding T^0. Second, *Mechanism II, a specific acid followed by general base mechanism,* involves a water attack on the protonated amide with formate anion acting as a general base to assist water attack to once again give T^0. Finally the third possibility is *Mechanism III, a nucleophilic mechanism,* where a formate anion attacks the protonated amide to produce the transient anhydride intermediate.

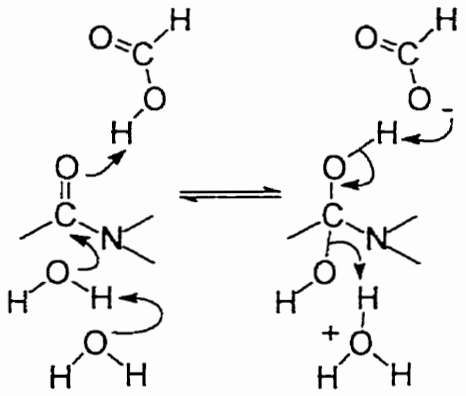

Mechanism I

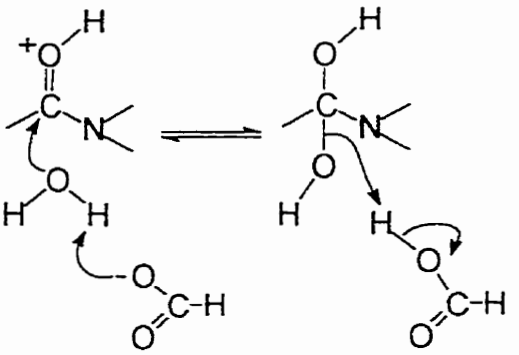

Mechanism II

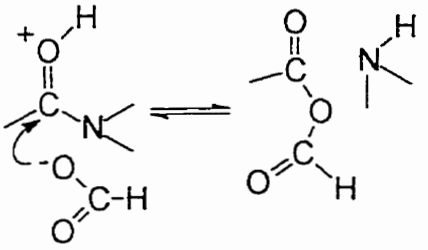

Mechanism III

However, these mechanisms are kinetically equivalent processes, since the stoichiometric composition (HCOOH or $HCOO^-$ and H^-) of the rate limiting transition states are the same in all three mechanisms.[55] As the observed SKIE on k_{1r} is close to unity (0.96±0.12, Table 2), *Mechanism I* is unlikely, since this mechanism would exhibit a primary SKIE. At this point it is not possible to differentiate between *Mechanism II* and *Mechanism III*, and data regarding formation and aminolysis of formic anhydride should be useful for this purpose. Similarly, the breakdown of T^0 leading to formanilide, can occur via general acid or specific acid catalysis followed by general base catalysis or via attack of amine on anhydride which is formed by nucleophilic attack of formate on protonated formic acid.

C. Effect of pH on the conditional equilibrium constant K'.

At constant $[formate]_{total}$, the conditional equilibrium constant K' increases with pH (up to pH 3.6) attaining a maximum value, and then decreases at higher pH (Table 10). This is because non-ionized acid and unprotonated aniline are the reactive species. The conditional equilibrium constant K' includes the $[formate]_{total}$, so eq 15 can be expanded as

$$K' = K''[HCOOH]_{total} = [anilide]^{eq}_{total} / [aniline]^{eq}_{total}$$

$$K'' = \frac{[HCONHPh]}{([HCOOH] + [HCOO^-])([H_3\overset{+}{N}Ph] + [H_2NPh])} \qquad (21)$$

and the optimum pH for formation can be calculated using $a_H = \sqrt{K_A K_B}$, where a_H is the hydrogen ion activity and K_A and K_B are the ionization constants of formic acid and anilinium ion respectively.[12] Using this relation between the dissociation constants of acid/amine and hydrogen ion concentration, the optimum pHs for formation of formanilide can be computed as 3.83 and 3.71 at 80 °C and 100 °C, respectively. Under the experimental conditions used here the pK_a of formic acid is 3.63 while that for anilinium ion is 3.78 (4.02 at 80° C). Thus at pH lower than 3.6, [RCOOH] is maximal while the majority of the aniline is protonated. At higher pH, the situation is reversed, but in both cases the concentration of the reactive species, RCOOH and H_2NAr, decreases (see Figure 9). Hence there is an optimum pH at which a maximal value for the conditional equilibrium constant, K', can be obtained. Laskowski has also reported[14] similar observations for the conditional equilibrium constant of the protease catalyzed hydrolysis and formation of peptide bonds.

Figure 9. Plot of speciation vs pH for formic acid (pK_a = 3.63) and aniline (pK_a = 3.78) at 100 °C. The speciation curve of a hypothetical amine with pK_a 6 has also been included (dotted line). Note that the pH corresponding to the maximum value for K' occurs at the point of intersection of the acid and ammonium ion curves.

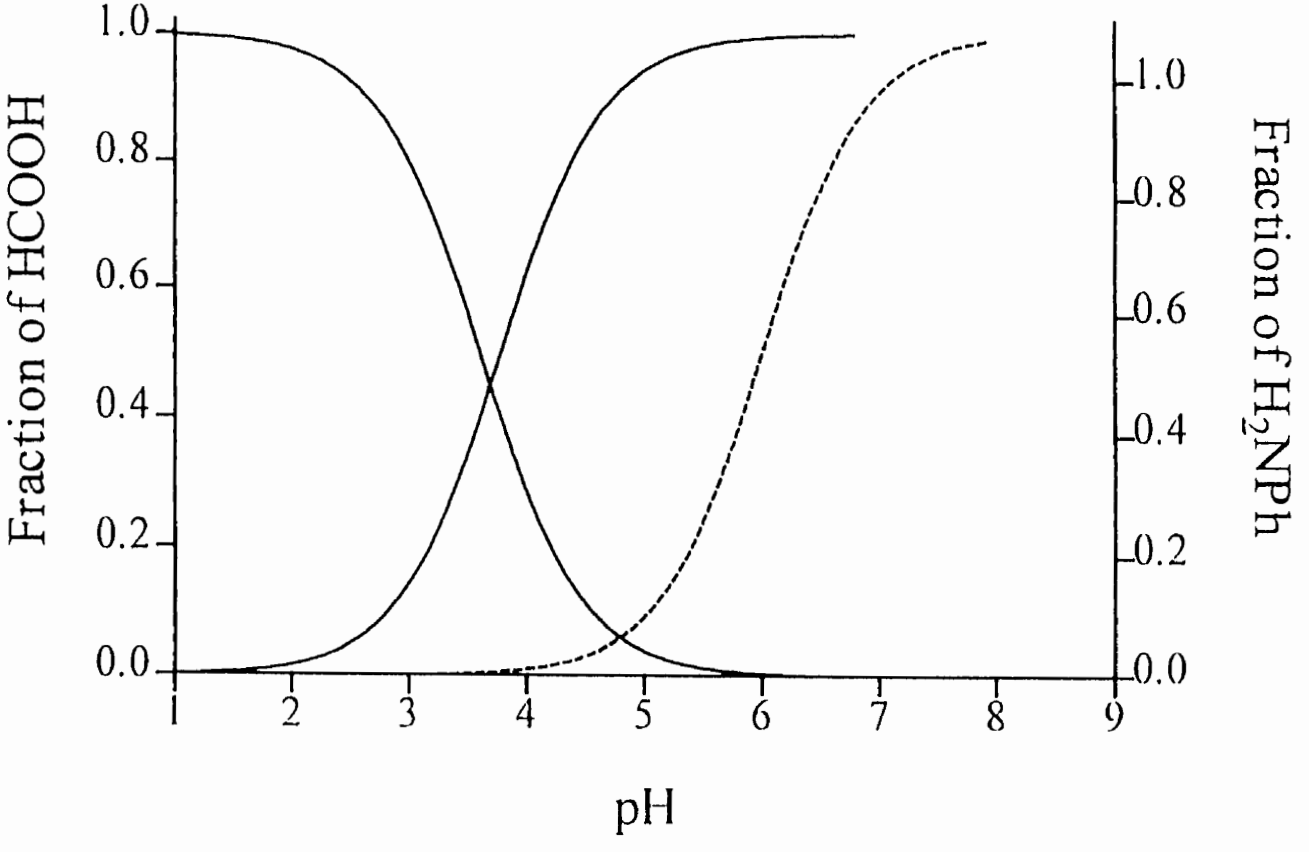

There is an apparent SKIE and on K' of formanilide. $K'_H/K'_D = 1.56$ at pH (pD) 3.60 at 80 °C (Table 10). This effect can be accounted for by the change in pK_a of formic acid and anilinium ion in D_2O. The SKIE becomes unity for K'_{eq} after correcting for these effects.

D. Effect of the amine basicity and the structure of the acyl moieties on the amide formation equilibria.

Fersht has shown[8] that for a number of aliphatic amines log K'_{eq} of formamide formation at 25 °C and μ = 1.0 follows eq 13. This demonstrates that the amide formation

$$\log K'_{eq} = 0.50 + 0.51\ pK_a\ (\text{ammonium}) \qquad (13)$$

equilibrium is directly proportional to the ammonium ion pK_a. However, Fersht's experimental K'_{eq} value for formanilide, was 8 times smaller than would be predicted using eq 13. This is because eq 13 relates to a series of aliphatic amines. In the present study it is seen that for formanilides, at 80 °C and μ=1.0, log K'_{eq} vs pK_a of anilinium ion obeys eq 22. Figure 10. This indicates that the equilibrium constants of formation of anilides are also directly proportional to the basicity of the aromatic amines.

$$\log K'_{eq} = -0.95 + 0.57\ pK_a \qquad (22)$$

Morawetz and Otaki have observed[7] that the amide formation equilibrium constants for a series of higher fatty acids were nearly the same under aqueous basic conditions. They have also observed that in base formate reacts with methyl amine about 140 times faster than does acetate at 44.4 °C. In the present study it is seen that in aqueous acid media the rate constant for the attainment of equilibria, k_{obs}, of formanilide

Figure 10. Plot of log of the experimentally determined formanilide equilibrium constant (K'_{eq}) against the pK_a of amine constituent at 80 °C, μ = 1.0.

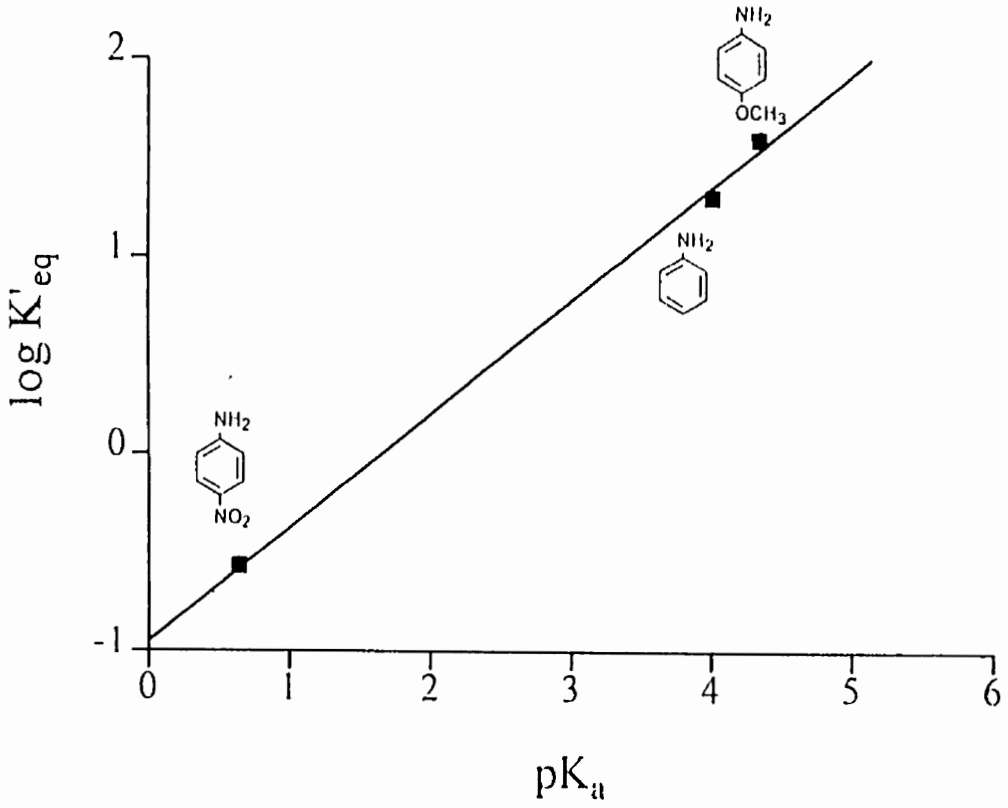

is 240 times greater than that of acetanilide at 100 °C and under similar conditions of pH and $[RCOOH]_{total}$. This high reactivity of formate compared to acetate can be explained in terms of steric factors, since the nucleophilic attack on the formate would be less

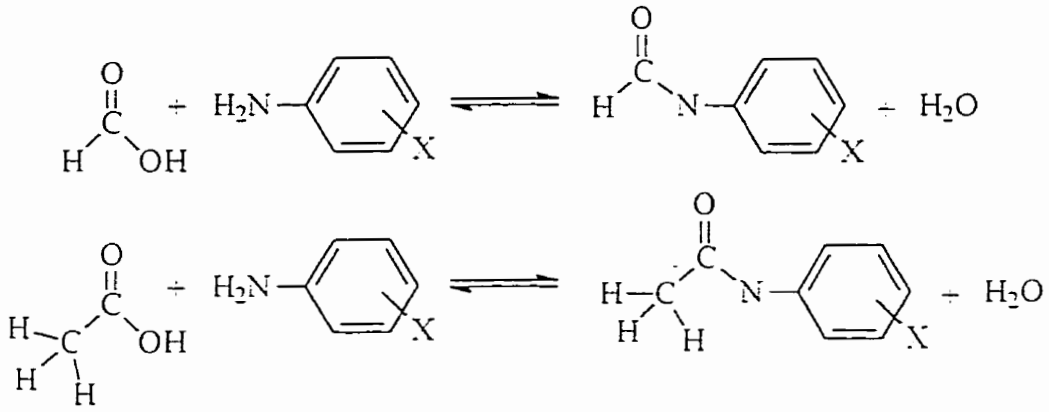

hindered compared with acetae. Nevertheless, the equilibrium constant, K'_{eq} is only 3.7 times greater for formanilide than that of acetanilide, under similar conditions, Table 10. Thus, the equilibrium positions are less sensitive to the acyl functionality of the amide.

E. Effect of temperature on the on the amide formation equilibria.

Log K'_{eq} (corrected equilibrium constant) for formanilide is inversely proportional to temperature, increasing 2.6 times from 100 °C to 60 °C, Table 10. When log K'_{eq} is plotted against 1/T a straight line with positive slope is obtained as seen in Figure 11. Fersht's value[8] of K'_{eq} for formamide, obtained by a different method at 25 °C, also falls on the line. From the slope of the line a ΔH_{eq} of 6.60±0.25 kcal/mole can be calculated. This ΔH_{eq} value is very close to ionization $\Delta H_{ionization}$ of anilinium ion (7.38 kcal/mole).[48] The pK_a of anilinium ion decreases 1.11 pK_a units from 25 °C to 100 °C, whereas the change in pK_a of formic acid over the same range of temperature is negligible. Thus the temperature effect on K'_{eq} is mostly due to the change in pK_a of the anilinium ion.

Figure 11. Plot of log of corrected equilibrium constant (K'_{eq}) against 1/T for equilibrium formation of formanilide, μ = 1.0 (KCl).

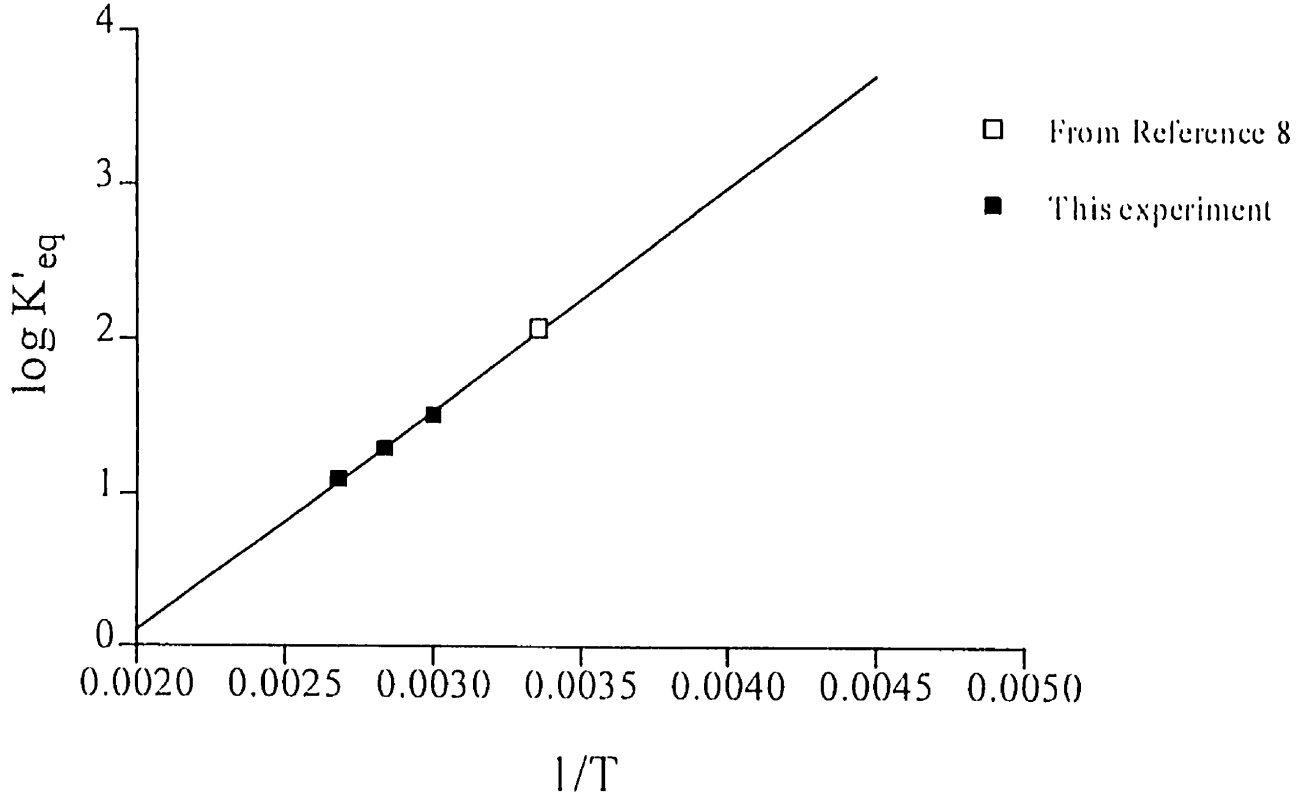

However, in practical terms, temperature has very little effect on the observed conditional equilibrium constant (K') as the values of K' range from 2.82, 2.77 and 2.64 at 60 °C, 80 °C and 100 °C, respectively, (at pH 3.6 and [formate] = 1.0 M) Table 10. This is because, at a given pH (3.6) when the temperature increases, the pK_a of anilinium ion decreases, increasing the concentration of non-protonated amine, hence, shifting the equilibrium more towards formation. Nevertheless, this effect is opposed by the decreasing basicity of aniline (see section D). These opposing factors reduce the effects of temperature on K', however it should be noted that this is only true at pHs above the pK_a of anilinium ion. Below the pK_a, since $[H_3N^+Ar]$ would remain constant, only the basicity is reduced so K' would drop too.

F. Effect of added phosphate ion on the amide formation.

Phosphate catalyses the formation and hydrolysis of formanilide. However, as expected, the equilibrium position is not changed by the addition of KH_2PO_4. It is known that phosphate ions[56, 57] are able to mediate acyl transfer, in this case to amine or water, probably through proton addition and removal in the formation and breakdown of tetrahedral intermediates.

In some cases it is known that phosphate can act as a nucleophile toward RCOX to give acyl phosphate intermediates. In a recent paper[58] Brown provided evidence that phosphate can act as a nucleophilic catalyst towards ester and thiolester hydrolysis. This mechanism generally occurs when the conjugate acid of the departing group, X, has a low pK_a and X can leave readily as an anion. It is unlikely to be operative for phosphate catalysis of amide equilibriation. Nevertheless, for the formation and hydrolysis of

formanilide, a speculative possibility exists where phosphate nucleophilically attacks to give the formyl phosphate intermediate. The hypothetical mechanism of nucleophilic catalysis by phosphate for amide bond formation is presented in Scheme 13.

Scheme 13

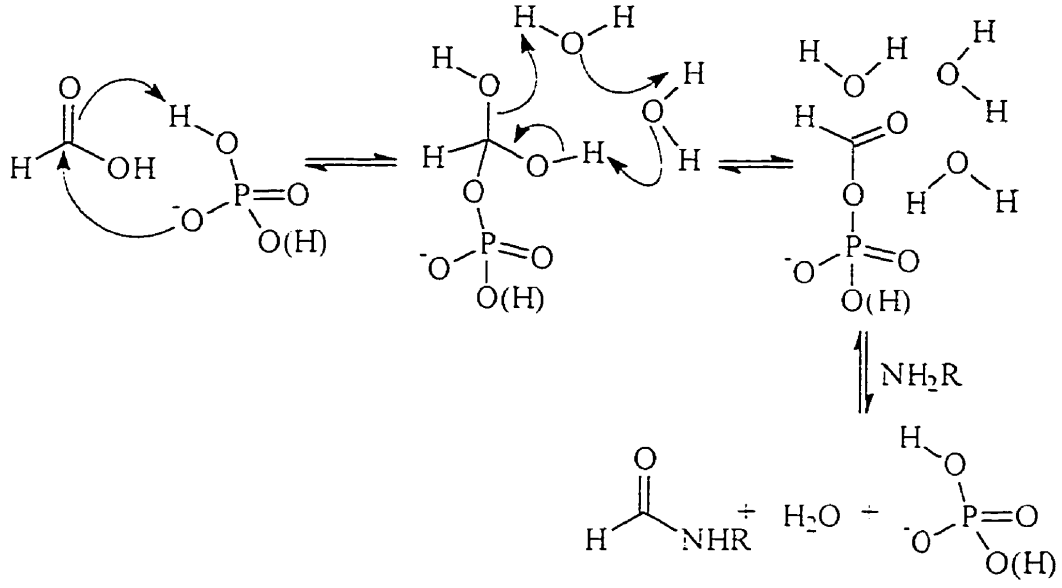

Keillor *et al* have suggested[35] that the catalytic mechanism of phosphate assisted formation and hydrolysis of amides proceeds via either sequential general base/general acid process or a bifunctional concerted general base/general acid processes, Scheme 14.

Scheme 14

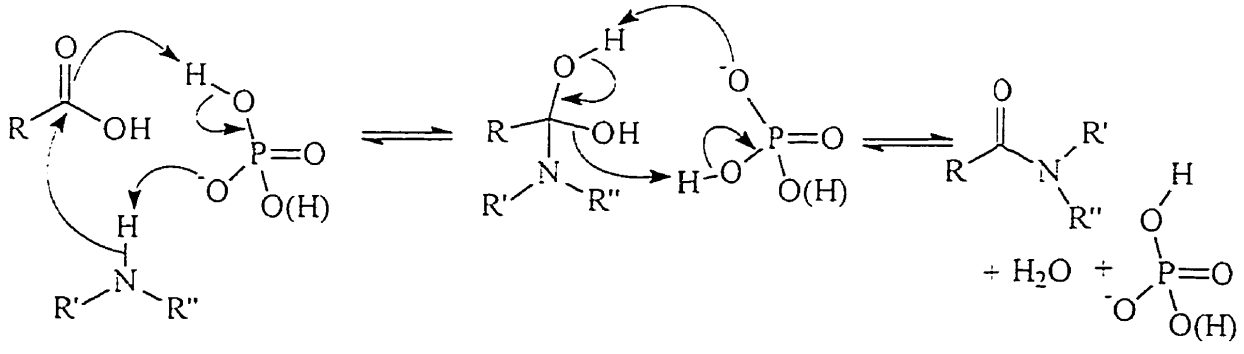

In earlier work, Kirby observed[38] phosphate catalysis of lactam formation from **15** and **16a.** To account for the accelerated rate of ring closure, the authors invoked the role of phosphate as both a general base and a general acid, Scheme 15. Bifunctional catalysis by phosphate buffers has also been observed for amide[56] and imidate ester[57] hydrolysis and suggested to occur by the same sort of mechanism as depicted in Schemes 14 and 15.

Scheme 15

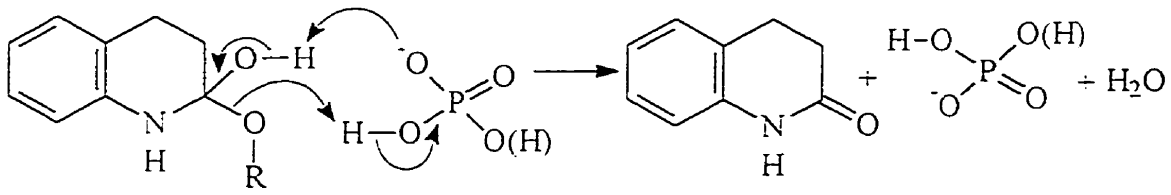

R = H, CH_3

G. Formation and hydrolysis of formanilide in aqueous ethanol.

To study the effect of the solvent polarity on the equilibrium constant, the formation and hydrolysis of formanilide was carried out in both 20 and 80 percent (v/v) ethanol/water mixtures. Under comparable conditions, both the rate constant for attainment of equilibrium (k_{obs}) and the conditional equilibrium constant (K') increased about 3.5 times in changing from 0 to 80 percent ethanol (see Table 10). The pK_a of formic acid increases with the addition of ethanol in aqueous media.[53] Under the experimental conditions of the present study, the pK_a of formic acid changes to 4.88 in 80 percent ethanol from 3.63 in aqueous media. On the other hand the pK_a of anilinium ion decreases to 3.33 in 80 percent ethanol from 4.30 in aqueous media. These changes in pK_as due to the addition of ethanol increase the concentration of the non-ionized forms of both aniline and formic acid at a given pH (here 3.6). Hence, the equilibrium lies more

towards the formation. However, it should be noted that if the observed change in K' only results from changes in effective concentration of reactive species (*ie* [HCOOH] and [H_2NPh]), the change would be higher than 3.5-fold in 80 percent ethanol since the effective concentration of both acid and amine increases. The other factor which reduces the overall effect on K' is the basicity of the amine. Although the reduction in amine pK_a increases the effective concentration of amine at a given pH it also reduces basicity of the amine, so the net effect on K' is somewhat dampened.

Similar observations for addition of organic solvents to the reaction media were made in studies of enzymatic formation of amide bonds.[1, 14] It was reported that, in the enzyme catalysed processes, the addition of organic solvents shifted the equilibrium more towards amide bond formation. In a chymotrypsin catalyzed formation of benzyloxycarbonyl-L-tryptophanylglycineamide a dipeptide, (from benzyloxycarbonyl-L-tryptophan, **18** and glycineamide, **19**), the addition of 85 percent 1,4-butanediol increased

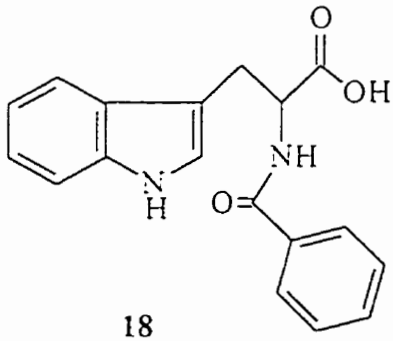

18

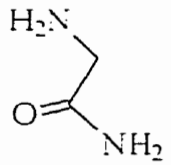

19

the formation by a factor of 84.[14] The pK_a of the carboxylic acid group of benzyloxycarbonyl-L-tryptophan shifted from 3.6 in aqueous solution to 5.3 in 85 percent 1,4-butanediol, without a significant change in the pK_a of the amine group of glycineamide (which changed from 8.2 to 8.1). Hence, in that study the enhancement in dipeptide formation in the above solvent system was attributed mostly to the change in

pK_a of the carboxylic acid group of benzyloxycarbonyl-L-tryptophan. Presumably such effect could be operative in the non-ezymatic coupling of these two species as well.

Although the effects of the addition of ethanol can be explained in terms of the change in pK_as, another possibility exists wherein ethyl formate is formed as a reactive intermediate and amide formation will occur through the aminolysis of ethyl formate, Scheme 16.

Scheme 16

$$H_3O^+ + HCOOH + NH_2Ph \underset{k_{-1}}{\overset{k_1}{\rightleftharpoons}} H_3O^+ + HCONHPh + H_2O$$

$$H_3O^+ + HCOOH + EtOH \underset{k_{-2}}{\overset{k_2}{\rightleftharpoons}} H_3O^+ + HCOOEt + H_2O$$

$$H_3O^+ + HCOOEt + NH_2Ph \underset{k_{-3}}{\overset{k_3}{\rightleftharpoons}} HCONHPh + EtOH + H_3O^+$$

A century ago, Kistiakowsky studied[59] the equilibrium formation and hydrolysis of ethyl formate in acidic aqueous ethanol, and showed that the acid catalyzed rate of attainment of equilibria ($(k_2 + k_{-2})$ in Scheme 16) varied from 2.3×10^{-3} M^{-1} s^{-1} to 3.3×10^{-3} M^{-1} s^{-1} when the solvent composition was varied from 21 to 80 percent ethanol at 25 °C. The equilibrium position lay 17, 61 and 72 percent towards formation of ethyl formate in 21, 73 and 84 percent ethanol, respectively. The author also reported an 8-10 percent increase in the rate of attainment of equilibria when the temperature was increased to 30 °C from 25 °C, without changing the equilibrium position. The possibility of formanilide formation via aminolysis of ethyl formate cannot be ruled out at this point. However, with more information from studies involving aminolysis of ethyl formate under the experimental conditions reported in this thesis, a definitive picture would likely emerge.

CHAPTER 5: CONCLUSION

Equilibria can be attained for formanilide, acetanilide, *p*-nitroformanilide and *p*-methoxyformanilide and their constituent acids and amines under dilute aqueous acidic conditions starting from both formation and hydrolysis directions. At moderately acidic pH, these amides can be formed in reasonable amounts in reasonable times under appropriate conditions. The conditional equilibrium constant, K', gives an indication of where the equilibrium position lies under a given set of conditions. The equilibrium position for formanilides shifts more towards formation with the increasing basicity of constituent amine. At 1.0 M $[formate]_{total}$ and at pH 3.2, K' for formanilide, *p*-methoxyformanilide and *p*-nitroformanilide are 2.05, 1.88 and 0.19 respectively at 80 °C. This indicates that for the first two anilides the equilibrium position lies more than 65% in favour of formation while the later compound sits only at about 16% towards formation. In the present study the optimum conditions for formanilide formation in aqueous media was found to be at pH 3.6, 1.0 M $[formate]_{total}$, where more than 73% formation was observed. The half life ($t_{1/2}$) for the rate of attainment of the equilibrium under the conditions described above, range from 1.6 hr to 8.6 hr for the different anilides, so for practical purposes, equilibrium can be reached within 8 to 42 hr (*i.e.*5 $t_{1/2}$). The corrected equilibrium constant (K'_{eq}) for formanilide is inversely proportional to temperature, while a minimal change in K' is observed.

While the rate of attainment of equilibrium decreases by 249 times when going from formanilide to acetanilide under comparable conditions, the effect on the corrected equilibrium constant (K'_{eq}) is much smaller, decreasing by a factor of only 3.7. These differences are believed to be largely due to the steric effects.

Phosphate catalyzes the attainment of both formation and hydrolysis of formanilide without changing the equilibrium position. At pH 3.6, and constant ionic strength (μ = 1.0), it was found that 0.5 M phosphate increased the rate of attainment of equilibrium for formanilide by 1.6 times, while K' remained constant at 2.7, denoting an unchanged equilibrium position as expected. In practical terms phosphate accelerates attainment of equilibria (5 $t_{1/2}$) from about 12 hr to 7 hr at pH 3.6, $[formate]_{total}$ = 1.0 M and at 80 °C, a considerable savings in time.

Both the rate of attainment of equilibrium and the apparent formation equilibrium constant for formation increases with increasing amounts of ethanol in the medium. In a solution system of 80 percent ethanol both the rate of attainment of equilibrium and the K' increase by a factor of 3.5 at pH 3.6, $[formate]_{total}$ = 1.0 M and at 60 °C. From a practical point of view, going from 0 to 80 percent ethanol in solution at pH 3.6 and $[formate]_{total}$ = 1.0 M, resulted in an enhancement of the yield from 73% to 91%, with the equilibrium being attained within 12 hr instead of 42 hr.

So from a synthetic point of view, simply adjusting pH and changing the solvent in an overnight reaction produces up to 91% formanilide using formic acid in excess of aniline as the starting materials. Actually, in aqueous media, using higher aniline concentrations while maintaining the excess formic acid will lead to formanilide precipitating out from solution, thus driving the reaction more completely towards formation.

Future work.

In the present study the equilibrium of formation and hydrolysis of formanilide and acetanilide have been studied. However, it would be useful to obtain such equilibrium constants for amides which were previously studied for hydrolysis such as:

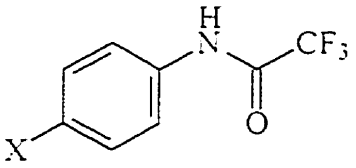

3a X = H
3b X = NO_2

In an initial study[60] with compound **3b** more than 10% formation was observed at equilibrium. (At pH 1.23, $[CF_3COOH]_{total}$ = 0.1 M, μ = 1.0 (KCl) at 100 °C).

Previously Keillor et al showed[35] that compound **8** catalyzed the formation and hydrolysis equilibria of N-formylmorpholine. It would be interesting to see the effect of **8** and other bifunctional catalysts such as (**4-6**) and (**9-11**), on the formation and hydrolysis equilibria of anilides and other amides. It is reported here that phosphate catalyses the rate at which equilibrium is attain for formanilide without effecting the equilibrium position. A logical extension of this work would be to study the effect of phosphate on the rate and equilibrium of formation and hydrolysis of other amides.

The formation and hydrolysis reaction of formanilide in aqueous ethanol may proceed via an intermediate ethyl formate (Scheme 16). Knowledge of the rate of formation of ethyl formate and the rate of ethyl formate aminolysis under the experimental conditions used in this study would be helpful to understand the processes occurring in aqueous ethanolic media.

REFERENCES

(1) Fruton, J.S. In *Adv. Enzymol.* Meister, A., Ed.; J. Wiley and Sons: New York, 1982; pp. 239-306.

(2) (a) Oie, T.; Loew, G. H.; Burt, S. K.; Binkley, J. S.; MacElroy, R. D. *J. Am. Chem. Soc.* **1982**, *104*, 6169.

(b) Oie, T.; Loew, G. H.; Burt, S. K.; Binkley, J. S.; MacElroy, R. D. *J. Am. Chem. Soc.* **1983**, *105*, 2221.

(3) (a) Chung, N. M.; Lohrmann, R.; Orel, E.; Rabinowiz, J. *Tetrahedron.* **1971**, *27*, 1210.

(b) Yamanaka, J.; Inomata, K.; Yamagata, Y. *Orig. Life* **1988**, *18*, 165.

(c) Rabinowitz, J.; Flores, J.; Krebsbach, R.; Rogers, G. *Nature* **1969**, *224*, 795.

(d) Rabinowitz, J.; Hampai, A. *J. Mol. Evol.* **1985**, *21*, 199.

(4) (a) Steinman, G. D.; Kenyon, D. H. and Calvin, M. *Biochem. Biophys Acta.* **1966**, *124*, 339.

(b) Ponnamperuma, C.; Peterson, E. *Science*, **1965**, *147*, 1572.

(c) Steinman, G.; Kenyon, D. H.; Calvin, M. *Nature* **1965**, *206*, 707.

(5) Rishpon, J.; O'Hara, P.; Lahav, N.; Lawless, J. G. *J. Mol. Evol.* **1982**, *18*, 179.

(6)(a) Bujdak, J.; Rode, B. M. *J. Mol. Evol.* **1997**, *45*, 457.

(b) Schwendinger, G. M.; Rode, B. M. *J. Mol. Evol.* **1992**, *22*, 349.

(7) Morawetz, H.; Otaki, P. S. *J. Am. Chem. Soc.* **1963**, *85*, 436.

(8) Fersht, A. R.; Requena, Y. *J. Am. Chem. Soc.* **1971**, *93*, 3499.

(9) Keller, M.; Blochl, E.; Wachtershauser, G.; Stetter, K. O. *Nature* **1994**, *368*, 836.

(10) Inovyl, K.; Watanabe, K.; Morihara, K.; Tochino, Y.; Kanaya, T. Emura, J.; Sekakibaras, S. *J. Am. Chem. Soc.* **1979**, *101*, 751.

(11) Carpenter, F. H. *J. Am. Chem. Soc.* **1960**, 82, 1111.

(12) Dobry, A.; Fruton, J. S.; Sturtevant, J. M.. *J. Biol. Chem.* **1952,** *195*, 149.

(13) Homandberg, G. A.; Laskowski, M. *Biochemistry*, **1979,** *18*, 586.

(14) Homandberg, G. A.; Mattis; Laskowski, M. *Biochemistry*, **1978,** *17*, 5220.

(15) Gawron, O.; Glaid, A. J.; Boyle, R. E.; Odstrchel, G. *Arch. Biochem. Biophys.* **1961**, *95*, 203.

(16) Kullmenn, W. *J. Biol. Chem.* **1980,** 255, 8234.

(17) (a) Esowa, Y.; Ohmori, M.; Ichikawa, T.; Kurite, H.; Sato, M.; Mori, K. *Bull. Chem. Soc. Japan.* **1977**, *50*, 2762.

(b) Westeneys, H.; Borsook, H. *Physiol. Rev.* **1930,** *10*, 110.

(18) Morihara, K.; Oka, T.; Tsuzuki, H.; *Arch. Biochem. Biophys.* **1969,** *132*, 489.

(19) Brown, R. S.; Bennet, A. J.; Slebocka-Tilk, H. *Acc. Chem. Res.* **1992,** *25*, 481.

(20) Brown, R. S. In "Biological Significance of the Amide Linkage", Eds. Greenburg, A.; Breneman C.; Liebman, J. Chapter 2. Chapman Hall: London. In Press.

(21) (a) Lowry, T. H.; Richardson, K.S. "Mechanism and Theory in Organic Chemistry" 3rd Edition. Harper and Row: New York, 1987, pp. 710-723.

(b) March, J. "Advanced Organic Chemistry" 4th Edition. Wiley-Interscience: New York, 1992, pp. 330-335, 378-386.

(c) Jencks, W. P. "Catalysis in Chemistry and Enzymology", McGraw-Hill: New York, 1969, pp. 7-242, 463-554.

(22) (a) Slebocka-Tilk, H.; Bennet, A. J.; Keillor, J. W.; Brown, R. S.; Guthrie, J. P.; Jodhan, A. *J. Am. Chem. Soc.* **1990**, *112*, 8507.

(b) Brown, R. S.; Bennet, A. J.; Slebocka-Tilk, H,; Jodhan, A. *J. Am. Chem. Soc.* **1992**, *114*, 3092.

(23) (a) Slebocka-Tilk, H,; Brown, R. S.; Olekszyk, J. *J. Am. Chem. Soc.* **1978**, *109*, 4620

(b) Bennet, A. J.; Slebocka-Tilk, H.; Brown, R. S.; Guthrie, J. P.; Jodhan, A. *J. Am. Chem. Soc.* **1990**, *112*, 8497.

(c) Bennet, A. J.; Slebocka-Tilk, H.; Brown, R. S. *J. Am. Chem. Soc.* **1992**, *114*, 3088.

(24) Guthrie, J. P. *J. Am. Chem. Soc.* **1974**, *96*, 3608.

(25) (a) Bender, M. L.; Thomas, R. J. *J. Am. Chem. Soc.* **1961**, *83*, 4183.

(b) Bunton, C. A.; Farber, S. J.; Milbank, A. J. G.; O'Connor, C.J.; Turney, T. A. *J. Chem. Soc.: Perkin Trans. 2*, **1972**, 1869 and references therein.

(c) Smith, C. R.; Yates, K. *J. Am. Chem. Soc.* **1972**, *94*, 8811.

(26) McClelland, R. A. *J. Am. Chem. Soc.* **1975**, *97*, 5281.

(27) (a) Pollack, R. M.; Dumsa, T. C. *J. Am. Chem. Soc.* **1973**, *95*, 4465.

(b) Biechler, S. S.; Taft, Jr. R. W. *J. Am. Chem. Soc.* **1957**, *79*, 4927.

(c) Menger, F. M.; Donohue, J. A. *J. Am. Chem. Soc.* **1973**, *95*, 432.

(28) (a) Bender, M. L. *J. Am. Chem. Soc.* **1951**, *73*, 1626.

(b) Bender, M. L. *Chem. Rev.* **1960**, *60*, 53.

(c) Bender, M. L.; Ginger, R. D.; Kemp, K. C. *J. Am. Chem. Soc.* **1954**, *76*, 3350.

(d) Slebocka-Tilk, H.; Bennet, A. J.; Hogg, H. J.; Brown, R. S. *J. Am. Chem. Soc.* **1991**, *113*, 1288.

(29) Slebocka-Tilk, H.; Rescorla, C. G.; Shirin, S.; Bennet, A. J.; Brown, R. S. *J. Am. Chem. Soc.* **1997**, *119*, 10969.

(30) (a) Skorey, K. I.; Somayaji, V.; Brown, R. S. *J. Am. Chem. Soc.* **1989**, *111*, 1445.

(b) Skorey, K. I.; Somayaji, V.; Brown, R. S. *J. Am. Chem. Soc.* **1988**, *110*, 5205.

(c) Somayaji, V.; Brown, R. S.; Ball, R. G. *J.Org. Chem.* **1986**, 51, 4866.

(31) Skorey, K. I.; Brown, R. S. *J. Am. Chem. Soc.* **1985**, *107*, 4070.

(32) Street, J. P.; Skorey, K. I.; Brown, R. S.; Ball, R. G. *J. Am. Chem. Soc.* **1985**, *107*, 7669.

(33) Keillor, J. W.; Brown, R. S. *J. Am. Chem. Soc.* **1991**, *113*, 5114.

(34) Keillor, J. W.; Brown, R. S. *J. Am. Chem. Soc.* **1992**, *114*, 7983.

(35) (a) Keillor, J. W.; Neverov, A. A.; Brown, R. S. *J. Am. Chem. Soc.* **1994**, *116*, 4669.

(b) Note that the apparent equilibrium constant, K", reported by Keillor *et al* can be expressed as $K'' = K'/[acid]_{total}$ where K' is the conditional equilibrium constant (see eq 15, Results).

(36) Kellogg, B. A.; Neverov, A. A.; Aman, A. M.; Brown, R. S. *J. Am. Chem. Soc.* **1996**, *118*, 10829.

(37) Somayaji, V.; Keillor, J. W.; Brown, R. S. *J. Am. Chem. Soc.* **1988**, *110*, 2625.

(38) (a) Kirby, A. J.; Mujahid, T.G.; Camilleri, P. *J. Chem. Soc. Perkin Trans. 2*, **1979**, 1610.

(b) Camilleri, P.; Ellul, R.; Kirby, A.; Mujahid, T. G. *J. Chem. Soc. Perkin Trans. 2*, **1979**, 1617.

(39) Fife, T. H.; Duddy, N. W. *J. Am. Chem. Soc.* **1983**, *105*, 74 and reference therein.

(40) Blackburn, G. M.; Jencks, W. P. *J. Am. Chem. Soc.* **1968**, *90*, 2638.

(41) Jencks, W. P.; Caplow, M.; Gilchrist, M.; Kaller, R.G. *Biochemistry*, **1963**, *2*, 1313.

(42) Guthrie, J. P.; Pike, D. C.; Lee, Y. *Can. J. Chem.*, **1992**, *70*, 1671.

(43) Krishnamurthy, S. *Tetrahedron. Lett.* **1982**, *23*, 3315.

(44) Perrin, C. L.; Thoburn, J. D.; Kresge, J. *J. Am. Chem. Soc.* **1992**, *114*, 8800.

(45) DeWolfe, R. and Newcomb, C. R. *J. Org. Chem.* **1971**, *36*, 3870.

(46) Glasoe, P. K.; Long, F. A. *J. Phys. Chem.*, **1960**, *64*,188.

(47) Huguet, J. Ph. D. Thesis, University of Alberta, 1980

(48) Isaacs, N. S. In "Physical Organic Chemistry", Longman Group UK Ltd: New York, 1987, pp. 210-213.

(49) Perrin, D. D.; Dempsey, B.; Serjeant, E. P. In "pKa Prediction for Organic Acids and Bases" Chapman and Hall, London, 1981, pp. 6-9.

(50) Bell, R. P.; Kuhn, A. T.; *Trans. Faraday Soc.*, **1963**, *59*,1789.

(51) (a) Perrin, D. D. In "Dissociation Constants of Organic Bases in Aqueous Solution", Butterworths, London, 1965.

(b) Biggs, A. I *J. Chem. Soc.* **1961**, 2572

(52) Johnson, C. D.; Katritzky, A. R.; Shapiro, S. A. *J. Am. Chem. Soc.* **1969**, *91*, 6654.

(53) Grunwald, E.; Berkowitz, B. *J. Am. Chem. Soc.* **1951**, *73*, 4939.

(54) Gutbezahl, B.; Grunwald, E. *J. Am. Chem. Soc.* **1953**, *75*, 1953.

(55) Lowry, T. H; Richardson, K. S. "Mechanism and Theory in Organic Chemistry" 3rd Edition. Harper and Row: New York, 1987, pp. 676-680.

(56) (a) Schepartz, A.; Breslow, R.; *J. Am. Chem. Soc.* **1987**, *109*, 1814.

(b) Cunningham, B; Schmir, G. L. *J. Am. Chem. Soc.* **1967**, *89*, 917.

(57) (a) Lee, Y.; Schmir, G. L. *J. Am. Chem. Soc.* **1979**, *101,3026*.

(b) Cunninghum, B.; Schmir, G. L. *J. Am. Chem. Soc.* **1966**, *88*, *551*.

(58) Gill, M. S.; Neverov, A.; Brown, R.S. *J. Org. Chem.* **1997**, *62*, 7351

(59) Kistiakowasky, *Z. Physik. Chem.* **1898**, *27*, 250.

(60) Present work.

Part 2: Studies of Acyl Transfer from a Strained Amide to Thioglycolic Acid and Intramolecular Catalysis of Thiol Ester Hydrolysis.

CHAPTER 1: BACKGROUND

Amide bond hydrolysis is very slow under mild conditions of temperature and at pH values close to neutrality which resemble physiological conditions. For example, in a recent report Smith and Hansen studied the hydrolysis of N-(phenylacetyl)glycyl-D-valine at 37 °C and at various conditions of pH.[1] At pH 7, the corresponding half life ($t_{1/2}$) for (phenylacetyl)glycyl bond hydrolysis has been computed to be 243 years, and that for hydrolysis of the glycyl-D-valine bond to be 267 years, Scheme 1. Nevertheless,

Scheme 1

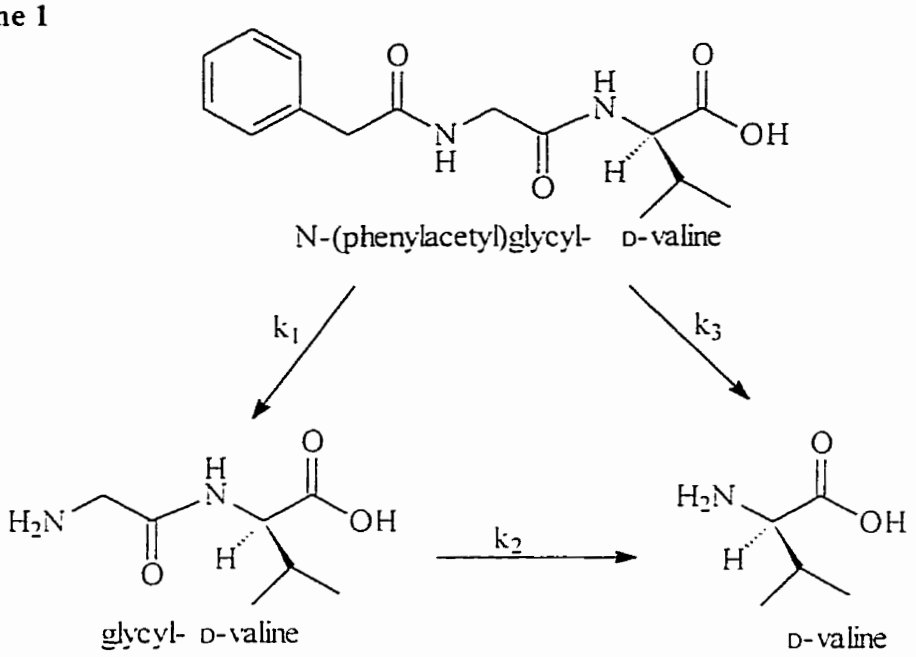

hydrolytic enzymes called proteases are capable of rapid cleavage of amide (peptide) bonds under physiological conditions. One such example is the enzymatic hydrolysis of benzoyl glycyl-L-phenylalanine by carboxypeptidase A with a $t_{1/2}$ of 6 milliseconds.[2] At present, proteases are classified into four main categories according to the functional groups present in the active site. The categories are Serine, Cysteine, Aspartate and Metallo (Zn^{2-}) proteases. In the following section, the three non-metallo proteases are discussed.

Serine proteases:

The serine proteases comprise a large group of enzymes for which the optimum pH for activity is close to neutrality.[3] The active site of most of these enzymes contains a catalytic triad of serine (Ser-OH), histidine (His-Im) and aspartate (Asp-COO$^-$).[4] The hydroxyl group of serine becomes acetylated, giving an acyl enzyme intermediate during the course of amide bond hydrolysis. Chymotrypsin is one of the most studied[4,5,6,7] serine proteases, with an active site containing Ser-195, His-57 and Asp-102 as the catalytic triad. Also present in the active site of chymotrypsin are the backbone NH groups of Gly-193 and Ser-195 forming the so-called "oxyanion hole".[4] The steps involved in the catalytic process for amide bond hydrolysis by chymotrypsin are detailed in Scheme 2, in which it is seen that the initial formation of the non-covalent enzyme substrate complex (ES) is followed by nucleophilic attack from the Ser-195 hydroxyl group on the substrate carbonyl carbon, forming a tetrahedral intermediate (T_O^-). The nucleophilic attack of the Ser-195 hydroxyl group is facilitated by general base assistance from the imidazole of His-57. The tetrahedral intermediate (T_O^-) subsequently breaks down to the acyl-enzyme (EA) intermediate via a proton transfer from the imidazolium of His-57. At this point, the cleaved amine is expelled from the active site and replaced by a water molecule.
In the deacylation process, the steps involved are nucleophilic attack of a water molecule on the carbonyl carbon of EA with general base assistance by the imidazole to produce the second tetrahedral intermediate T'_O^-, which subsequently breaks down to form products, regenerating the enzyme. Throughout the hydrolytic process, the role of the carboxylate moiety of Asp-102 is to orient the imidazoyl group of His-57 to enable it to

perform its general base/acid role and also to electrostatically stabilize the imidazolium ion and increase the basicity of imidazole.[4,7]

Scheme 2

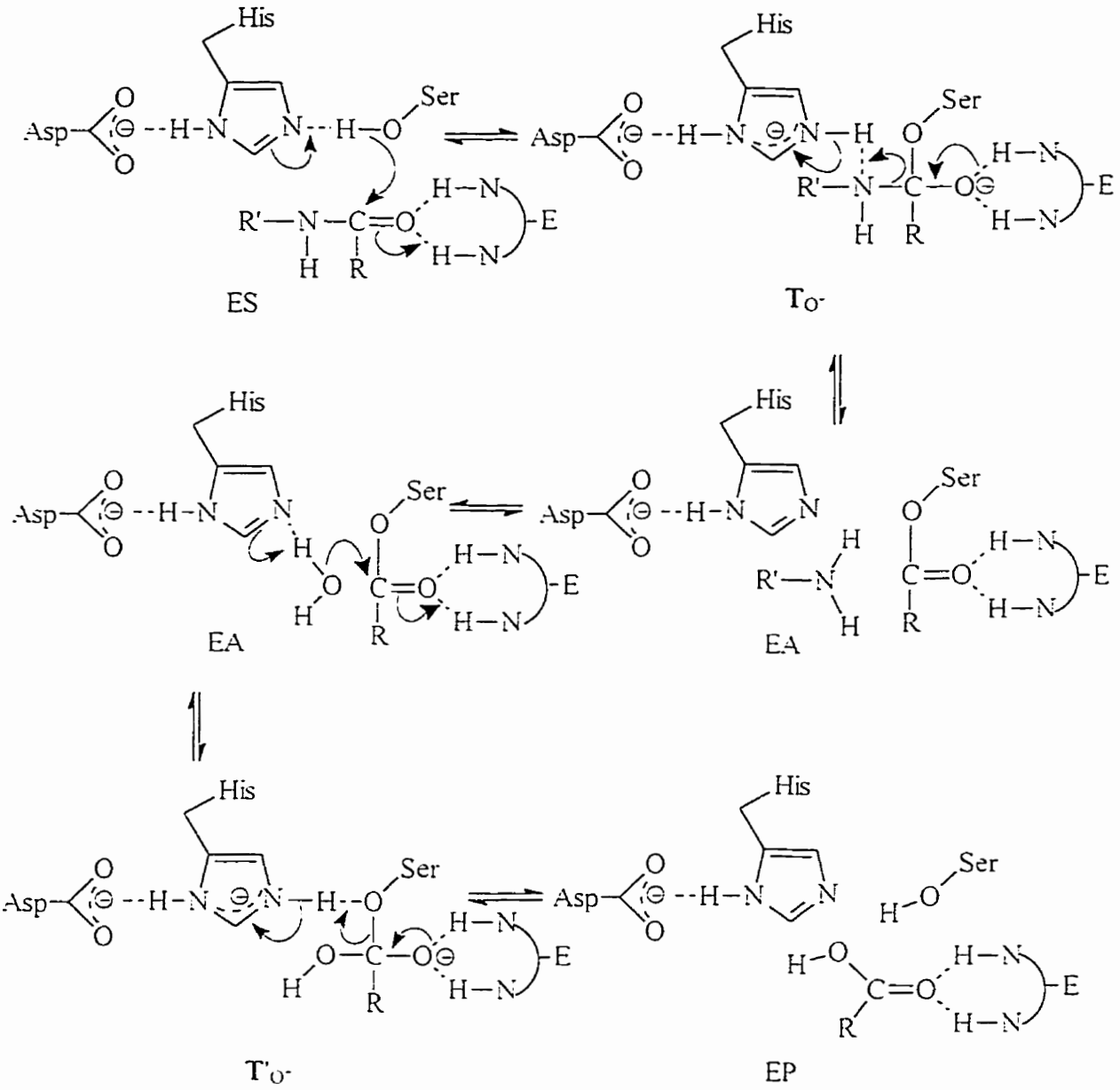

Aspartate proteases:

Aspartate proteases are also known as carboxyl proteases because these enzymes have two catalytically essential carboxyl groups of aspartate in the enzyme active site.[8] The two well known enzymes of this class are the mammalian enzyme pepsin[8,9,10,11] and the fungal enzyme penicillopepsin.[12,13] However, possibly the most famous aspartate protease is the human immunodeficiency virus (HIV) protease.[14,15,16] Most of these proteases are active at low pHs (ranging from pH 1.9 to 4.0), which is why these enzymes were formerly known as acid proteases. The pK_as of the two carboxylic acid groups of the active site aspartate are 1.4 and 4.5 (for pepsin the two aspartate groups are Asp-32 and Asp-215, respectively). The former carboxylic acid group, when deprotonated, acts a nucleophile or a general base while the other supplies a proton to the nitrogen of the tetrahedral intermediate, Schemes 3 and 4.

Scheme 3

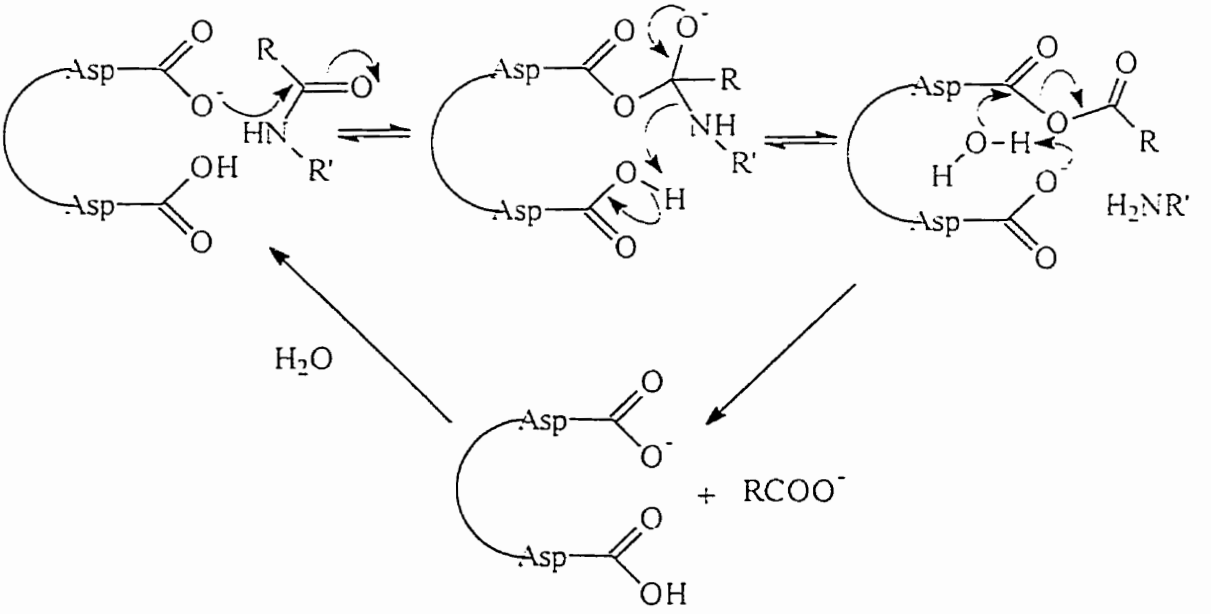

Scheme 4

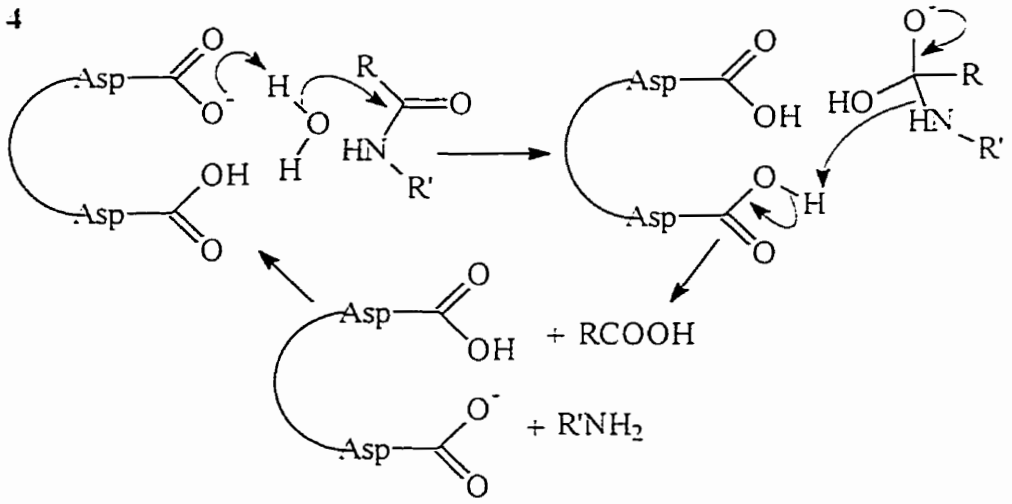

The catalytic mechanism of these enzymes is still controversial, because the initial attack of an aspartate carboxylate on the substrate can either be nucleophilic to form an acyl enzyme intermediate, Scheme 3, or general base without going via an acyl enzyme, Scheme 4. However, a recent postulated mechanism of aspartate proteases, depicted in Scheme 5, includes one aspartate residue as a general base/acid, while the second residue acts solely to stabilize the developing charge on the acyl oxygen.[15,17,18]

Scheme 5

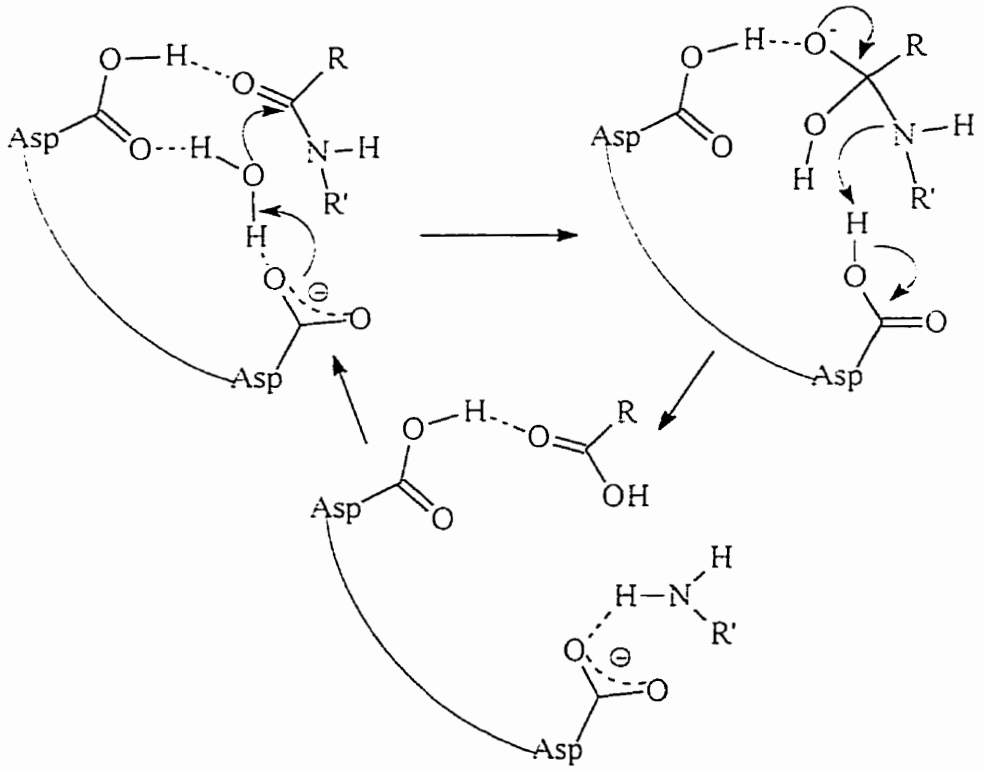

Cysteine proteases:

Cysteine proteases are widely distributed in nature and contain an essential cysteine thiol and a histidine imidazole within the active site.[19] The plant protease papain was the first enzyme to be recognized as a thiol-containing protease:[20a] this is also the best studied cysteine protease.[20,21,22] The pH rate profile of papain follows a bell shaped curve which is consistent with the fact that two ionizable groups are essential for the catalytic process. It is now generally accepted that the catalytically active enzyme contains the thiolate-imidazolium ion pair.[23] Scheme 6.

Scheme 6

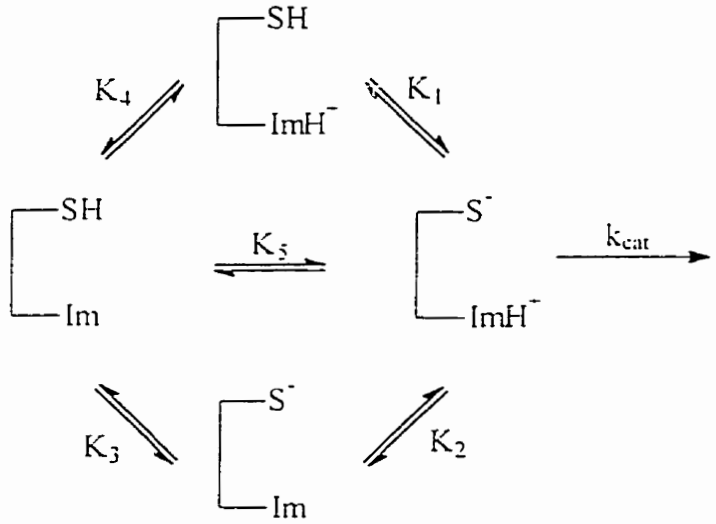

The two apparent pK_a values obtained from the bell shaped pH rate profile are ~ 4 and ~ 8.5. The lower pK_a value is considered to be mostly due to the ionization of the cysteine thiol group, while the higher pK_a value is attributed mostly to the ionization of the imidazolium ion. It was suggested that,[24] at physiological pH, the active site largely contains the catalytically active thiolate imidazolium zwitterionic pair.

The basic features involved in the catalytic mechanism of cysteine proteases are presented in Scheme 7. The first step is the formation of the non covalent enzyme

substrate (ES) complex, followed by the acylation of the cysteine thiol group to form an acyl enzyme intermediate (EA). The latter step is initiated by the attack of cysteine thiolate on the substrate carbonyl carbon to produce a tetrahedral intermediate which then breaks down to give the ester intermediate and the amine product via a proton

Scheme 7

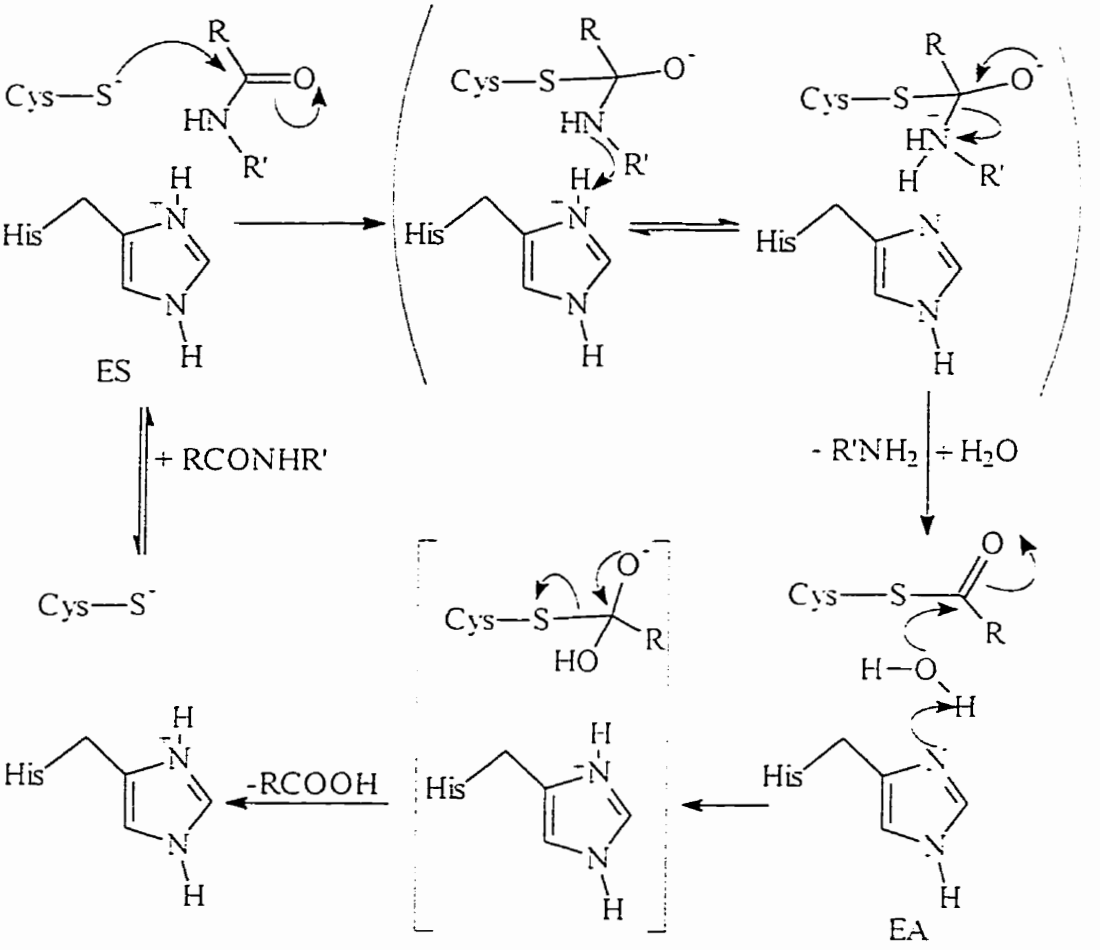

transfer from the imidazolium ion. In the following deacylation step, the histidine imidazole acts as a general base, delivering a water molecule to hydrolyse the thiol ester intermediate, subsequently regenerating the enzyme.

Small molecular models for enzymatic amide bond hydrolysis:

Enzymes are large proteins, with a major portion of the protein serving as the substrate binding site thereby controlling the specificity of the enzyme by holding the substrate in proper orientation. The catalytically active parts of the enzymes are relatively small. To investigate the detailed catalytic mechanisms, many small molecular models containing reasonable approximations of the essential functionalities of enzyme active sites have been studied.[25,26,27,28] The following section is a summary of some small molecular models of the proteases discussed above.

Small molecular models for serine proteases

Brown and coworkers have studied the reaction of a number of bifunctional molecules with the distorted[29] amide 1 as a model for the reactions believed to occur in

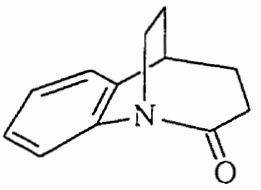

1

the active site of proteases. As the model for the acylation steps of the serine proteases, the reaction of a series of imidazole and amino alcohols such as **2-4**[30]

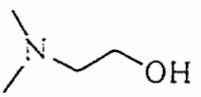

2

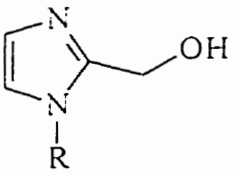

3a R = H
b R = CH_3

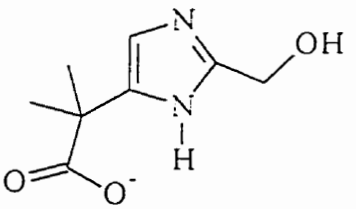

4

with 1 have been studied. In all cases, the initial products were the O-acylated esters. The

pH rate profile for acylation showed a plateau above the amine pK_a, indicating the basic (or zwitterionic) form was active, suggesting the reaction mechanism shown in Scheme 8.

Scheme 8

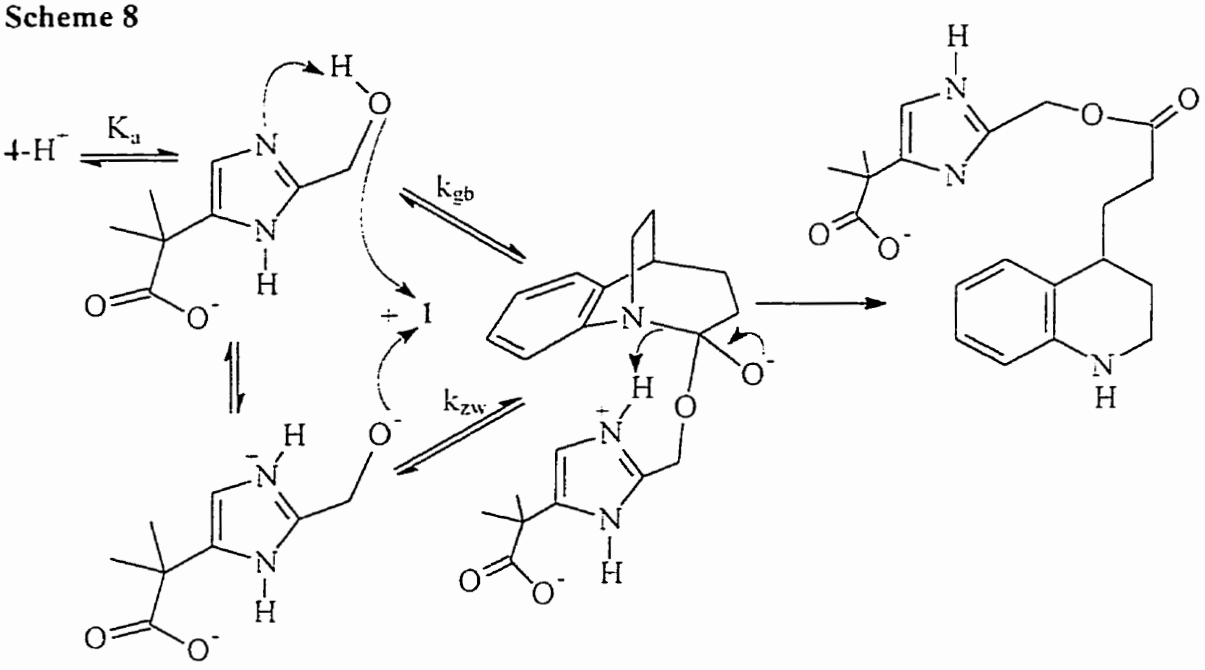

The reactivity of the amines increased with increasing ammonium ion pK_a and the plot of pK_a vs the second order rate constants for O-acylation of amino alcohols produced a straight line indicating a Brønsted relationship. The rate constant for acylation of the imidazole alcohol **4** containing the pendant carboxylate group also fit on the same Brønsted line as defined by other amino alcohols showing that the reaction rate is controlled by amine basicity. For compound **4**, the role of the carboxylate was suggested to electrostatically increase the basicity of the imidazole. The common mechanism for these amino alcohols involves either the initial nucleophilic attack of the OH with general base assistance from the pendant amino group or attack by O^- of the zwitterion to form the zwitterionic tetrahedral intermediate, $T^{\pm}$. This intermediate breaks down to the product by an intramolecular proton transfer from the pendant ammonium ion.

Solvent kinetic isotope effects (SKIE) of 1 to 2 were observed for the acylation of amino alcohols by **1**. For imidazole alcohols, the SKIE decreased with increasing amine pK_a. This effect was explained by the possible involvement of zwitterionic ammonium alkoxide (lower part of Scheme 8).

In an effort to mimic the catalytic triad of serine proteases, and to provide a binding pocket for the substrate, Bender and coworkers synthetically modified[25,31] β-cyclodextrin to include an imidazole and a carboxylate functionality in molecule (**5**). It was shown that **5**, an "artificial enzyme" as termed by the authors, significantly enhances the hydrolysis of *p-tert*-butylphenyl acetate and the suggested[25] mechanism is given in Scheme 9.

Scheme 9

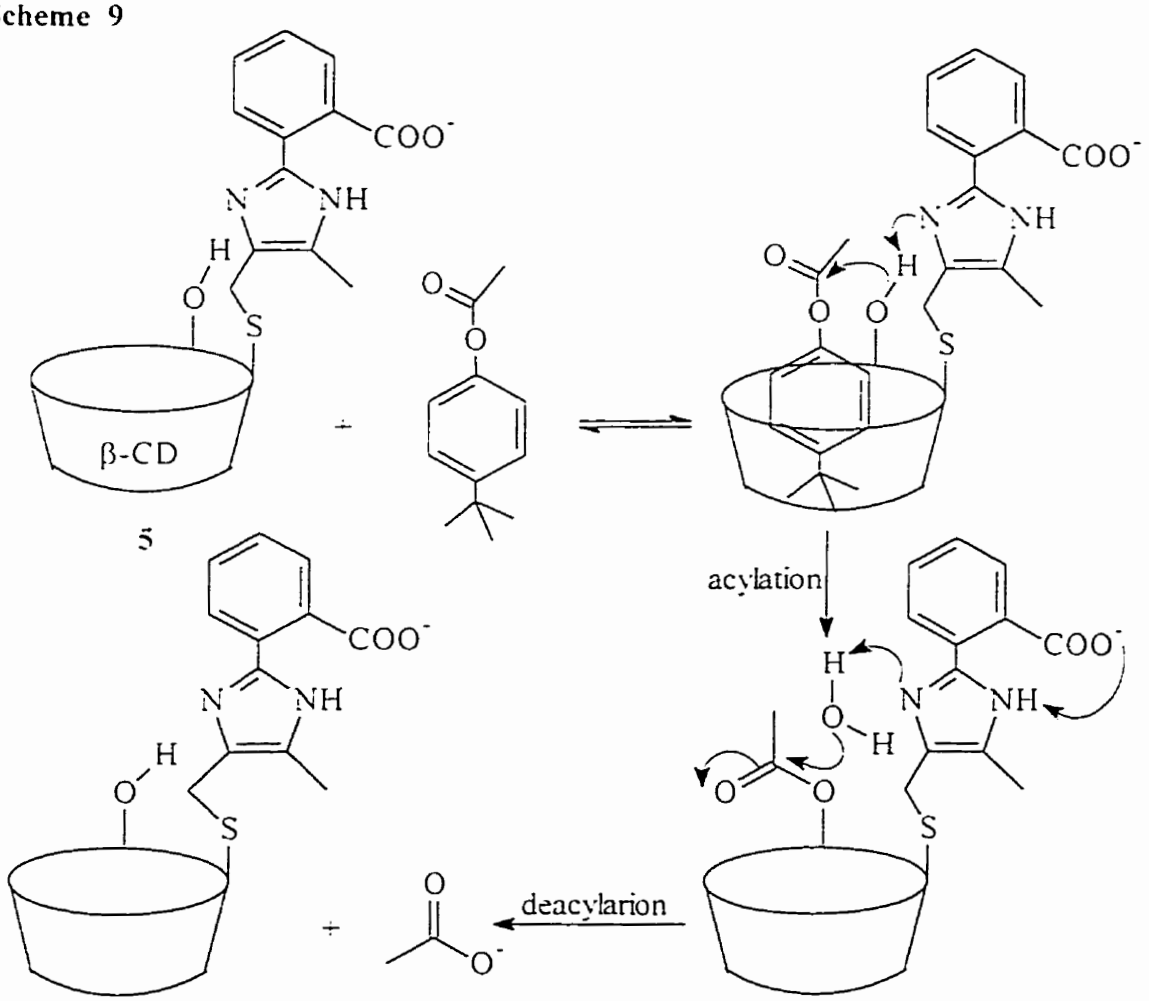

However, no amide hydrolyses catalyzed by this 'artificial enzyme' were reported. Later it was shown[32] that the imidazole and carboxylate functional groups incorporated in **5** did not participate in the hydrolysis of ester substrates by cyclodextrin, but in fact retarded the reaction because of steric hindrance.

In a recent paper,[33] De Clercq *et al* have reported the synthesis and reactivity of a series of γ-amino alcohols (**6-9**) towards esterification by acetylimidazole (**10**) and

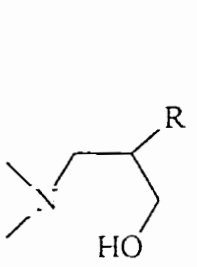

6 = H
7 = tBu

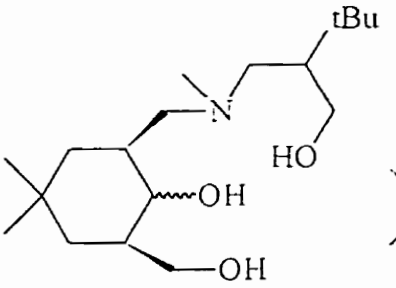

8a = *cis*
8b = *trans*

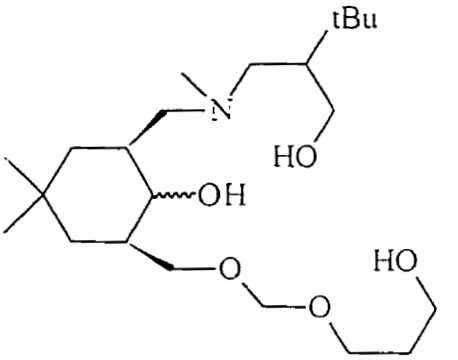

9a = *cis*
9b = *trans*

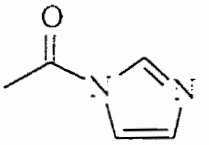

10

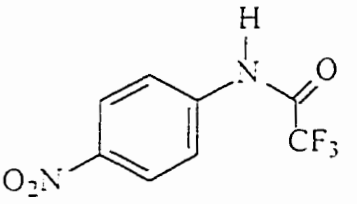

11

p-nitrotrifluoroacetanilide (**11**). The acyl transfer reactions, suggested to occur as in Scheme 10, were carried out in acetonitrile at 23 °C. The reaction of 1,6-hexanediol with **10** and **11** in acetonitrile in the presence of triethyl amine were taken as the base reactions for comparison, and the half lives ($t_{1/2}$) for these reactions were found to be

Scheme 10

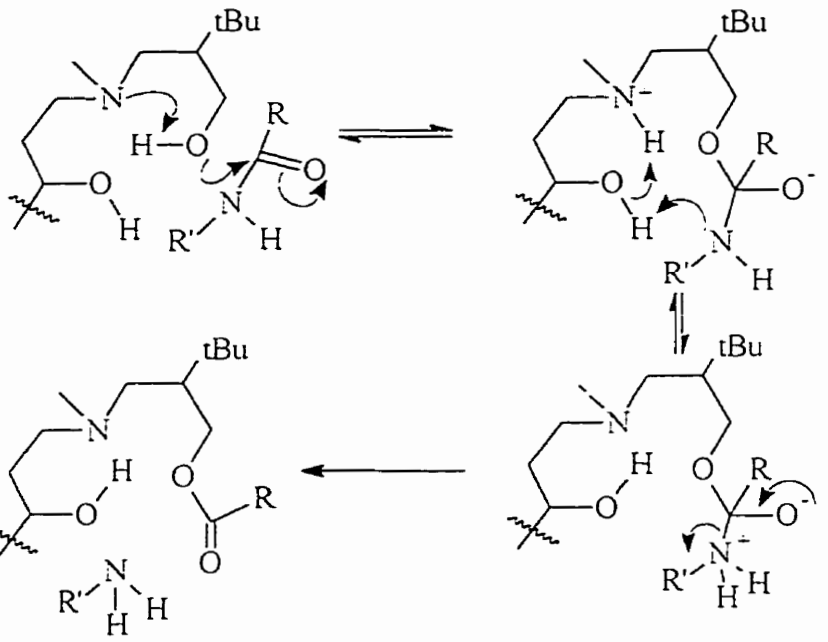

2240 hr and 412 hr, respectively. Considerable rate enhancements were observed for the reaction of amino alcohols **6-9** with acetyl imidazole (**10**) compared to the base reaction (in the best case as high as $5*10^3$ times). On the other hand, the reaction rates of **6-9** with *p*-nitrotrifluoroacetanilide (**11**) did not show as much enhancement (only about 4 times for the best case). For compounds **8** and **9**, the *cis* isomers (**8a** and **9a**) were more reactive with compound **10** than were the *trans* isomers. Compound **9a** (the *cis* isomer) was also more reactive than **9b** (the *trans* isomer) with **11**. These results were explained by a hydrogen bonding network such as that shown in **12**, which gives rise to extra stabilization of the tetrahedral oxyanion.

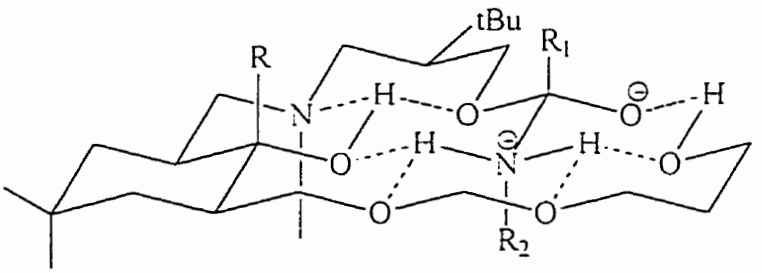

12

Small molecular models for aspartate proteases.

The hydrolysis reactions of a series of maleamic acid derivatives (**13**) were studied[34] as the model for the deacylation step of the aspartate proteases. The steps

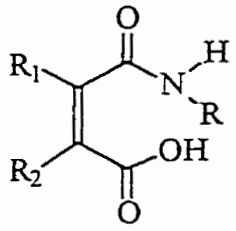

13

involved in the hydrolytic process of **13** are described in Scheme 11. As seen in the scheme, the reaction proceeds via intramolecular attack to yield maleic anhydride. The rate determining step (or steps) depends on both leaving group basicity and on the acidity of the solution.

Scheme 11

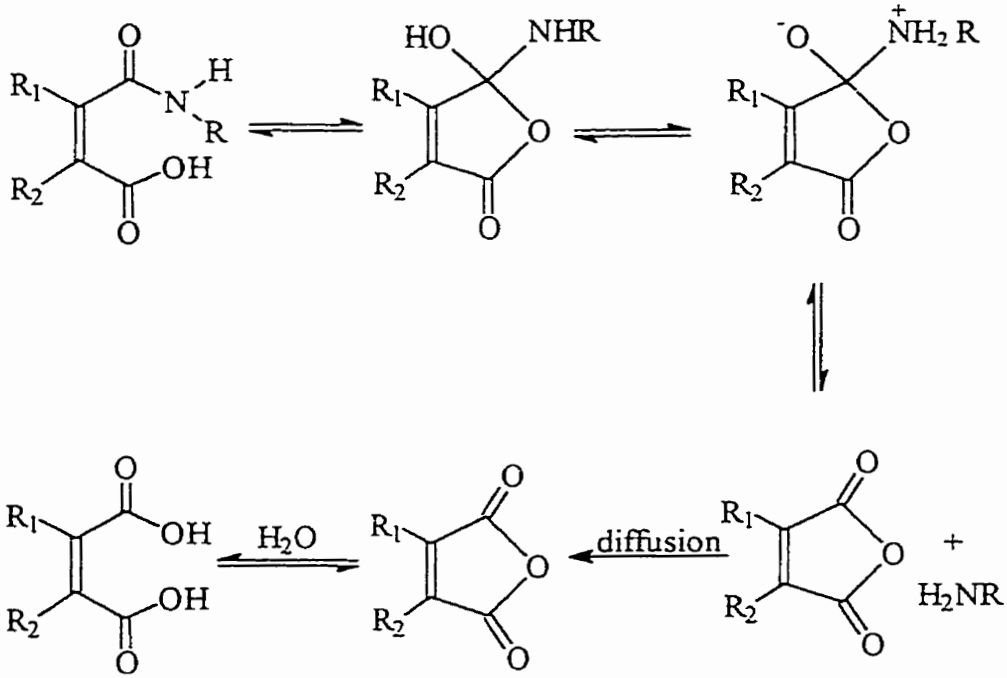

As a model for the acylation process of aspartate proteases which contain two aspartate COO(H) in the active site. Brown *et al* have studied[35] the reaction of certain carboxylic diacids with the strained amide **1**. They found that dicarboxylic acids (**14-16**)

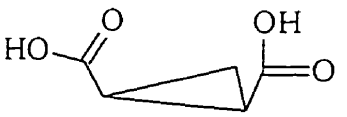

14

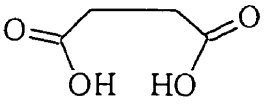

15

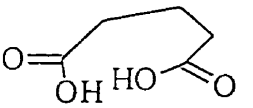

16

capable of forming cyclic anhydrides can attack **1** with high efficiency. The hydrolytic process was found (Scheme 12) to proceed through a reversible nucleophilic attack of monoanionic carboxylate on amide **1**, yielding the linear anhydride intermediate. This linear anhydride undergoes rapid intramolecular nucleophilic attack by the second

Scheme 12

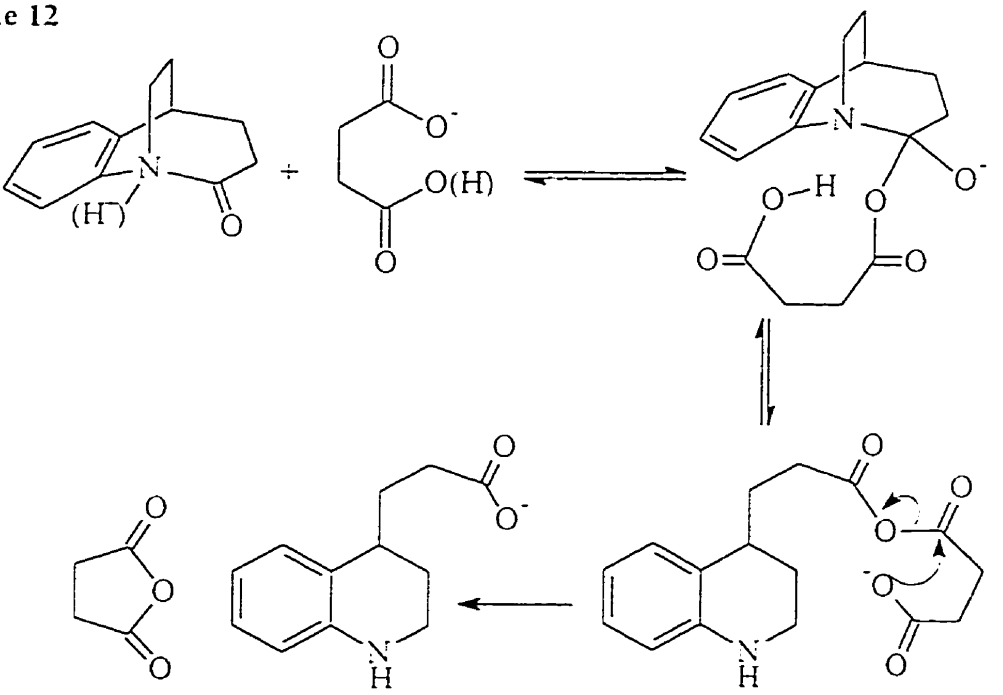

(pendant) carboxylate to form the cyclic anhydride of the diacid. In the pH-rate profile for the reaction of **14-16** with **1**, three domains were observed corresponding to attack of the monoanion on 1-H$^+$, monoanion on 1 and dianion on 1.

Small molecular models for cysteine proteases

In earlier studies,[36] Brown *et al* investigated the reaction of imidazole-thiols **17a,b** and **18** with reactive esters **19a,b** as the models for the acylation step of cysteine

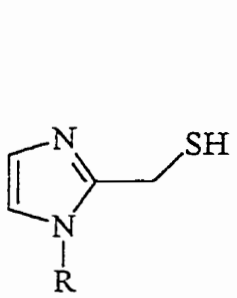

17a R = H
17b R = CH_3

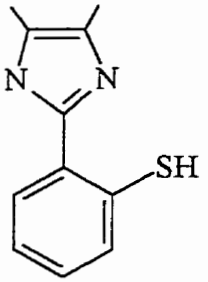

18

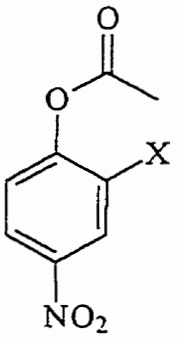

19a R = H
19b R = NO_2

proteases. More recently, Keillor *et al* in this laboratory have studied[37] the reactivity of a series of amino thiolates, **17b, 20a-c** and **21** towards the distorted amide **1**. In the former

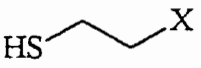

20a X = NH_2
20b X = $N(CH_3)_2$
20c X = CH_2NH_2

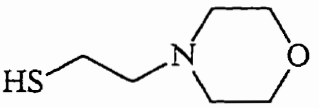

21

studies, it was seen that although the ammonium thiolates showed high reactivity towards **1**, neither thiolates nor amines/ammonium alone was reactive. While the thiolate functionality was required for the initial nucleophilic attack on the carbonyl carbon of the amides, the pendant ammonium (or imidazolium) was needed to serve as a general acid to supply a proton to the unstable intermediate. The reaction of **17b** with **1** showed a bell shaped pH-rate profile indicating that only the zwitterionic ammonium thiolate was the reactive species. The overall reaction of ammonium thiolates with amides is summarized

in Scheme 13 (only **17b** and **1** are shown), where the initial attack on the amide carbonyl carbon from the zwitterionic ammonium thiolate leads to the tetrahedral intermediate $T^{\pm}$.

Scheme 13

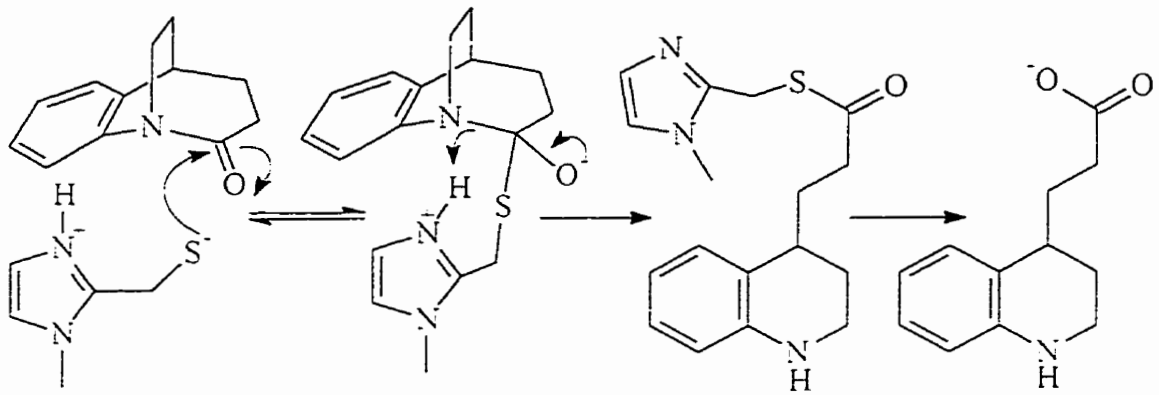

This intermediate is then captured by a proton transfer from the pendant imidazolium group to form the thiol ester, which subsequently hydrolyses to the open amino acid. In subsequent studies,[38] hydrolysis of four nonactivated amides (**22a-c**) and **23** were followed in the

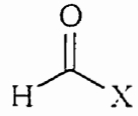

22a X = NH_2
22b X = $N(CH_3)_2$
22c X = NHPh

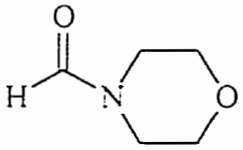

23

presence of **17b** and the same general features were observed.

All model systems for acylation indicate that for good catalysis one needs a bifunctional nucleophile where one group acts as the nucleophile, while the other as a proton transfer agent. The unifying feature of such catalysts is that at each intermediate stage of the reaction, the catalyst is born in a state of protonation where it facilitates the next reaction.

Intramolecular hydrolysis of thiol esters: Model for deacylation of cysteine proteases.

As seen in Scheme 7, the acyl enzyme (thiol ester) is hydrolysed in a deacylation step via a general base assisted delivery of water by the active site histidine imidazole. To investigate the intramolecular role of imidazole, the hydrolysis of several imidazole containing thiol esters, such as **24** and **25**, had been studied.[39,40] However, in these studies it was found that the pendant imidazole acted as a nucleophile rather than as a general base to effect S to N acyl transfer prior to hydrolysis.

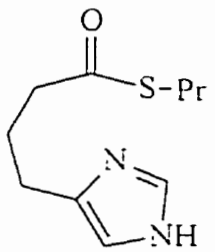

24

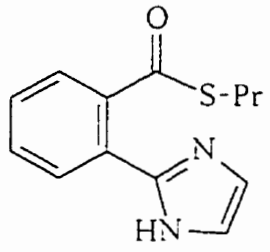

25

Bruice has studied[39] the hydrolysis of **24** at various pHs. The proposed mechanism involved reversible formation of lactam **24a** (Scheme 14) via an initial nucleophilic attack of the deprotonated pendant imidazole. This lactam then slowly hydrolysed to give the imidazole acid, **24b**. However, in the presence of added thiol, **24a** reformed the initial thiol ester, and at high enough concentration (ca 0.2M) of free thiol the hydrolysis of **24** was completely inhibited. This demonstrated the reversibility of the formation of lactam **24a**.

Scheme 14

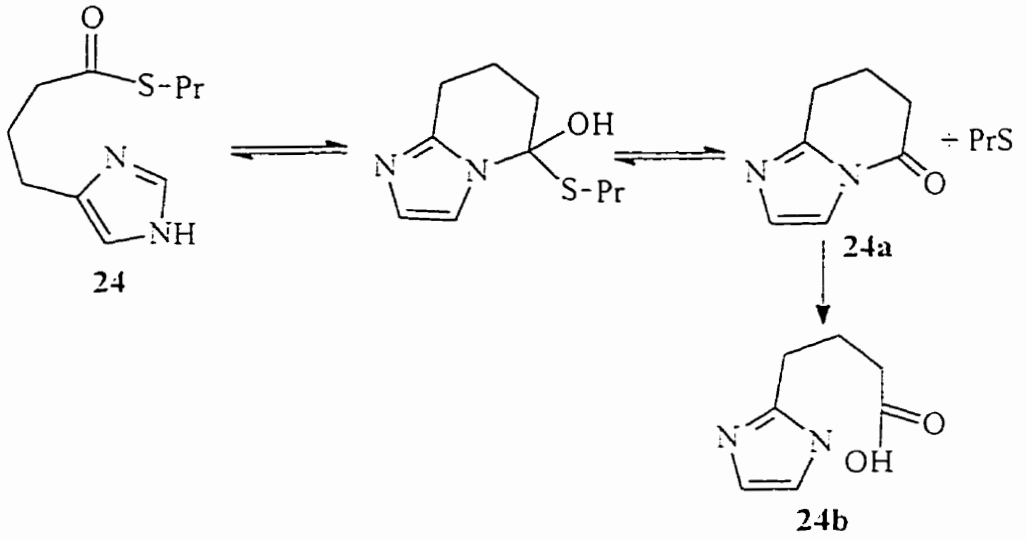

In another paper, Fife and DeMark reported the intramolecular aminolysis of thiol ester **25**.[40] They found (Scheme 15) that the formation and reversal (to the starting thiol ester **25**) of the tetrahedral intermediate, T^0, proceeding through nucleophilic attack by the imidazole moiety was an equilibrium process. The breakdown of the intermediate T^0 was subject to intermolecular general base catalysis yielding the lactam **25a**, which was subsequently hydrolysed. No intramolecular general base assistance from the imidazole

Scheme 15

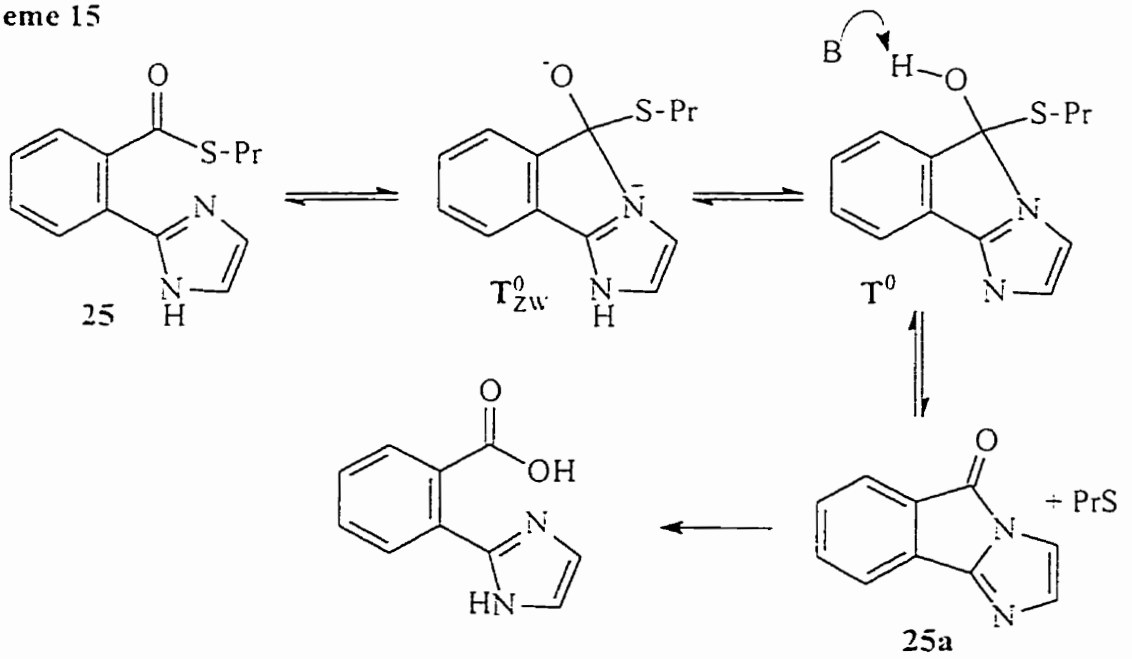

pendant was observed. However, it should be noted that in these small molecular models, the pendant imidazole is on the acyl part of the molecule and, as a result, the thiol part of the molecule is expelled upon ring closure, whereas in the enzyme the imidazole and the thiol remain in the active site.

More recently Brown *et al* have studied[36b,41] the hydrolytic reaction of the thiol esters **26-28** as a function of pH. Solvent deuterium kinetic isotope effects on the

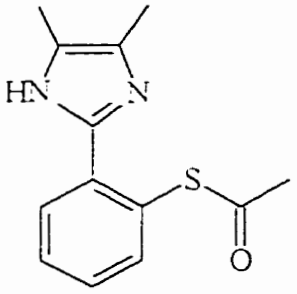

26

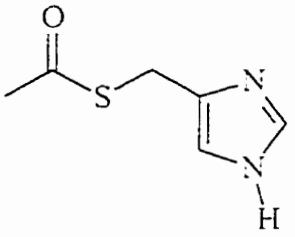

27

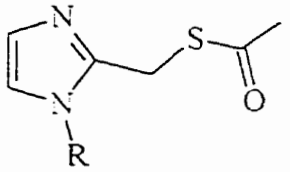

28a R = H
28b R = CH_3

hydrolysis were also studied for **26** and **27** at neutral pH and were found to be 3.8 and 1.9, respectively. Experiments performed in the presence of thiolate trapping reagents (Ellman's reagent) showed that acyl transfer from S to N (*i.e.* an intramolecular nucleophilic reaction) was not an important process. From these observations, it was suggested that the major hydrolytic pathway for these thiol esters at neutral pH proceeds through a mechanism in which the pendant imidazole acts as a general base. The proposed hydrolytic mechanism is shown in Scheme 16, using **28b** as an example.

Scheme 16

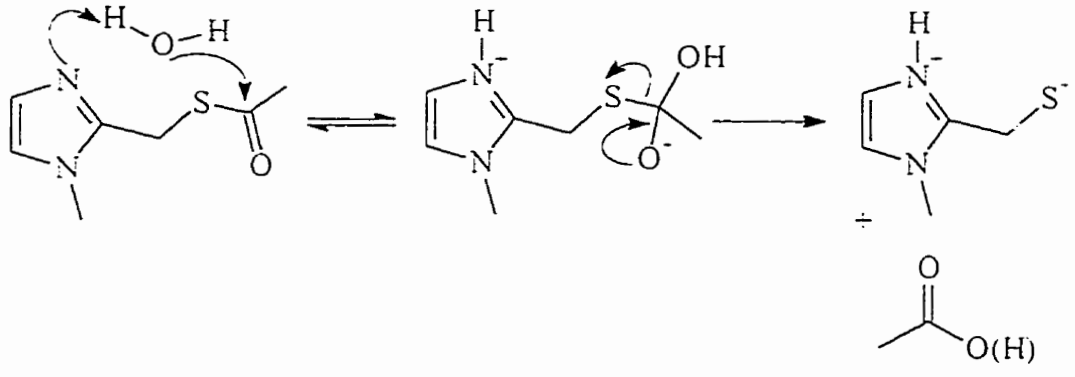

CHAPTER 2

A. Objective of this work.

All three classes of naturally occurring non-metallo enzymes have a nucleophile (or a general base) and a group which acts as a general acid in the enzyme active site. Although the mechanistic details of aspartate protease are still uncertain, the steps involved in the amide bond hydrolysis by all three non-metallo proteases have similarities (Scheme 2- 4 and 7). In each case, the first step is a nucleophilic attack by the enzyme on the carbonyl carbon of the substrate. However, it should be noted that in a recently proposed mechanism[17,18] (Scheme 5) for amide bond hydrolysis by aspartate protease, the first step is attack of H_2O with general base assistance from an Asp-COO^-. In all cases, the next step is the nitrogen protonation of the departing amine by an active site general acid prior to, or concerted with, C-N cleavage. To mimic these catalytic features of proteases, bifunctional molecules containing nucleophilic/acid-base groups have been studied in this laboratory, and recent work has shown that the distorted aniline 2,3,4,5-tetrahydro-2-oxo-1,5- ethanobenzazepine, **1**, is susceptible towards nucleophilic attack by bifunctional nucleophiles such as β-amino alcohols,[30] β-amino thiols[36,37,38] and dicarboxylic acids which are capable of forming cyclic anhydrides.[35] These reactions mimicked chemical processes belived to occur in the active site of serine, cysteine, and aspartate proteases, respectively. The common feature of the reaction of bifunctional nucleophiles is that after the initial attack, the acid/base pendant is born in a state of ionization that is correct for assisting the subsequent step. To study the effect of other pairs of nucleophilic/acid-base groups that are not simultaneously present in a natural

protease, and to develop a catalyst for amide hydrolysis at neutral pH, the reaction of **1** with thioglycolic acid, **29**, and ethyl-2-mercaptoacetate, **30**, have been investigated.

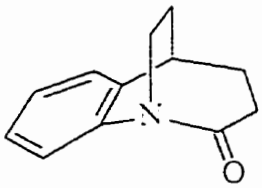

1

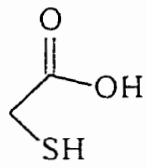

29

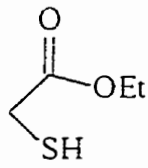

30

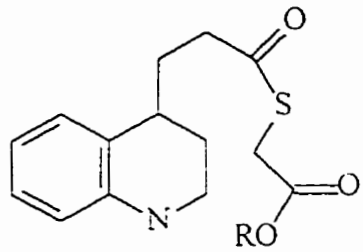

31a R = H
31b R = Et

Preliminary work from these laboratories[42a] has shown that the reaction of **1** and both **29** and **30** produce the corresponding thiol ester, and part of the pH rate profile for **29** with **1** from pH 4.0 - 9.0 and pH 10.5 - 10.9, were obtained. However, the second order rate constants of the reaction of **29** with **1** at pHs lower than the first pK_a (3.55) of **29** were not obtained, and consequently the reaction mechanism at lower pH was unclear. In addition, data closer to second pK_a (10.22) of **29** was missing from the previous study. Thus, to determine the reaction mechanism at lower pH and to define completely the pH rate profile, the second order rate constants of **29** reacting with **1** at low pH and at pHs close to the pK_a's of **29** were obtained in the present work.[42b]

B. Experimental.

Materials and Methods.

The following compounds were obtained from different commercial suppliers: thioglycolic acid (Aldrich), sodium thioglycolate (Sigma), 5,5'-dithio-bis(2-nitrobenzoic acid) (DTNB; Ellman's reagent) (Sigma), potassium chloride (BDH), potassium dihydrogen orthophosphate (BDH) and potassium hydrogen orthophosphate (BDH). 2,3,4,5-Tetrahydro-2-oxo-1,5-ethanobenzazepine (**1**), was synthesized by a previous[42a] worker using methods described by Brown *et al.*[29] Acetonitrile was dried over 3A molecular sieves and distilled from phosphorous pentoxide under argon. Purified and deoxygenated water from an Osmonics Aries water purification system was used for all buffer preparations and these were further degassed by bubbling Ar through them for several hours before use. All pHs were measured using a Radiometer Vit 90 Video Titrator equipped with a GK2321C combined electrode, standardized by Fisher certified pH 2.01, 4.00, 7.00 and 10.00 buffers.

Kinetics.

At pH 2.0 to 2.2, HCl (titrated) was used as the buffer, μ = 1.0 (KCl). Thioglycolic acid was used as the buffer at pHs close to the pK_as of thioglycolic acid (pK_1 = 3.55 and pK_2 = 10.22). At high pH (~10) the rate of ring opening of the strained amide 1 in the presence of excess thiol was followed by observing the increase in absorbance at 291 nm. At lower pH (2-3.5) the rate of reaction was followed by observing the decrease in absorbance of 1 at 230 or 240 nm. A modified Cary-17 UV-vis spectrophotometer interfaced to an IBM 486 PC fitted with OLIS software (On-line

Instrument Systems. Jefferson. Ga., 1992) was used to follow the reaction at high pH values. In a typical run 3 mL of deoxygenated thioglycolate buffer ([buffer] = 0.05 to 0.20 M, μ = 1.0 (KCl)) was transferred to Ar flushed cuvettes which were then thermally equilibrated in the cell holder of the spectrophotometer for 10 min. at 25 °C. To initiate the reaction, 10 μL of 0.08 M stock solution of 1 in dry acetonitrile was injected in to the cuvettes. The final pH of the cuvettes was measured after each run to ensure constancy of pH. At lower pH, the rate of the reaction was followed by a Sequential Stopped Flow ASVD Spectrophotometer from Applied Photophysics (UK), interfaced with an Arcon A5000 PC fitted with RISC OS3 software. One drive syringe was loaded with a 3.2×10^{-4} M solution of 1 in dilute phosphate buffer (pH = 6.9, [buffer] = 2×10^{-4} M, μ = 1.0 (KCl)). The other drive syringe was loaded with a solution of thioglycolic acid in HCl buffer ($[thiol]_{total}$ = 0.10 to 0.40 M, μ = 1.0 (KCl)). In all cases an excess of thiol of at least 10-fold (over [amide 1]) was used so that reactions were pseudo-first order. The pseudo-first order rate constants (k_{obs}) were obtained for each run by nonlinear least squares (NLLSQ) fitting of the absorbance (A) vs time (t) data to a standard exponential model ($A_t = A_\infty + (A_0 - A_\infty) \exp(-kt)$). The second order rate constants (k_2^{obs}) were obtained from the slopes of plots of k_{obs} vs $[thiol]_{total}$ at each pH (3-4 thiol concentrations were used).

Thiol solutions were titrated with Ellman's reagent[43] in order to determine the concentration of free thiols.

C. Results.

The pseudo-first order rate constants (k_{obs}) of the reaction of the strained amides **1** $(1.3 - 2.6)*10^{-4}$ M with thioglycolic acid, **29**, to give the corresponding thiol ester **31a** were obtained at various pH values and $[thiol]_{total}$ at 25 °C, μ = 1.0 (KCl). The runs were followed by observing the rate of decrease in absorbance at 230 or 240 nm at low pH (pH<3.5) using a stopped flow spectrophotometer and by following the increase in absorbance at 291 nm at higher pH using a UV-vis spectrophotometer. The pseudo-first order rate constants (k_{obs}) are given in Appendix 2, Table 1S.

At each pH, k_{obs} was obtained at 3 or 4 different $[thiol]_{total}$. The observed second order rate constants (k_2^{obs}) were obtained from the slope of a plot of k_{obs} vs $[thiol]_{total}$ at each pH according to eq 1.

$$k_{obs} = k_0 + k_2^{obs}[thiol]_{total} \qquad (1)$$

where k_0 is the background reaction (combination of acid, base and water reactions). The values of k_2^{obs} at various pHs are given in Table 1 and the pH vs rate constant profile for the reaction of **29** with amide **1** is shown in Figure 1. As seen in Figure 1, going from high pH (> 10) to lower pH, the pH-rate profile increases with decreasing pH until the second pK_a of **29** (pK_2=10.22), whereupon the profile attains a limiting plateaued value down to pH 2. It should also be noted that there is a small and almost imperceptible inflection at the first pK_a of **29** (pK_1 =3.55) followed by another plateau. The second order rate constant k_2^{obs} could not be obtained below pH 2 since background acid catalyzed reactions become faster and high absorbancies were encountered. The pH rate profile of the reaction of **29** with amide **1** can be explained by the processes described in

Table 1. Second order rate constants for the reaction of thioglycolic acid (**29**) with the strained amide 1 obtained at various pH. T = 25 °C, μ = 1.0 (KCl).

pH	Buffer	[buffer] (M)	k_2^{obs} (M^{-1} s^{-1})[a]
2.02	HCl	9.5×10^{-3}	1.46 ± 0.15
2.19	HCl	6.5×10^{-3}	1.38 ± 0.17
3.43	thioglycolic acid	0.05-0.20	1.72 ± 0.10
4.00[b]	thioglycolic acid	0.05-0.20	1.60 ± 0.15
4.50[b]	Acetate	0.05	1.78 ± 0.18
5.16[b]	Acetate	0.20	1.41 ± 0.02
5.40[b]	MES	0.05	1.52 ± 0.15
5.90[b]	MES	0.05	1.35 ± 0.04
7.00[b]	MOPS	0.05	1.73 ± 0.17
7.08[b]	Phosphate	0.20	1.69 ± 0.18
7.20[b]	1,2-dimethylimidazole	1.00	1.33 ± 0.08
7.94[b]	HEPES	0.05	1.65 ± 0.15
8.20[b]	HEPES	0.20	1.46 ± 0.08
9.00[b]	CHES	0.05	1.86 ± 0.05
9.75	thioglycolic acid	0.05-0.20	0.83 ± 0.01
10.06	thioglycolic acid	0.05-0.20	0.78 ± 0.06
10.47	thioglycolic acid	0.05-0.20	0.27 ± 0.06
10.50[b]	thioglycolic acid	0.05-0.20	0.432 ± 0.003
10.90[b]	thioglycolic acid	0.05-0.20	0.24 ± 0.03

[a]The errors quoted are obtained from the standard deviation in the slope calculated by the linear regression fitting of k_{obs} vs $[thiol]_{total}$ data to eq 1 at each pH.

[b]Obtained from reference 42a.

Figure 1. Plot of the log second order rate constant (k_2^{obs}) for the attack of thioglycolic acid (**29**, ●) and ethyl 2-mercaptoacetate (**30**, ■, data obtained from reference 42a)on the strained amide **1** at various pH, T = 25 °C, μ = 1.0 (KCl). The solid lines are computed from the NLLSQ fit of the data to eq 2. and eq 4. The dashed line is obtained excluding k_2 from eq 2.

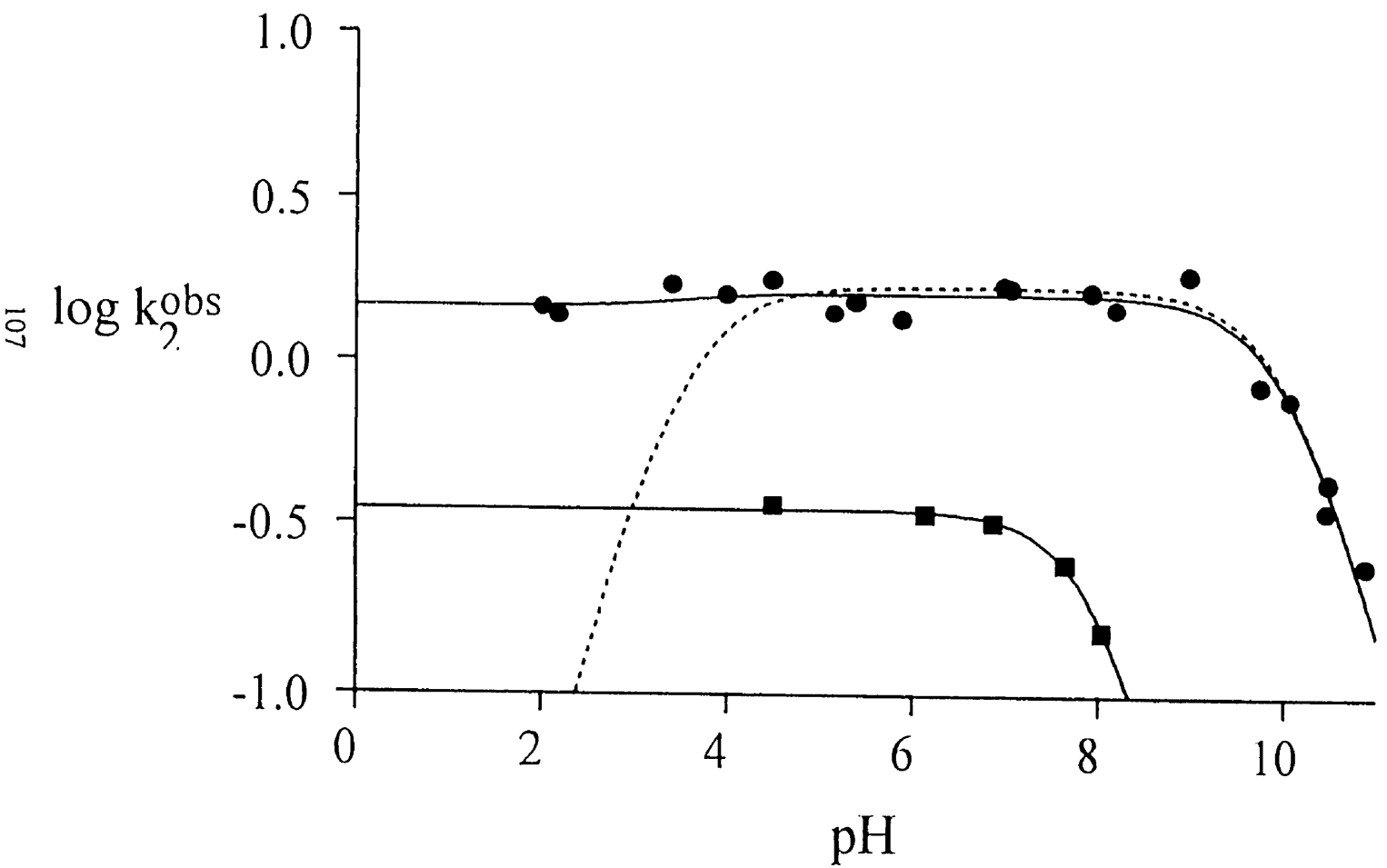

Scheme 17, where the monoanionic form of thioglycolic acid **M** can react with both the neutral and protonated form of amide **1** to give products. From this scheme, it can be

Scheme 17

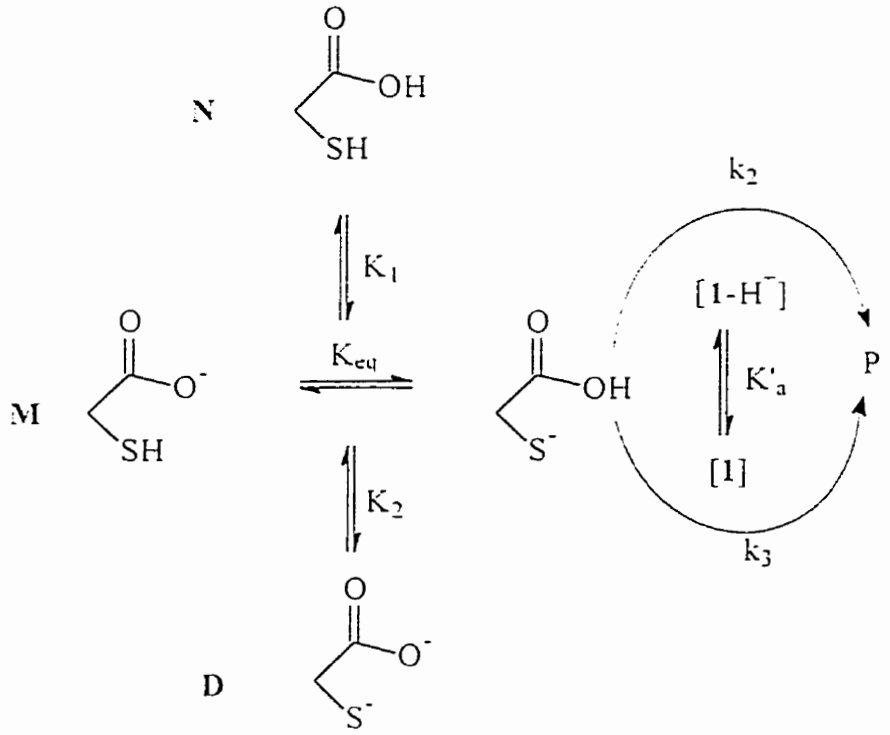

shown that the observed rate constant k_2^{obs} at a given pH, when $[H^-] << K'_a$, can be described by eq 2.[44]

$$k_2^{obs} = ((k_2/K'_a)K_1[H^-]^2 - k_3K_1[H^-])/([H^-]^2 + K_1[H^-] + K_1K_2) \qquad (2)$$

where k_2 and k_3 are the rate constants for attack of a monoanionic **M** on the protonated, 1-H^-, and neutral amide **1** respectively. K_1 and K_2 are the first and second macroscopic dissociation constants for thioglycolic acid and K'_a is the dissociation constant of protonated amide **1**. The solid line through the data in Figure 1 was obtained by non-linear least square (NLLSQ) fitting of the data in Table 1 to eq 2, where the known values of K_1 ($2.82*10^{-4}$ M),[45] K_2 ($6.02*10^{-11}$ M) [45] and K'_a (1.9 M)[46] were fixed as constants. From the fit, values of k_2 and k_3 can be obtained as $9.9*10^3$ M^{-1} s^{-1} and 1.63 M^{-1} s^{-1}.

D. Discussion

Mechanism at low pH.

The observed variations in the second order rate constant, k_2^{obs}, for the reaction of thioglycolic acid **29** with amide **1** at various pHs, is consistent with the process depicted in Scheme 17, where a monoanionic thioglycolic acid **M** reacts with both neutral and protonated amide **1**. In eq 2, both processes, namely attack of **M** on 1-H$^+$(k_2) and attack of **M** on neutral **1** (k_3), have been incorporated into the NLLSQ fit of the experimental data to the equation which generates a line passing through most of the points. However, when the k_2 (the term describing a attack of **M** on 1-H$^+$) is excluded from eq 2 (*i.e.* k_2 = 0) the fit to the experimental data is poor in the low pH region, as is indicated in Figure 1 by the dotted line. In absence of the attack of **M** on 1-H$^+$, the observed rate constant would have to drop linearly with pH below 3.55, which is the first pK_a of **29** (pK_1 = 3.55). None of the above data allows us to ascertain which monoanionic form of thioglycolic acid is responsible for the attack on 1-H$^+$.

However, some guidance for the species responsible for attack on **1** at various pH values can be obtained from the reaction of the blocked derivative **30**.[42a] Kellogg has shown[42a] that for the reaction of ethyl 2-mercaptoacetate **30** with **1**, the pH rate profile shows a plateau at low pH, followed by a linear decrease at pH values above the pK_a (8.0) of the thiol,[42b] consistent with the process described in eq 3, where the monoanionic

$$\begin{array}{ccc} EtOOCCH_2SH & \rightleftharpoons & EtOOCCH_2S^- \xrightarrow[[1\text{-}H^+]]{} P \\ & & \Big\| K'_a \\ & & [1] \end{array} \qquad (3)$$

30 attacks 1-H^-. Fitting the experimental k_2^{obs} vs pH (see Figure 1) data to the kinetic expression given in eq 4, derived from eq 3, gives a value of be $6.35*10^7$ M^{-1} s^{-1} for k_2, the rate constant

$$k_2^{obs} = (k_2/K'_a)K_a^{SH}[H^-]/(K_a^{SH} + [H^-]) \qquad (4)$$

for the attack of monoanion of **30** on 1-H^-. The large apparent (almost 4 orders of magnitude) difference between the rate constant (k_2) for the attack of **M** of **29** on 1-H^- ($9.9*10^3$ M^{-1} s^{-1}) and that of **30** on 1-H^- is noteworthy. One expects that the nucleophilicity of these two thiolates, $EtO_2CCH_2S^-$ and $HO_2CCH_2S^-$, should not substantially differ towards 1-H^-, with only minor differences potentially arising from variation in the pK_as of the thiols. To explain the large apparent difference in k_2 values between the thiols **29** and **30** we need to analyze the various microscopic forms of thioglycolate as in Scheme 18. Note that the dominant monoanionic form of **29** is thiocarboxylate, **29**-COO^-, since carboxylic acids are more

Scheme 18

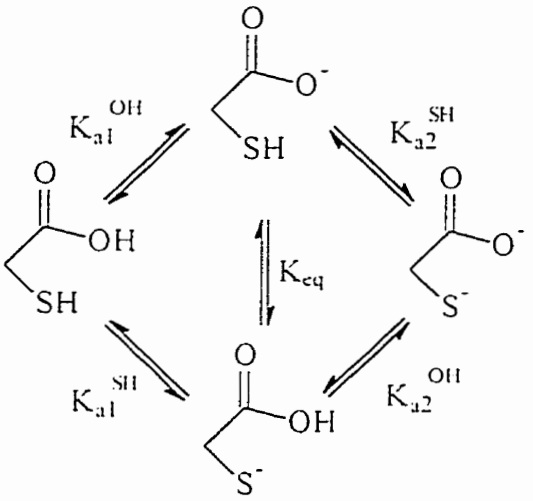

acidic than thiols. The first macroscopic pK_2 of **29** (3.55) is mostly attributable to the microscopic pK_a of **29**-COOH (hence, $pK_{a1}^{OH} \approx 3.55$ in Scheme 18). It can also be reasonably assumed that the dissociation constant of **29**-SH would be similar to that of

30-SH: thus pK_{a1}^{SH} is equal to ~8.0. Given the above, the ratio [$^-$OOC-**29**]/[**29**-S$^-$] at any given pH is calculated to be $2.8*10^{-4}$. It follows then, that only a small part of the total monoanionic species of **29**, **M**, represents the thiolate, **29**-S$^-$. The corrected second order rate constant for the attack of **29**-S$^-$ on **1**-H$^+$ is ($9.9*10^3$ M^{-1} s^{-1} x $2.8*10^{-4}$) = $2.8*10^8$ M^{-1} s^{-1}, which is similar to that obtained for **30**-S$^-$ attack on **1**-H$^+$, indicating that both proceed via thiolate attack on the protonated amide **1**.

Mechanism at pH>4.

At pHs above 4 and below 9, thioglycolic acid exists mostly as the monoanion **29**-COO$^-$ and for the reasons described above. Although product analysis[42] revealed that the reaction of **29** with **1** produced the corresponding thiol ester **31a**, suggesting a process where **29**-S$^-$ attacks **1** or **1**-H$^+$, two other possible mechanisms can be envisioned, Scheme 19. The second mechanism proceeds via an initial attack of **29**-COO$^-$ on **1** to produce the

Scheme 19

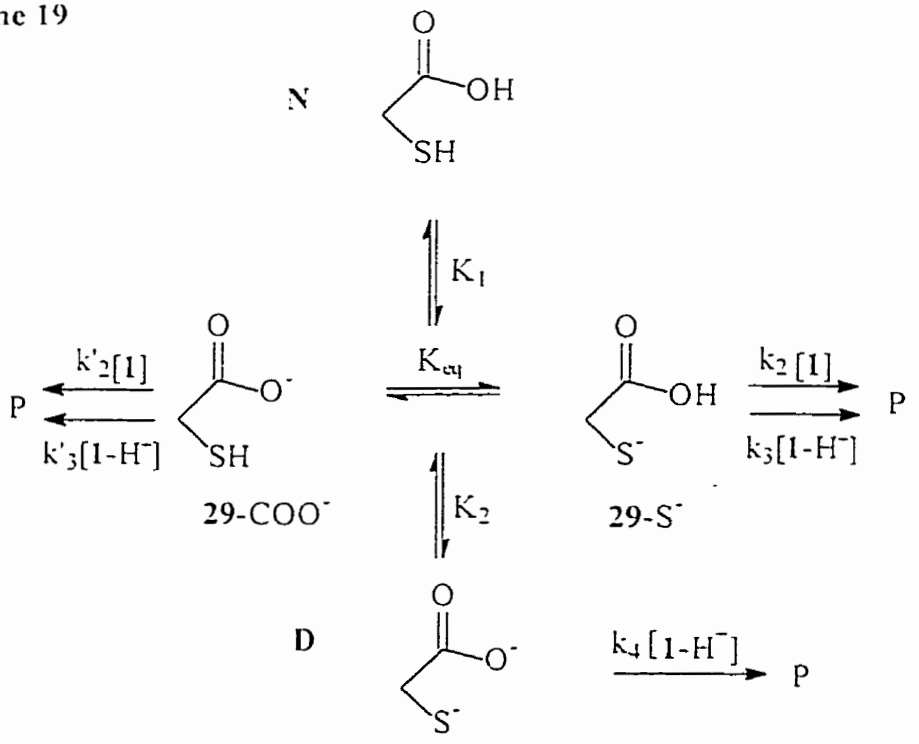

intermediate anhydride, which subsequently breaks down to **31a** in a fast step, Scheme 20. Although in this pH region, **29**-COO$^-$ is the dominant anion it should also be noted

Scheme 20

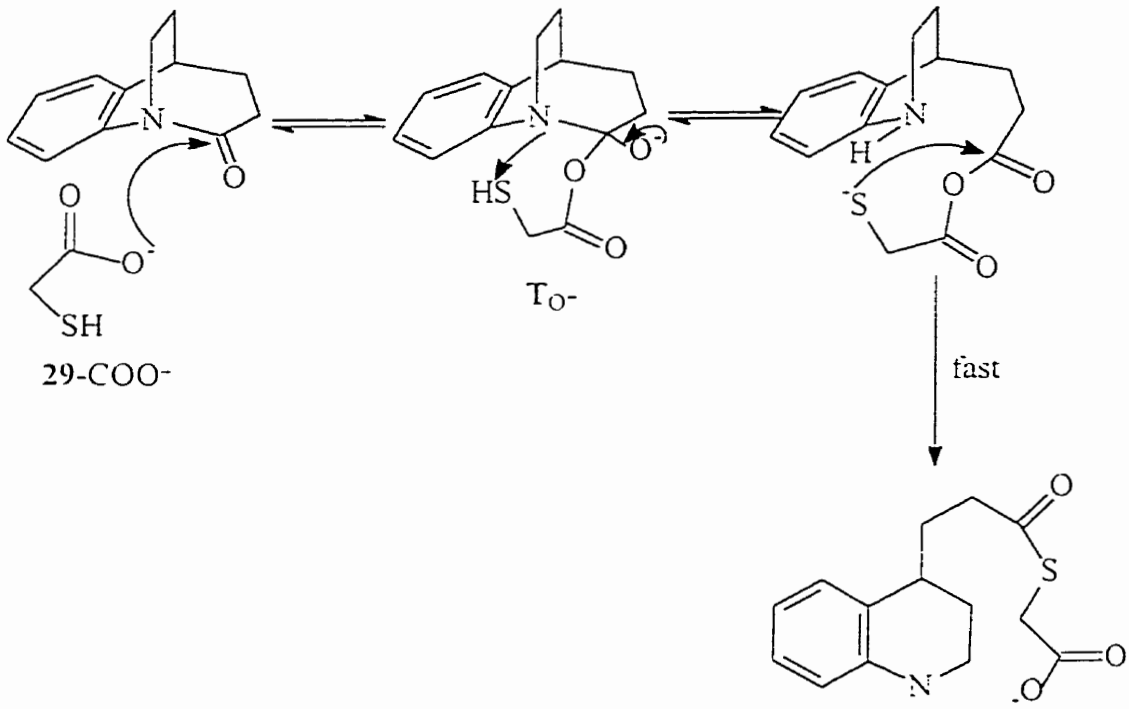

that carboxylates are much less nucleophilic than thiolates[47] and no activity was detected[35,46] for acetate with neutral **1** although acetate does react with **1**-H$^+$.[46] Hence it might be expected that the attack of **29**-COO$^-$ on **1** should also be negligible. However, considering the presence of the SH pendant in **29**-COO$^-$ it might be argued that the activity of **29**-COO$^-$ is not similar to that of simple carboxylic anions, and that there may be an intramolecular proton transfer from the SH to trap the tetrahedral intermediate ($\mathbf{T}_O^-$) in a subsequent step after the initial nucleophilic attack, Scheme 20. If this process were operative, glycine zwitterion, **32**$_{ZW}$, which is isostructural to **29**-COO$^-$, should show a similar second order rate constant for reaction with **1** to that of **29**-COO$^-$. However, it was found[42] that the glycine zwitterion is 200 times less reactive than **29**-COO$^-$. Thus, it

32 **32_{ZW}**

can be concluded that at this pH region the reaction of monoanion of **29** with **1** does not proceed via an anhydride intermediate.

The third mechanism, operative throughout the plateau region from pH 3.5 to 10, might be a kinetically equivalent process where the thiolate dianion, $^-$S-**29**-COO^- attacks the protonated amide **1**. It can be inferred from the above discussion that the thiolate part of the dianion would attack **1**-H^+, not the carboxylate moiety also because the pH profile should be linear in $[H^+]$ if the COO^- part of the dianion of **29** were nucleophilic towards **1**-H^+. However, the second order rate constant (k_4, Scheme 19) for such a process would be $5.2*10^{10}$ M^{-1} s^{-1}, which is at the higher end for a diffusion controlled[48] process, considering the reaction involves a dianion ($^-SCH_2$-COO^-) and a positively charged (**1**-H^+) species. It should be noted that the reaction of $HOOCCH_2S^-$ with **1**-H^+ proceeds with rate constant of $2.8*10^8$ M^{-1} s^{-1}, which is 200 times smaller than that of $^-SCH_2COO^-$. There is an increase in the pK_a of the thiolate of $HSCH_2COO^-$ (pK_a = 10.2) relative to that in $HOOCCH_2SH$ (pK_a^{SH} = 8), which may result in an increase in thiolate nucleophilicity.[49] The reaction of the anions of thiols of comparable pK_a should have similar rate constants for this process. However, the second order rate constant ($2*10^9$ M^{-1} s^{-1})[37a] for the reaction of the thiolate of ethanethiol, which has slightly higher pK_a (10.55)[50] than $^-OOCCH_2SH$, is 20 times smaller than that of the latter thiolate. As mentioned above, there may be some kinetic enhancement due to the attack of an anion on a positively charged substrate that could account for the extra factor of 20. However,

there is no significant difference between the rate constant for the attack of the zwitterionic (though formally neutral) dimethyl cysteamine versus the attack of anionic mercaptopropionitrile on **1**-$H^{\pm}$, indicating that there is no enhancement of the reactivity due to the overall charge of the nucleophilic species. Thus, it can be concluded that the attack of $^{-}S\text{-}CH_2\text{-}COO^{-}$ on **1**-$H^{\pm}$ is not responsible for the reaction from pH 10 to 3.5.

There exists another possibility where the SH attacks **1** with intramolecular general base assistance from carboxylate to produce T_O^{-} as in Scheme 21.General base

Scheme 21

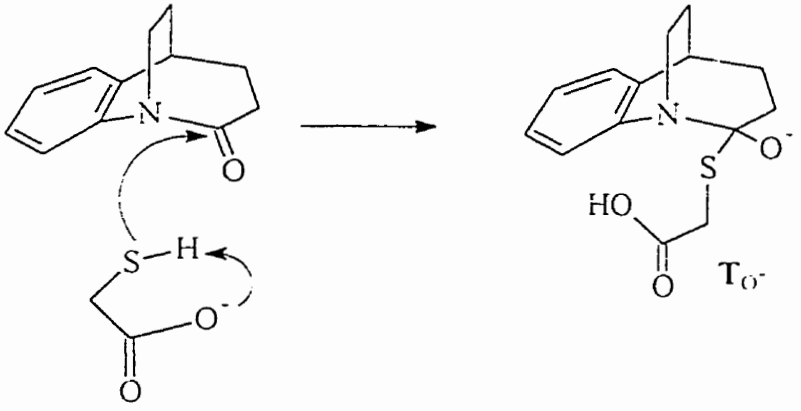

assistance of thiol attack has not been observed previously[51] in systems such as RSH plus *p*-nitrophenyl acetate; at this point, this intramolecular process, while unlikely, cannot be ruled out with certainty.

It follows from the above discussion that the favored mechanism at neutral pH proceeds with the attack of the thiolate monoanion, **29**-S^{-} on neutral **1** to give the intermediate T_O^{-}, Scheme 22. In the subsequent steps, the intermediate T_O^{-} is captured by a proton transfer from the pendant COOH to form T_N^{-} which ultimately breaks down to form the thiol ester **31a**. It should be noted that the mechanism outlined in Scheme 22 is similar to that proposed by Keillor *et al* for the reaction of ammonium thiolates[37a] on **1**.

Scheme 22

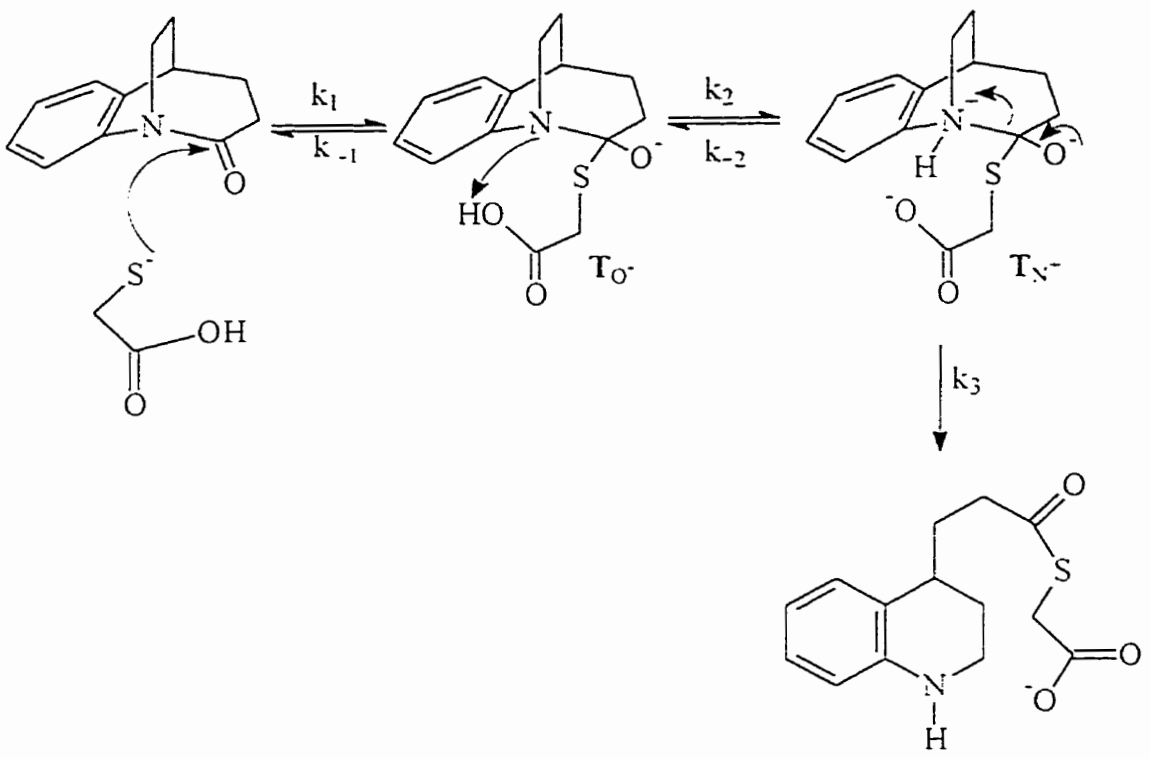

From fits of the k_2^{obs} data vs pH to eq 2 the observed second order rate constant (k_3) for the attack of **29**-S^- on neutral **1** is 1.6 M^{-1} s^{-1}. However, after correcting for the actual concentration of thiolate present at a given pH, *vide infra*, it becomes (1.6 M^{-1} s^{-1} x $2.8*10^{-4}$ =) $4.6*10^{-4}$ M^{-1} s^{-1}, which is more than 750 times larger than that of the strong nucleophile HO^- (60 M^{-1} s^{-1}). This enhanced effect arises due to the nuclophilicity of **29**-S^-, and to its bifunctional character. As shown in Scheme 22, bifunctional nucleophiles generally react with **1** in a multistep reaction proceeding through an anionic tetrahedral intermediate $\mathbf{T_O}^-$. Unless the intermediate is trapped by a proton transfer from some adjacent pendant, $\mathbf{T_O}^-$ simply reverses back to **1**. Thus, the bifunctional nucleophiles generally function by trapping $\mathbf{T_O}^-$ via intramolecular proton transfer from the pendant thereby preventing reversal.

When compared to other bifunctional[42b] nucleophiles such as **17b** (100 $M^{-1} s^{-1}$), **29**-S^- ($4.6*10^4$ $M^{-1} s^{-1}$) was found to be the most reactive towards neutral **1**. This might be explained by fact that proton transfer to the anilino nitrogen in T_O^- from COOH is thermodynamically more favored, since the COOH group has a lower pK_a than other possible pendants (e.g. Im-H^+) of the different bifunctional catalysts.

E. Conclusion.

In previous work, it was shown that bifunctional small molecular models of naturally occurring proteolytic enzymes containing nucleophilic/acid-base groups had a high propensity to react with the distorted amide **1**. The common mechanism for all the model systems involves an initial nucleophilic attack followed by intramolecular proton transfer from the pendant to trap the unstable intermediate. The initial goal of the present study was to design systems that did not mimic naturally occurring enzymes by coupling a good nucleophile with a pendant not seen in the enzymes. As seen in this work, thioglycolic acid (**29**) containing both the thiol(ate) and carboxylic acid group, functionalities which are not simultaneously present in natural enzymes, is also reactive towards **1**. It should be noted, however, that a mutant β-lactamase enzyme has been reported[52] to contain a catalytically active thiol and an acid group at the enzyme active site. This mutant β-lactamase was produced using site directed mutagenesis techniques where an active site serine (Ser-70) was substituted by cysteine. It was also suggested that the active form of the enzyme for hydrolysis of β-lactam substrates contained the ionized thiolate (Cys-70) and protonated carboxylic acid (Glu-166).

It is also shown here that the active form of the bifunctional nucleophile is $^{-}SCH_2COOH$, where both a strong nucleophile (thiolate) and a pendant capable of transferring a proton (carboxylic acid) are present. In the present study, the lower and upper limits of the pH rate profile for the reaction of **29** with **1** were defined so that it was possible to determine which of several mechanisms were operative, and it was further shown that in the low pH domain, the monoanion of **29** attacks 1-H^{-}. These findings, coupled with previous observations, reaffirm an important feature for catalysis. For

bifunctional compounds to be active towards acyl transfer from amides. both nucleophilic and general acid (to trap the unstable tetrahedral intermediate via an intramolecular proton transfer) functionalities are required.

CHAPTER 3

A. Objective of this work.

As discussed in Chapter 2 and in previous work from this research group,[42] both thioglycolic acid (**29**) and 2-(*N*,*N*-dimethylamino)ethane thiol (**20b**) react with distorted amide **1** yielding the corresponding thiol esters (**31a, 33**). These reactions have been taken as models for the acylation reaction that occurs in the active

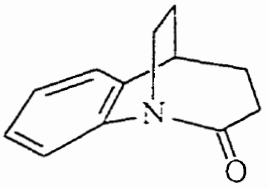

1

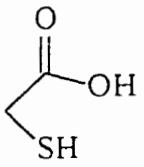

29

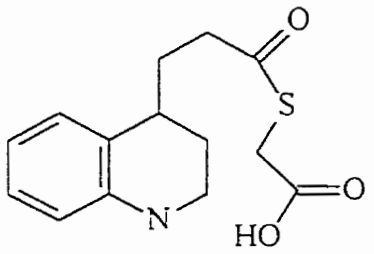

31a

20b

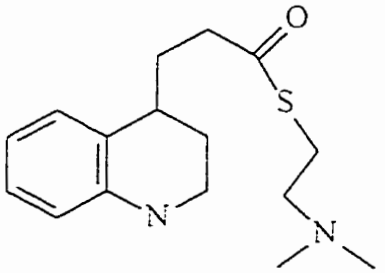

33

site of cysteine proteases where the catalytic cycle also proceeds via an intermediate thiol ester. In the enzyme-catalyzed reaction, the thiol ester intermediate is subsequently hydrolyzed to regenerate the enzyme. If **20b** and **29** are considered to be true catalysts for the hydrolysis of **1**, the intermediate thiol esters **31a** and **33** must be hydrolyzed rapidly with intramolecular catalysis by the pendant carboxylate or amine. The widely accepted mechanism of cysteine protease acyl enzyme intermediate hydrolysis is believed to proceed via a general base assisted attack of water by the active site histidine imidazole.[19] There are only a few small molecular models available that demonstrate intermolecular

assisted hydrolysis of the thiol ester[39,40,41] and even fewer[41] examples where intramolecular general base catalysis has been observed.

Described in this Chapter is the propensity for intramolecular assistance by carboxylate and tertiary amine towards the hydrolysis of thiol esters. For this purpose, 4-nitrobenzoate esters of ethyl 2-mercaptoacetate, thioglycolic acid, 2-(*N,N*-dimethylamino)ethanethiol, and 2-(*N,N,N*-trimethylammonium)ethanethiol iodide (**34-37**) have been synthesized. The rates of hydrolysis of these thiol esters have been studied

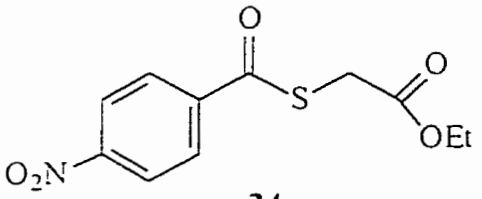

34

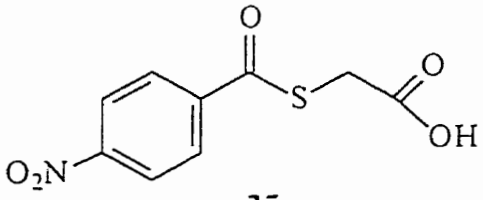

35

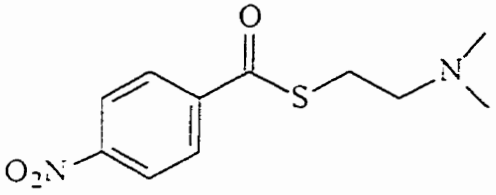

36

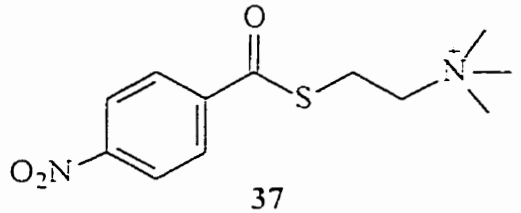

37

as a function of pH at 50 °C. Reported herein are the findings which indicate compounds **35** and **36** show intramolecular general base catalyzed hydrolysis at neutral pH, whereas the control compounds, **34** and **37**, only exhibit specific base catalysis.

B. Experimental.

Materials and General Methods:

The following materials were obtained from commercial suppliers: 4-nitrobenzoyl chloride (Aldrich), 5,5'-dithiobis(2-nitrobenzoic acid) (DTNB; Ellman's reagent, Sigma), 2-(*N,N*-dimethylamino)ethane thiol:HCl (Aldrich), ethyl 2-mercaptoacetate (Aldrich), thioglycolic acid (Sigma), iodomethane (BDH), glacial acetic acid (Fisher Scientific), sodium acetate (General Intermediates of Canada) and triethylamine (BDH). Buffers, MES (4-morpholineethanesulfonic acid), MOPS (4-morpholinepropanesulfonic acid) and EPPS (4-[2-hydroxyethyl]-1-piperazenepropanesulfonic acid), were reagent grade (Sigma) and were used as supplied. Purified deoxygenated water from an Osmonics Aries water purification system was used for buffer preparation. Acetonitrile was dried over 3A molecular sieves and distilled from phosphorous pentoxide under argon prior to use. pH was measured using a Radiometer Vit 90 Video Titrator equipped with a GK2321C combination electrode, standardized by Fisher Certified pH 2, 4, 7, and 10 buffers.

^{1}H and ^{13}C NMR spectra were obtained using a Bruker AC-200 or a Bruker AM-400 spectrometer. Infrared spectra were obtained using a Bomem MB-120 FTIR spectrometer. High resolution mass spectra were obtained using a Concept 2H (Kratos) spectrometer. All melting points were obtained using a Fisher-Johns melting apparatus and are uncorrected.

Synthesis:

The thiol esters **34** - **37** were prepared by the typical procedure described below.

***p*-Nitrobenzoate ester of ethyl 2-mercaptoacetate (34):**

p-Nitrobenzoyl chloride (4.64 g, 0.025 mole) was dissolved in 10 mL CH_3CN and then added to a mixture of 3.00 g (0.025 mole) $HS\text{-}CH_2\text{-}COOEt$ and 2.52 g (0.025 mole) $N(Et)_3$ in 15 mL of CH_3CN. The reaction mixture was then stirred at room temperature for 1 h after which the CH_3CN was evaporated to obtain reddish-yellow crystals which were dissolved in 50 mL of CH_2Cl_2. This solution was washed with 3 X 100 mL each of 1N HCl, a saturated solution of $NaHCO_3$, and with water. The CH_2Cl_2 layer was then dried with $MgSO_4$ and the solvent removed by rotary evaporation to obtain 5.73 g of the crude product (85% crude yield.). A 2 g portion of this was recrystallized from acetone (10 mL)-hexane (a few drops) to yield light yellow, needle shaped crystals: mp 51-52 °C. IR (KBr) 3113, 2982, 2935, 1730, 1667 cm^{-1}; ^1H NMR ($CDCl_3$) δ 1.27 (t, J = 7.1, 3H), 3.89 (s, 2H), 4.20 (q, J = 7.1, 2H), 8.07-8.30 (m, 4H); ^{13}C NMR ($CDCl_3$) δ 13.98 (CH_3), 31.67 (CH_2), 62.00 (CH_2), 123.84 (aromat. CH) 128.28 (aromat. CH), 140.53 (aromat. C), 150.58 (aromat. C), 167.89 (C=O), 188.60 (C=O). Exact mass, m/z calcd for $C_{11}H_{11}NO_5S$: 269.03528; found: 269.03477 (4.1%). Anal. calcd for $C_{11}H_{11}O_5NS$: C, 49.07, H, 4.09, N, 5.20, S, 11.90; found: C, 49.26, H, 3.83, N, 5.21, S, 12.08.

***p*-Nitrobenzoyl ester of mercaptoacetic acid (35):**

This was prepared in 71% crude yield as above. A part (~1.5 g) of the product was crystallized from acetone (15 mL)-hexane (few drops) to give light yellow crystals, mp 155-156 °C. IR (KBr) 2727 -3363 (s,br), 3111, 2914, 1704, 1670 cm^{-1}: ^1H NMR (CD_3CN) δ 4.06 (s, 2H), 8.12-8.49 (m, 4H). ^{13}C NMR (CD_3CN) δ 32.29 (CH_2), 125.12

(aromat. CH), 129.33 (aromat. CH), 141.54 (aromat. C), 150.84 (aromat. C), 169.67 (C=O), 189.90 (C=O). Anal. Calcd for $C_9H_7O_5NS$: C, 44.81, H, 2.90, N, 5.81, S, 13.28: found: C, 44.81, H, 2.62, N, 5.79, S, 12.96.

_p_-Nitrobenzoyl ester of 2-(*N*,*N*-dimethylamino)ethanethiol (36):

_p_-Nitrobenzoyl chloride (4.64 g, 0.025 mole), $HS(CH_2)_2N(CH_3)_2$ (3.54 g, 0.025 mole) and pyridine (3.96 g, 0.025 mole) and 25 mL of $CHCl_3$ were mixed using the above procedure. After 6 hr. the reaction mixture was filtered. The $CHCl_3$ solution was extracted with 1N HCl and the pH of the aqueous wash was adjusted to 7 with NaOH (pH paper). The mixture was extracted with $CHCl_3$, this layer being dried over $MgSO_4$, filtered, and evaporated to give a yellow solid in 93% crude yield (5.90 g). A part (~2 g) of it was recrystallized from $CHCl_3$ (7 mL)-hexane (2 mL) to give a yellow solid, mp 32-33 °C. IR (KBr) 2953, 2769, 1664 cm^{-1}: ^1H NMR ($CDCl_3$) δ 2.29 (s, 6H), 2.59 (t, J = 6.8, 2H), 3.25 (t, J = 6.8, 2H), 8.08-8.29 (m, 4H): ^{13}C NMR ($CDCl_3$) δ 27.33 (CH_2), 44.88 (CH_3), 57.75 (CH_2), 123.60 (aromat. CH), 128.01 (aromat. CH), 141.30 (aromat. C), 150.26 (aromat. C), 190.12 (C=O). Exact mass m/z calcd for $C_{11}H_{14}N_2O_3S$: 254.07114: found: 254.06976 (4.2%).

_p_-Nitrobenzoyl ester of thiocholine iodide (37):

Into 10 mL of dry diethyl ether was placed 0.41 g (1.6 mmol) of **36** followed by 0.28 g (2 mmol) of CH_3I. The reaction mixture was stirred overnight at room temperature. The bright yellow precipitate was collected by filtration and recrystallized from methanol (3 mL)-acetonitrile (few drops) to give 0.61 g of solid (96% crude yield), mp 224-225° C (decomp.). ^1H NMR (60% $CDCl_3$, 40% CD_3OD) δ 3.12 (s, 9H), 3.25-3.51 (m, 4H), 7.86-8.22 (m, 4H): Exact mass (FAB) m/z calcd. for $C_{12}H_{17}N_2O_3S$:

269.0960: found: 269.0880. Anal. calcd for $C_{12}H_{17}N_2O_3SI$: C. 36.36. H. 4.29. N. 7.07. S. 8.08: found: C. 36.10. H. 4.43. N. 7.07. S. 8.48.

Kinetics:

The pH rate constant profiles of hydrolysis of esters **34-37** were determined at 50 °C. μ=0.1 (KCl). To control pH in the 6.6-9.8 range. tertiary amine buffers were used (MES. MOPS. EPPS and Et_3N). Acetate buffer was used at pH 3.8-4.8. In all cases two buffer concentrations. 0.05 and 0.10 M. were used to check for buffer catalysis. At pH ≥11.5. NaOH was used as the buffer and at pH ≤ 2.3 . HCl was used: in both cases the ionic strength was maintained at 0.10 (KCl). All pH readings were measured before and after the reaction. the reported values being the average of the two readings.

Rates of disappearance of the starting esters were followed at 270 nm using a modified Cary-17 UV-vis spectrophotometer interfaced to an IBM 486 PC fitted with OLIS software (On-line Instrument Systems. Jefferson. Ga.. 1992). Reactions were initiated by injecting 20 - 25 μL of a 0.009 - 0.012 M solution of the ester in dry acetonitrile into 3 mL of buffer solution held in 1-cm quartz cuvettes which were thermally equilibrated at 50 ± 0.7 °C in the cell holder for 10 min. prior to initiation of the run. The pseudo-first order rate constant for the reaction (k_{obs}) was obtained by NLLSQ fitting of abs. vs time data to a standard exponential model ($A_t = A_\infty + (A_0 - A_\infty) \exp(-kt)$). Values reported are the averages of at least duplicate runs. The pseudo-first order rate constant at [buffer] = 0. k_1. is derived from extrapolation of rate constants obtained at two [buffer].

D_2O Studies:

The rate of hydrolysis of **36** was determined in D_2O at pD 10.20 ± 0.04 (pD = pH + 0.4)[53] in triethylamine buffer ([buffer] = 0.05 and 0.10 M, μ = 0.10 (KCl)). pD was adjusted by additions of 3M DCl. The kinetic data were obtained as above, also at 50 ± 0.7 °C.

Hydrolysis of 36 in the presence of DTNB:

The rate of generation of the Ellman's anion accompanying the hydrolysis of **36** was determined in the presence of Ellman's reagent (DTNB) at pH 9.77 ± 0.04, triethylamine buffer ([buffer] = 0.05 and 0.10 M, μ = 0.10 (KCl)) at 50 ± 0.7 °C. For this series of reactions, 125-250 μL aliquots of DTNB solution (3.2×10^{-3} M in the same buffer) were injected into 3 mL of the thermally equilibrated buffer in 1-cm cuvettes (giving a final [DTNB] = $1.3\text{-}2.5 \times 10^{-4}$ M), immediately followed by 4 - 8 μL of the stock solution of **36** (0.012 M in dry acetonitrile). The rate of appearance of the Ellman's thiolate anion from DTNB was followed at 412 nm. Since DTNB itself decomposes under these conditions, the pseudo-first order rate constants were obtained by nonlinear least squares fitting of the abs. vs. time data to a double exponential model ($A_t = ((A_0 - A_{1\infty}) \exp(-k_1 t) + (A_0 - A_{2\infty}) \exp(-k_2 t) + (A_{1\infty} + A_{2\infty}))$ to obtain the rate constants for the thiolate induced and spontaneous productions of Ellman's anion. To verify the rate constants computed in this way, a second run was also performed wherein one cell containing buffer and DTNB only was used as a reference against a cell containing the identical amount of DTNB and **36**. These data were also fitted to a double exponential model equation.

C. Results.

The kinetics of the hydrolysis of the thiol esters **34-37** were investigated at various pHs ranging from 1.9 to 11.9 (T = 50 °C, μ = 0.10 (KCl)). The rate of hydrolysis was followed by observing the decrease in the absorbance of the starting thiol esters at 270 nm. The observed pseudo-first order rate constants (k_{obs}) for the hydrolysis at different [buffer] and various pHs are given in Appendix 2, Table 2S. The second order rate constants (k_{2buff}) for buffer catalysis are given in Appendix 2, Table 3S. The pseudo-first order rate constants (k_1) extrapolated to zero buffer concentration are given in Table 2.

The kinetic features for the hydrolysis of these thiol esters are evident from the pH-rate profiles given in Figure 2. It is observed that the hydrolysis of compounds **34** and **37** showed only a linear dependence on hydroxide ion concentration. For both compounds **35** and **36**, the hydrolysis rate constant increases with increasing pH until reaching a plateau beginning at the pK_a of the respective pendants (pK_a 2.8 and 8.1 for the carboxylic acid and the dimethylammonium group, see Discussion). At still higher pH, specific base catalysis predominates and the rate constants increase with increasing pH.

The rate constants for the hydrolysis of compound **36** in D_2O at pD = 10.20, which is in the pH independent region, where 0.05-0.10 M triethylamine was used as buffer, μ = 0.10 (KCl), are given in Table 3. Given in Table 4 are the rate constants for the appearance of Ellman's anion caused by the hydrolysis of **36** in the presence of excess DTNB in the pH independent region (pH 9.75, triethylamine buffer).

Table 2. Pseudo-first Order Rate Constants for Hydrolysis of Thiol Esters **34-37** [buffer]= 0. T = 50 °C. μ = 0.1 (KCl).[a]

	rate constant, k_1 (s^{-1})			
pH	**34**	**35**	**36**	**37**
1.98		$(4.63\pm1.00) \times 10^{-6}$		
2.33		$(5.67\pm1.00) \times 10^{-6}$		
3.83		$(1.44\pm0.07) \times 10^{-5}$		
4.77		$(1.73\pm0.08) \times 10^{-5}$		
6.60	$(1.49\pm0.60) \times 10^{-6}$	$(2.19\pm0.13) \times 10^{-5}$	$(4.08\pm0.61) \times 10^{-4}$	$(6.80\pm0.38) \times 10^{-6}$
7.61	$(3.83\pm0.06) \times 10^{-5}$	$(3.09\pm0.10) \times 10^{-5}$	$(3.15\pm0.04) \times 10^{-3}$	
7.72				$(6.20\pm0.20) \times 10^{-5}$
8.04	$(8.36\pm0.15) \times 10^{-5}$		$(6.82\pm0.12) \times 10^{-3}$	$(1.33\pm0.02) \times 10^{-4}$
8.09			$(9.32\pm0.27) \times 10^{-3}$	
8.55				$(4.94\pm0.08) \times 10^{-4}$
8.70	$(1.73\pm0.03) \times 10^{-4}$	$(5.90\pm0.10) \times 10^{-5}$	$(1.26\pm0.04) \times 10^{-2}$	$(6.13\pm0.22) \times 10^{-4}$
9.70				$(2.91\pm0.11) \times 10^{-3}$
9.78	$(2.26\pm0.03) \times 10^{-3}$	$(4.99\pm0.40) \times 10^{-4}$	$(1.61\pm0.14) \times 10^{-2}$	
11.46	$(8.30\pm0.23) \times 10^{-2}$ [b]	$(1.37\pm0.03) \times 10^{-2}$	$(3.05\pm0.05) \times 10^{-2}$	
11.90	$(1.50\pm0.10) \times 10^{-1}$ [b]		$(5.97\pm0.03) \times 10^{-2}$	

[a]Extrapolated to [buffer] = 0. Errors are standard deviations from fits of two or three replicates at each of two [buffer].

[b]Determined at 46 °C by stopped flow procedure.

Figure 2. Plot of the pseudo-first order rate constants for hydrolysis of thiol esters **34** (○), **35** (●), **36** (▲), and **37** (Δ) as a function of pH at 50 °C, μ = 0.10 (KCl). Lines are from fits of the data to eq 5 for **35** and **36** and from linear regression for **34** and **37**.

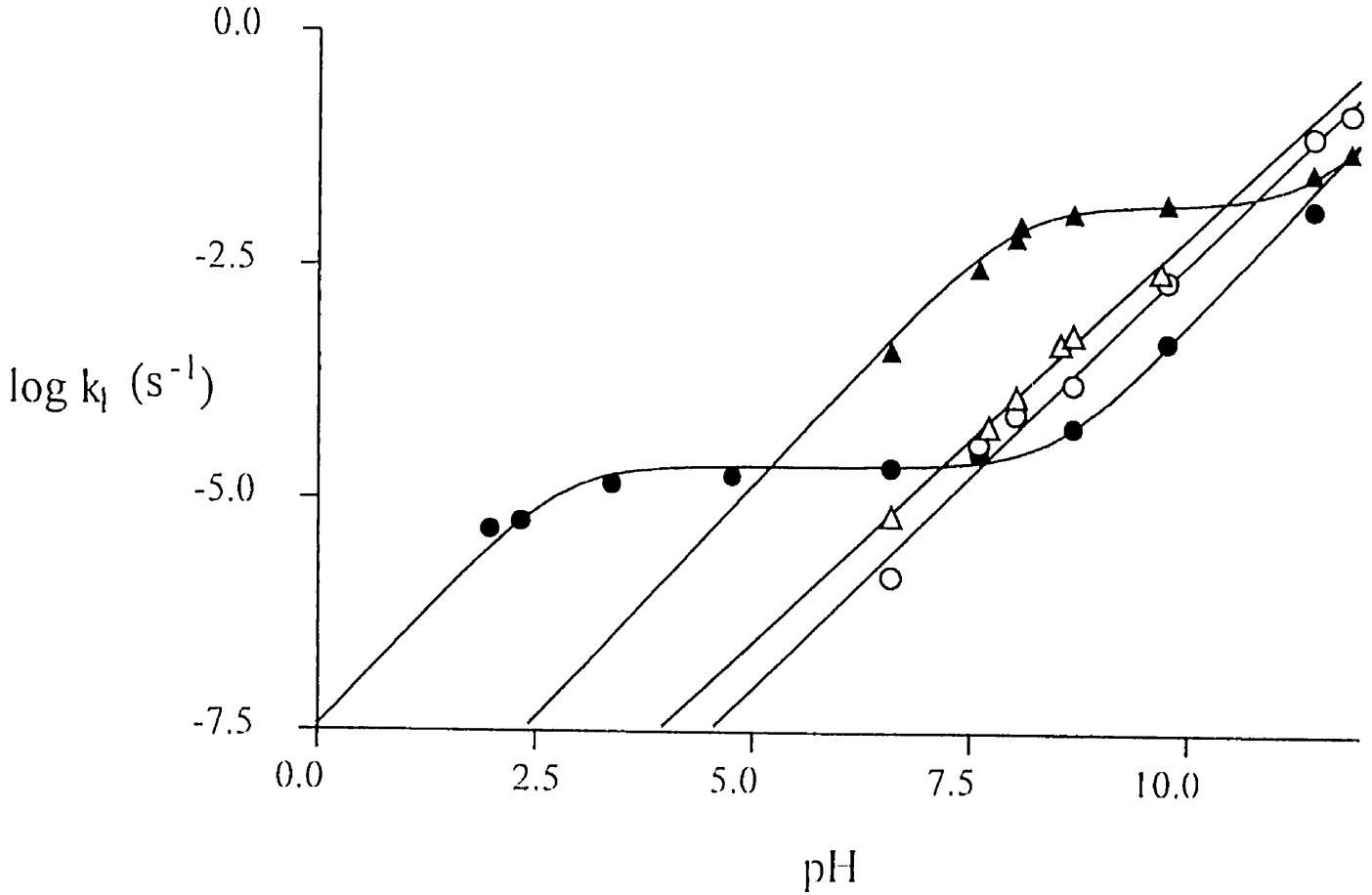

Table 3. Pseudo-first Order Rate Constants for the Hydrolysis of Thiol Ester **36** in D_2O, pD=10.20, T=50 °C, μ = 0.1 (KCl).

pD[a]	[buffer][b]	k_{obs} (s^{-1})	k_1 (s^{-1})[c]	k_H / k_D[d]
10.20	0.05	(9.28±0.15) x 10^{-3}	(8.02±0.18) x 10^{-3}	2.23
10.24	0.10	(10.55±0.08) x 10^{-3}		

[a]pD = pH ÷ 0.4.[53]

[b]Triethyl amine.

[c]Extrapolated to zero [buffer].

[d]Rate constant for hydrolysis of **36** at pH 10.2 is computed to be 1.78x10^{-2} s^{-1} using eq 5.

Table 4. Pseudo-first Order Rate Constant for the Appearance of Ellman's Anion Accompanying the Hydrolysis of **36** in the Presence of Ellman's Reagent. T=50 °C, μ = 0.1(KCl).[a]

pH	[buffer][b]	k_{obs} (s^{-1})	k_1 (s^{-1}) [c,d]
9.77	0.05	$(1.88\pm0.08) \times 10^{-2}$	$(1.66\pm0.10) \times 10^{-2}$
9.75	0.10	$(2.10\pm0.03) \times 10^{-2}$	

[a][Ellman's reagent, 5,5'-dithiobis(2-nitrobenzoic acid)] = 2.46×10^{-4} M

[b]Triethyl amine

[c]Extrapolated to zero [buffer]

[d]Pseudo-first order rate constant for hydrolysis of **36** at pH 9.78 extrapolated to zero [buffer] is $(1.61\pm0.14) \times 10^{-2}$ s^{-1}, (obtained from Table 2).

D. Discussion

Common mechanism for the hydrolysis of 35 and 36:

As seen in Figure 2, the pH rate profile has a plateau region from pH 3 to 11 in the case of **35** and pH 8 to 11 in the case of **36**, indicating that the deprotonated COO^- or the basic $N(CH_3)_2$ groups of the pendants are involved with the hydrolysis. The hydrolysis profiles for both **35** and **36** are consistent with the common process depicted in Scheme 23, where the deprotonated X group (either COO^- or $-CH_2-N(CH_3)_2$) assists a

Scheme 23

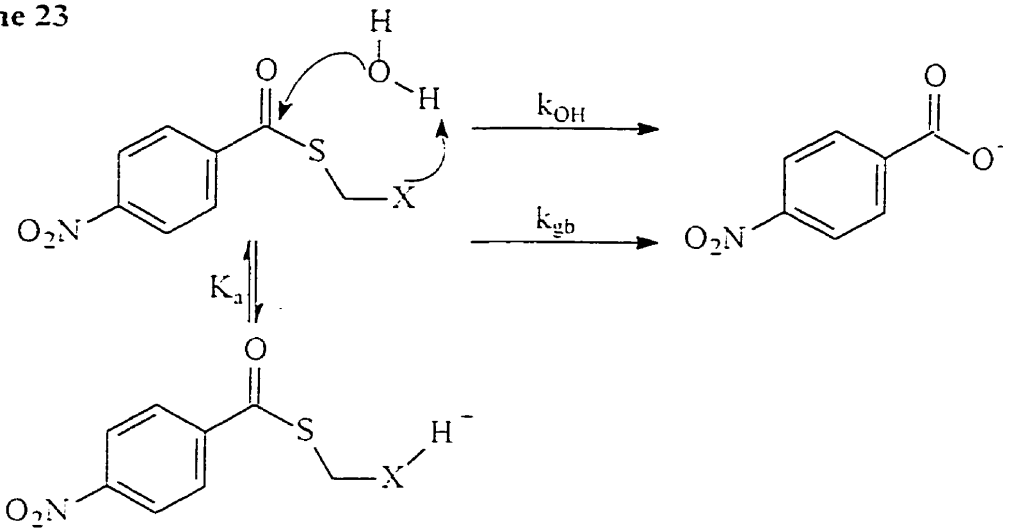

35 X = COO^-
36 X = $CH_2N(CH_3)_2$

water molecule in attacking the carboxyl carbon to yield hydrolyzed products, in addition to a concurrent ^-OH catalyzed process. From Scheme 23 can be derived the kinetic expression given in eq 5, where k_{OH} is second order rate constant for the hydroxide catalyzed process, where

$$k_1 = (k_{OH} (K_w / [H^-])) \div (k_{gb} K_a / (K_a \div [H^-])) \qquad (5)$$

k_{gb} is the rate constant for the intramolecularly assisted process, K_a is the acid dissociation constant of the pendant and K_w is the autoprotolysis constant of water.

The NLLSQ fitting of the k_I values at different pH values listed in Table 2 to eq 5 generates the values for k_{hyd}, k_{OH} and K_a for **35** and **36** given in Table 5. The kinetic pK_as of **35** and **36** are 2.8 and 8.18, obtained from the best fit of the kinetic data to eq 5. A thermodynamic pK_a of **36** was found to be 7.9 at 25 °C, μ = 0.10 (KCl), obtained by measuring the pH of half neutralized solution.[54] Also included in the Table are the second order rate constants for hydroxide attack on **34** and **37** as determined from linear regression of the k_I vs $[OH^-]$ plots.

General base or Nucleophilic assistance from the pendants:

Although, as described in Scheme 23, the favored mechanism for intramolecular assistance of thiol ester hydrolysis by the pendants proceeds via a general base process, there exist two more possibilities for the intramolecular catalysis. In the following section, these other possibilities will be explored and compared with the general base mechanism.

The solvent deuterium kinetic isotope effect (DKIE) for the hydrolysis of **36** has been determined in the plateau region at pH 10.2 where the reaction proceeds almost entirely via the intramolecular process. The value of k_H/k_D of 2.2 is consistent with the process described in Scheme 23, where the pendant is acting as a general base. Nevertheless, a primary solvent DKIE would also be observed when the pendant acts as a nucleophile, as shown in eq 6 and 7, in a rapid reversible step to form the anhydride

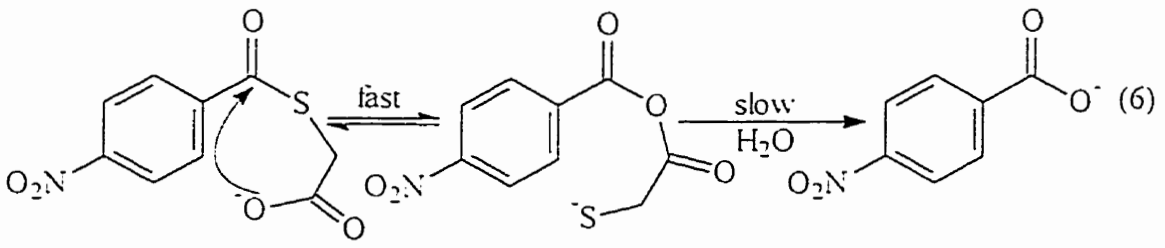

Table 5. Computed Rate and Acid Dissociation Constants for the Hydrolyses of Thiol Esters **34**-**37**.[a]

Thiol ester	k_{OH} ($M^{-1}s^{-1}$)	k_{gb} (s^{-1})[b, c]	kinetic pK_a
34	28.7±0.1 [d,e]		
35	4.7±0.1[e]	(5.58±2.71) x 10^{-5}	2.80
36	5.3±0.2[e]	(1.72±0.08) x 10^{-2}	8.18[f]
37	55.8±3.5[d]		

[a]T=50 °C, μ=0.1 (KCl)

[b]From fits of the k_I vs. pH data to eq 5.

[c]Standard error from NLLSQ fit of the k_I vs. pH data to eq 5.

[d]Standard error from fits of k_I at [buffer] = 0 against [OH^-].

[e]From fits of 5 data in Table 2 excluding two highest [NaOH] since the latter were at 46 °C.

[f]pH of 1/2 neutralized solution of **36** is 7.9 at 25 °C (see text).

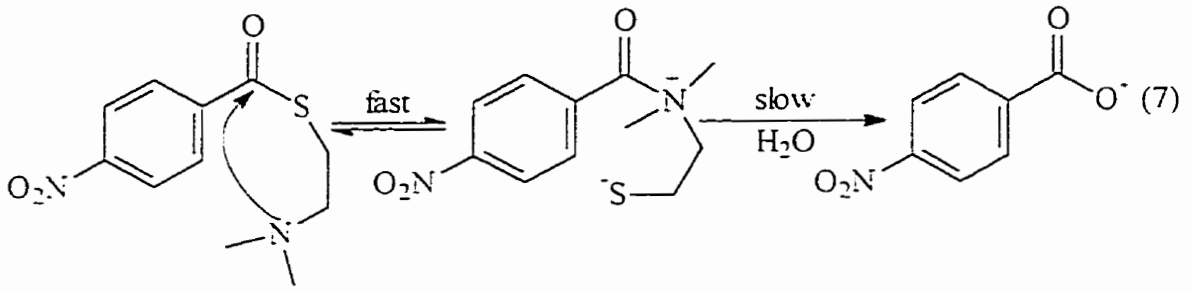

or the N-acyl ammonium ion intermediate which hydrolyzes into the final products by a subsequent rate limiting attack of water. The latter process is analogous to water promoted hydrolysis of several activated acyls,[55] such as N-acylimidazoles, which also show solvent DKIEs of 2.5 - 3.7. Hence, from the solvent DKIE data alone, it is not possible to differentiate between a general base catalyzed hydrolysis or nucleophilic role for the pendant.

In order to distinguish between the two possibilities, **36** was hydrolyzed in the plateau region (pH 9.7) in the presence of Ellman's reagent, Scheme 24. This reagent

Scheme 24

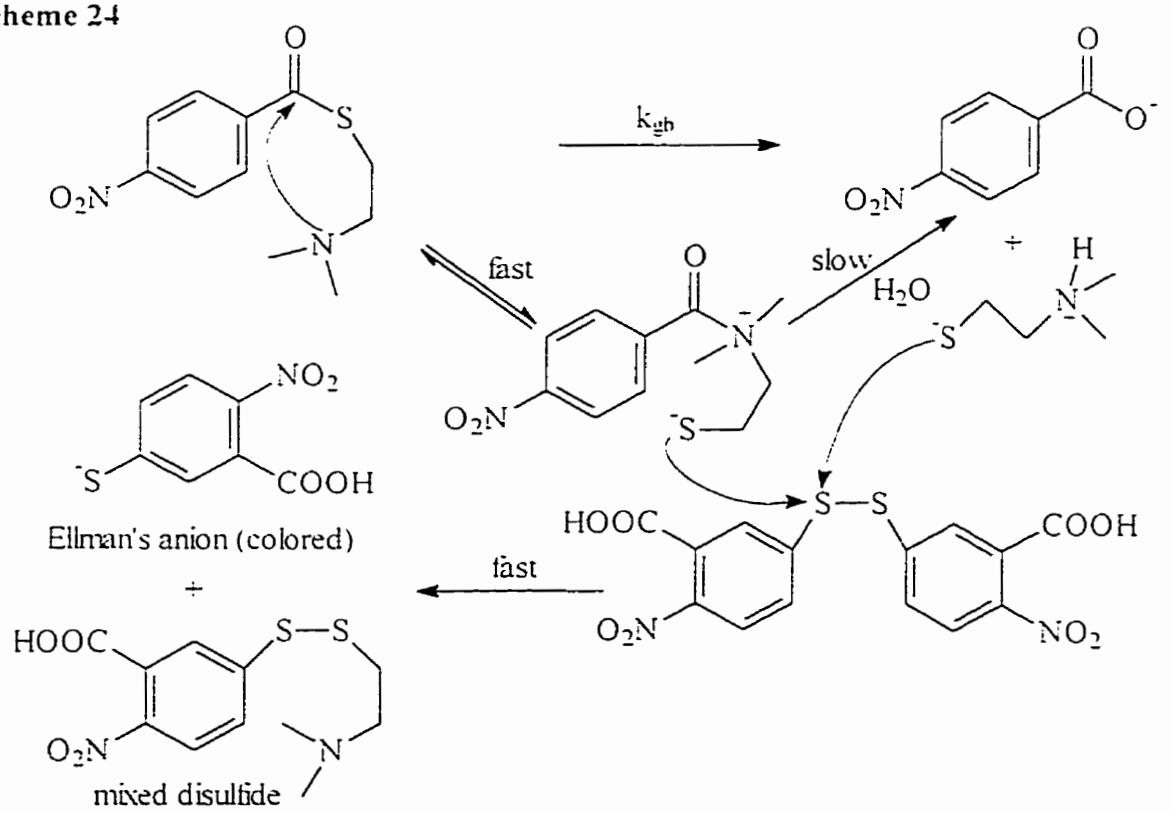

should react rapidly[36b,56] with the transiently formed thiolate to generate the highly absorbing Ellman's anion, a process which is followed at 412 nm. If the pendant acts as a nucleophile then added Ellman's reagent will trap the transient thiolate and prevent its return to starting thiol ester. This trapping process should depend on the [Ellman's reagent], ultimately displaying saturation behaviour where the rate limiting step becomes the intramolecular S to N acyl transfer. This technique has previously been used in this laboratory by Street *et al*[36b,41] to test for S to N acetyl transfer that could generate reversibly formed thiolates during the hydrolysis of the acetyl thio esters of **28b** and **26**.

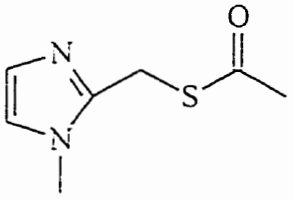

28b

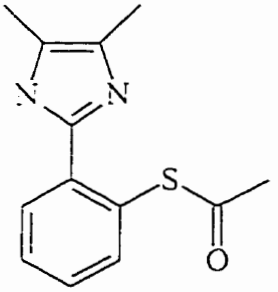

26

In the present study it was found that the appearance of Ellman's anion which accompanied the hydrolysis of **36** did not depend on the [Ellman's reagent], and from the data in Table 4, the rate of Ellman's anion generation was identical to the rate at which **36** disappears. From this, it is reasonable to conclude that the intramolecular nucleophilic process depicted in eq 7 neither predominates nor competes with general base assistance during the hydrolysis of **36**.

In another possible mechanism, the pendant can attack the carbonyl carbon in a rate limiting step, producing the N-acyl intermediate which then undergoes rapid hydrolysis, Scheme 25. This process will show no dependance on the [Ellman's reagent], but may show some solvent isotope effect[57] because of the solvation of the developing oxyanion (slow step Scheme 25). Nevertheless, this process is unlikely since it

Scheme 25

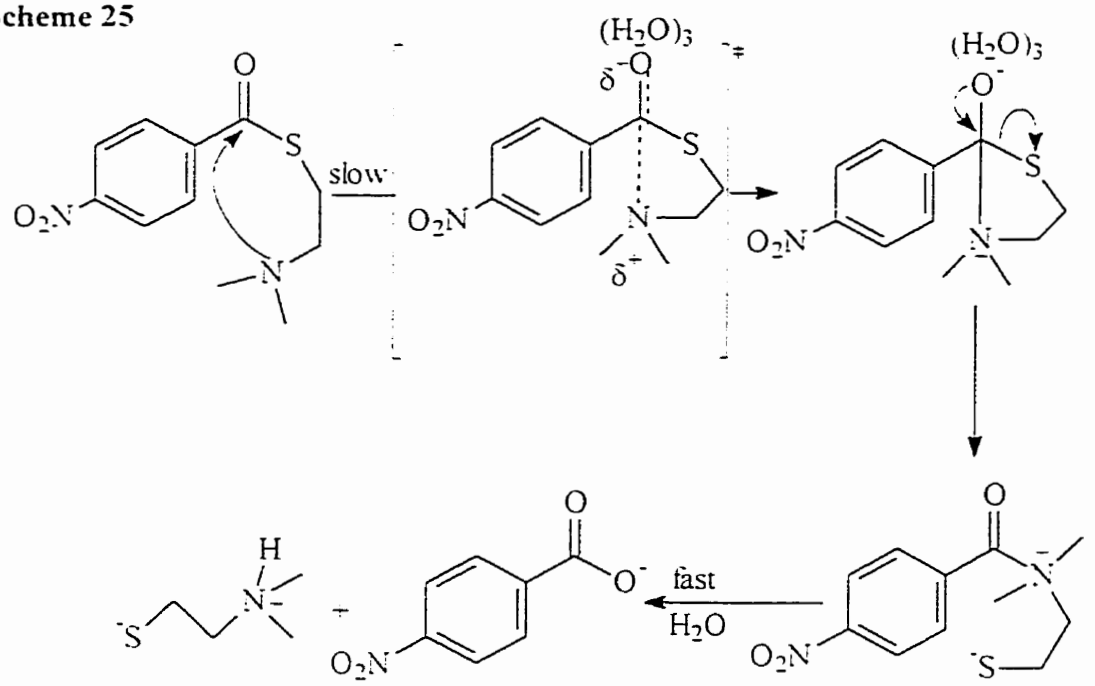

requires a more rapid intermolecular attack of water (which is a poor nucleophile) on the carbonyl carbon of the N-acyl ammonium intermediate,[58] relative to the intramolecular attack of the strong nucleophile, S^-. Here, it can be concluded that the rate limiting nucleophilic role of the pendant is not possible. Consequently, the most favored role of the pendants in the hydrolysis of the thiol esters is the general base assisted attack on the carbonyl carbon.

Given that the nucleophilicity of COO^- is much less than that of the $N(CH_3)_2$ group,[47] one can make the argument that in a scenario in which the $N(CH_3)_2$ group fails to act as nucleophile, then the COO^- will be unlikely to behave as a nucleophile.

Comparison of the specific base catalyze rate constants:

As seen in Table 5, the second order rate constants for hydroxide attack on the thiol esters **34-37** ranges from 4.7 $M^{-1}s^{-1}$ to 55.8 $M^{-1}s^{-1}$, the reactivity order being **37>34>36≥35**. The high reactivity of **37** may be explained on electrostatic grounds as there will be more stabilization of the transition state (for positively charged **37** compared to neutral **36** or anionic **35**) arising from the attack of the negatively charged ^{-}OH. The enhancement of the ^{-}OH attack on **34** over **35** can be explained by the fact that the ester group of **34** is an inductively electron withdrawing group. This increases the electrophilicity of the carbonyl carbon and also stabilizes the transition state for direct attack by ^{-}OH. The second order rate constants for hydroxide attack on **35** is the smallest because the anionic pendant, COO^{-}, would hinder this process.

Intramolecular vs intermolecular catalysis:

For intramolecular catalysis by COO^{-} and $N(CH_3)_2$, the effective molarities (EM)[59] can be calculated by comparing the k_{gb}, first order rate constants, with the appropriate second order rate constants for an intermolecular process. As defined, the effective molarities of a pendant group can be obtained from the ratio of the first order rate constant (unit s^{-1}) for the intramolecular reaction and the second order rate constant (unit $M^{-1}s^{-1}$) for an intermolecular reaction of a group with similar properties as the pendant. It is seen from Table 5 that the rate constant for the COO^{-} mediated intramolecular catalysis (k_{gb}) for the thiol ester hydrolysis is $5.6*10^{-5}$ s^{-1} and that of $N(CH_3)_2$ is $1.7*10^{-2}$ s^{-1} for compounds **35** and **36**, respectively. To compute EM, an appropriate intermolecular general base for each of these pendants would be a carboxylic

acid and a tertiary amine having similar pK_as to the respective pendants. The closest available intermolecular match for the pendants of **35** and **36** are acetate (pK_a 4.76) and EPPS (4-[2-hydroxyethyl]-1-piperazenepropanesulfonic acid), pKa = 8.00) respectively, which were used as buffers in this experiment. From data given in Appendix 2 Table 3S, it can be computed that the second order rate constant for the reaction of acetate with **35** is $(3.34\pm0.09)*10^{-5}$ $M^{-1}s^{-1}$ at pH 3.83 and $(9.98\pm0.07)*10^{-5}$ $M^{-1}s^{-1}$ at pH 4.77 and that for EPPS with **36** is $(3.74\pm0.13)*10^{-2}$ M^{-1} s^{-1} at pH 8.70. As expected for general base catalysis, the anionic or basic forms are the reactive species for catalysis as indicated by the increasing catalysis of the reaction by acetate with increasing pH. After correcting for only the anionic or basic form of the buffer species at the given pH, the true rate constants for anionic acetate with **35** and free EPPS with **36** become $2*10^{-4}$ $M^{-1}s^{-1}$ and $4.5*10^{-2}$ M^{-1} s^{-1}. Using these values as the intermolecular rate constants, the EM for **35** and **36** can be calculated as 0.2 - 0.3 M and 0.4 M. These EM values provide further support the general base role of the pendants of **35** and **36**, since it is commonly accepted that for a general base processes, the EM is generally less than 10 M,[27] whereas for a nucleophilic processes the EM is generally larger than 10 M (sometimes as high as 10^5 M).[60]

As the pK_a of acetic acid is 4.76, compared to the apparent pK_a of the pendant carboxylic acid (pK_a = 2.80) of **35**, it can be argued that the comparison is inappropriate. However, by assuming a Bronsted β of 0.5,[61] it is possible to calculate the intermolecular rate constant for a hypothetical carboxylic acid with pK_a of 2.8. When this is done, the effective molarity of **35** was seen to increase to roughly 2M, remaining within the limit of the general base process.

E. Conclusion.

The present study indicates that both the carboxylate and tertiary amine pendants are capable of intramolecular assistance towards the hydrolysis of thiol esters. The SKIE for the intramolecular catalysis of **36** hydrolysis is 2.2 consistent with a primary DKIE. This value, coupled with the fact that in the presence of Ellman 's reagent **36** produced the Ellman's anion at the same rate of disappearance of the thiol ester (at pH 9.75 where the hydrolysis proceeds mostly by intramolecular catalysis), indicates that the pendant is not acting as an intramolecular nucleophile. Hence, it is proposed that that both carboxylate and tertiary amine pendants act as intramolecular general bases. The effective molarities for the intramolecular catalysis by COO^- and $N(CH_3)_2$ pendants were found to be much less than 10M, which is also consistent with these having a general base role. The second order rate constant for hydroxide catalyzed hydrolysis of **34-37** span a 10-fold range and the order of reactivity is **37>34>35≥36**. The ordering is explained on the basis of electrostatics.

CHAPTER 4: GENERAL CONCLUSION

Acyl transfer from amide to thiolate and from thiol to water.

Amide bond hydrolysis by many non-metallo proteases (enzymes) proceeds via an acyl enzyme intermediate. To mimic the acylation process, the reactivity of several bifunctional catalysts containing a nucleophile and an acid/base group (simultaneously present in the enzyme acive site), towards various esters and amides have been studied previously. The current study has shown that a simple bifunctional molecule, thioglycolic acid (**29**), showed high reactivity towards amide **1**, although it has no obvious analogy to naturally occurring enzymes. The reactivity of **29** further illustrated that the general features necessary for activity of such bifunctional molecules toward **1** and presumably other amides include a powerful nucleophilic component and an acidic pendant capable of transferring a proton to trap the unstable tetrahedral intermediate. In this study it is seen that the active form of thioglycolic acid (**29**) consists of S^- and COOH. This observation is consistent with the findings of Pratt *et al.* who reported[52] that the active form of a mutant β-lactamase also contained ionized thiolate (Cys-70) and protonated carboxylic acid (Glu-166). The calculated second order rate constant for the attack of $^-SCH_2COOH$ on **1** is about 750 times higher than that of ^-OH, a powerful nucleophile.

The acyl enzyme intermediate formed in the active site of cysteine proteases during the hydrolytic process eventually hydrolyzes to regenerate the enzyme via general base assistance from an active site imidazole in a so-called "deacylation" process. In this study, we have shown that other intramolecular groups such COO^- and $N(CH_3)_2$ can participate in the hydrolysis of the thiol esters **35** and **36.** At around neutral pH, the

enhancement of hydrolysis due to the pendants are 16 and 50 times for **35** and **36**, respectively, compared to the control compounds **34** and **37**.

Future work.

Apart from 2-mercaptomethyl-N-methylimidazole (**17b**), other thiol containing tertiary amine or carboxylic acid pendants such as **20b**, **21** and **29** produced thiol esters

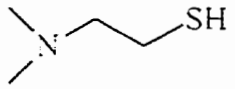

20b

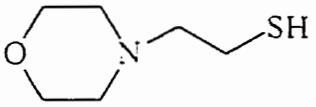

21

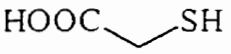

29

as the final products after reacting with amide **1**. Only in the case of the **17b** has it been demonstrated that the thiol ester thus produced proceeded further to hydrolyzed product via intramolecularly catalyzed deacylation, thereby regenerating the catalyst. As seen in the present study, tertiary amines and carboxylates can significantly enhance the rate of thiol ester hydrolysis. Hence, a logical extension of this work would be to study the hydrolysis of the intermediate thiol ester **31a**, **33** and **39**.

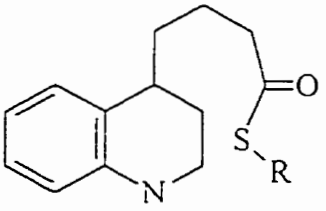

31a R = CH_2COOH

33 R = $CH_2CH_2N(CH_3)_2$

39 R = CH_2CH_2— 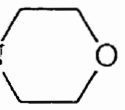

REFERENCES

[1] Smith, R. M.; Hansen, D. E. *J. Am Chem. Soc.* **1998**, *120*, 8910.

[2] Uren, J. R.; Neurath, H. *Biochemistry* **1974**, *13*, 3512.

[3] Fersht, A. In "Enzyme Structure and Mechanism"; 2nd ed.; W. H. Freeman: San Francisco, 1985; pp. 405-413.

[4] Fink A. L. In "Enzyme Mechanisms"; Page, M. I.; Williams, A. Eds.; Royal Society of Chemistry: London, 1987, pp. 159-177.

[5] Blow, D. M. *Acc. Chem. Res.* **1976**, *9*, 145.

[6] Walsh, C. In "Enzymic Reaction Mechanisms"; W. H. Freeman: San Francisco, 1979; pp. 56-97.

[7] (a) Sprang, S.; Standing, R J.; Fletterick, R. M.; Stroud, J. F-M.; Xuong, N-H.; Hamlin, R.; Rutter, W. J.; Craik, C. S. *Science*; **1987**, *237*, 905.

(b) Craik, C. S.; Roczniak, S.; Largman, C.; Rutter, W. J.; *Science*; **1987**, *237*, 909.

[8] Fersht, A. In "Enzyme Structure and Mechanism"; 2nd ed.; W. H. Freeman: San Francisco, 1985; pp. 422-426.

[9] Fruton, J. S. In "The Enzymes"; Boyer, P. D. Ed.; Academic Press: New York, 1971, Vol. 3, pp. 119-164.

[10] Walsh, C. In "Enzymic Reaction Mechanisms"; W. H. Freeman: San Francisco, 1979; pp. 98-104.

[11] Dunn, B. M.; Fink, A. L. *Biochemistry* **1984**, *23*, 5241.

[12] Fischer G. In "Enzyme Mechanisms"; Page, M. I.; Williams, A. Eds.; Royal Society of Chemistry: London, 1987, pp. 229-239.

[13] (a) Hofmann, T.; Fink, A. L. *Biochemistry* **1984**, *23*, 5247.

(b) Blum, M.; Cunninghham, A.; Pang, H.; Hofmann, T. *J. Biol. Chem.* **1991**, *266*, 9501.

[14] (a) Varney, M. D.; Appelt, K.; Kalish, V.; Reddy, R. M.; Tatlock, J.; Palmer, C. L.; Romines, W. H.; Wu, B.; Musick, L. *J. Med. Chem.* **1994**, *37*, 2274.

(b) Ettmayer, P.; Hubner, M.; Billich, A.; Rosenwirth, B.; Gstach, H. *Bioorganic. Med. Chem. Lett.* **1994**, *4*, 2851.

(c) Martin, J. A. *Antiviral Research*, **1992**, *17*, 265.

[15] Katz, R. A.; Skalka, M. *Annu. Rev. Biochem.* **1994**, *63*, 133.

[16] Yu, Z.; Caldera, P.; McPhee, F.; De Voss, J. J.; Jones, P. R.; Burlingame, A. L.; Kuntz, I. D.; Craik, C. S.; de Montellano, P. R. O. *J. Am Chem. Soc.* **1996**, *118*, 5846.

[17] (a) Suguna, K.; Padlan, E. A.; Smith, C. W.; Carlson, W. D.; Davis, R. D. *Proc. Natl. Acad. Sci. U. S. A.* **1987**, *84*, 7009.

(b) Hyland, L. J.; Tomaszek, T. A., Jr.; Meek, T. D. *Biochemistry* **1991**, *30*, 8454.

(c) Hyland, L. J.; Tomaszek, T. A., Jr.; Roberts, G. D.; Carr, S. A.; Magaard, V. W. *Biochemistry* **1991**, *30*, 8441.

[18] Cho, Y-K.; Northrop, D. B. *J. Biol. Chem.* **1998**, *273*, 24305.

[19] Brocklehurst, K. In "Enzyme Mechanisms"; Page, M. I.; Williams, A. Eds.; Royal Society of Chemistry: London, 1987, pp. 140-158.

[20] (a) Drenth, J.; Jansonius, J. N.; Koekoek, R.; Wolthers, B. G. In "The Enzymes": Boyer, P. D. Ed.; Academic Press: New York, 1971, Vol. 3, pp. 485-500.

(b) Glazer, A. N.; Smith, E L. In "The Enzymes"; Boyer, P. D. Ed.; Academic Press: New York, 1971, Vol. 3, pp. 501-546.

[21] Fersht, A. In "Enzyme Structure and Mechanism"; 2nd ed.; W. H. Freeman: San Francisco, 1985; pp. 413-416.

[22] Andrew, S. C.; Ménard, R. In "Methods in Enzymology, 244 (Proteolytic Enzumes: Serine and Cysteine Peptidases)"; Barrett, A. J. Ed.; Academic Press: San Diego Calif., 1994, pp. 486-500.

[23] (a) Ménard, R.; Khouri, H. E.; Plouffe, C.; Dupras, R.; Ripoll, D.; Vernet, T.; Tessier, D. C.; Laliberte, F.; Thomas, D.Y.; Storer, A. C. *Biochemistry* **1990**, *29*, 6706.

(b) Ménard, R.; Khouri, H. E.; Plouffe, C.; Laflamme, P.; Dupras, R.; Vernet, T.; Tessier, D. C.; Thomas, D.Y.; Storer, A. C. *Biochemistry* **1991** *30*, 5531.

[24] Angelides, K. J.; Fink, A. L. *Biochemistry* **1978**, *17*, 2659.

[25] D'Souza, V. T.; Bender, M. L. *Acc. Chem. Res.* **1987**, *20*, 146.

[26] Breslow, R. *Acc. Chem. Res.* **1995**, *28*, 146.

[27] Kirby, A. J.; In "Enzyme Mechanisms"; Page, M. I.; Williams, A. Eds.; Royal Society of Chemistry: London, 1987, pp. 67-77.

[28] (a) Klotz, I. M. In "Enzyme Mechanisms"; Page, M. I.; Williams, A. Eds.; Royal Society of Chemistry: London, 1987, pp. 14-32.

(b) Stoddart, J. F. In "Enzyme Mechanisms"; Page, M. I.; Williams, A. Eds.; Royal Society of Chemistry: London, 1987, pp. 35-55.

(c) Bender, M. L. In "Enzyme Mechanisms"; Page, M. I.; Williams, A. Eds.; Royal Society of Chemistry: London, 1987, pp. 56-65.

[29] Somayaji, V.; Brown, R. S. *J. Org. Chem.* **1986**, *51*, 2676.

[30] (a)Skorey, K. I.; Somayaji, V.; Brown, R. S. *J. Am. Chem. Soc.* **1989**, *111*, 1445.

(b) Skorey, K. I.; Somayaji, V.; Brown, R. S. *J. Am. Chem. Soc.* **1988**, *110*, 5205.

(c) Somayaji, V.; Brown, R. S.; Ball, R. G. *J.Org. Chem.* **1986**, 51, 4866.

[31] D'Souza, V. T.; Hanabusa, K.; O'Leary, T.; Gadwood, R. C.; Bender, M. L. *Biochem. Biophys. Res. Commun.* **1985**, *129*, 727.

[32] (a) Breslow, R.; Chung, S.*Tetrahedron Lett.* **1989**, *30*, 4353.

(b) Zimmerman, S. C. *Tetrahedron Lett.* **1989**, *30*, 4357.

[33] Madder, A.; De Clercq, P. J.; DeClercq J-P. *J. Org. Chem.* **1998**, *63*, 2548.

[34] (a) Kluger, R.; Chin, J. *J. Am. Chem. Soc.* **1982**, *104*, 2891.

(b) Aldersley, M. F.; Kirby, A. J.; Lancaster, P. W. McDonald, R. S.; Smith, C. R. *J. Chem. Soc., Perkin Trans. 2*, **1974**, 1487.

(c) Kirby, A. J.; Lancaster, P. W. McDonald, R. S.; Smith, C. R. *J. Chem. Soc., Perkin Trans. 2*, **1974**, 1495.

[35] Somayaji, V.; Keillor, J. W.; Brown, R. S. *J. Am. Chem. Soc.* **1988**, *110*, 2625

[36] (a) Skorey, K. I.; Brown, R. S. *J. Am. Chem. Soc.* **1985**, *107*, 4070.

(b) Street, J. P.; Skorey, K. I.; Brown, R. S.; Ball, R. G. *J. Am. Chem. Soc.* **1985**, *107*, 7669.

[37] (a) Keillor, J. W.; Brown, R. S. *J. Am. Chem. Soc.* **1991**, *113*, 5114.

(b) Keillor, J. W.; Brown, R. S. *J. Am. Chem. Soc.* **1992**, *114*, 7983.

[38] Keillor, J. W.; Neverov, A. A.; Brown, R. S. *J. Am. Chem. Soc.* **1994**, *116*, 4669.

[39] Bruice, T. C. *J. Am. Chem. Soc.* **1959**, *81*, 5444.

[40] Fife, T. H.; DeMark, B. R. *J. Am. Chem. Soc.* **1979**, *101*, 7379.

[41] Street, J. P.; Brown, R. S.; *J. Am. Chem. Soc.* **1985**, *107*, 6084.

[42] (a) Kellogg B. A. Ph. D. Thesis. University of Alberta, 1995.

(b) Kellogg, B. A.; Neverov, A. A.; Aman, A. M.; Brown, R. S. *J. Am. Chem. Soc.* **1996**, *118*, 10829.

[43] Ellman, G. L. *Arch. Biochem. Biophys.* **1959**, *82*, 70.

[44] For derivation of eq 2 see reference 42a.

[45] Hall, C. M.; Wemple, J. *J. Org. Chem.* **1977**, *52*, 2118

[46] Wang, Q. P.; Bennet, A. J.; Brown, R. S.; Santarsiero, B. D. *J. Am. Chem. Soc.* **1991**, *113*, 5757.

[47] Lowry, T. H.; Richardson, K. S. In "Mechanism and Theory in Organic Chemistry"; 3rd ed.; Harper and Row: New York, 1987 pp. 367-373.

[48] Fersht, A. "Enzyme Structure and Mechanism"; W. H. Freeman and Co.; New York, 1985 pp. 147-8.

[49] Hupe, D.; Jencks, W. P. *J. Am. Chem. Soc.* **1977**, *99*, 451.

[50] Nenasheva, T. N.; Salinove, G. A. *Zh. Org. Khim.* **1979**, *15*, 835.

[51] (a) Fersht, A. *J. Am. Chem. Soc.* **1971**, *93*, 3504.

(b) Barnett, R. E.; Jencks, W. P. *J. Am. Chem. Soc.* **1969**, *91*, 2358.

[52] (a) Knap, A. K.; Pratt, R. F. *Biochem. J.* **1987**, *247*, 29.

(b) Knap, A. K.; Pratt, R. F. *Proteins: Structure, Function, and Genetics* **1989**, *6*, 313.

(c) Knap, A. K.; Pratt, R. F. *Biochem. J.* **1991**, *273*, 85.

[53] Glasoe, P. K.; Long, F. A. *J. Phys. Chem.* **1960**, *64*,188.

[54] The thermodynamic pK_a of **36** was found to be 7.9 at 25 °C, obtained by measuring the pH of half neutralized solution. This solution was prepared by adding 80 μL of 0.62 M solution of **36** in acetonitrile and 252 μL of 0.0984 M HCl (Aldrich standard solution) to 10 mL distilled water and maintaining μ =0.10 by KCl.

[55] Fife, T. H. *Acc Chem. Res.* **1993**, *26*, 325 and references therein.

[56] Whitesides, G. M.; Lilburn, J. E.; Szajewski, R. P. *J. Org. Chem.* **1977**, *42*, 332.

[57] Alvarez, F. J.; Schowen, R. L. In "Isotopes in Organic Chemistry"; Buncel, E. Lee, C. C. Eds.; Elsevier:Amsterdam,1987, Vol. 7, pp. 1-60.

[58] For example rate constant for water catalyzed hydrolysis of $CH_3CON^-(Et)_3$ is $2.3*10^{-5}$ s. Williams, A. *J. Am. Chem. Soc.* **1976**, *98*, 5645.

[59] Isaacs, N. S. In "Physical Organic Chemistry"; Longman Scientific & Technical: Essex, 1987, pp. 601-604.

[60] Kirby, A J. In "Comprehensive Organic Chemistry"; Bartona, D. H. R.; Ollis, W. D. Eds. Pergamon: Oxford 1979, Vol. 5 pp. 389.

[61] Kirby, A J *Adv. Phys. Org. Chem.***1980**, *17*, 183.

APPENDIX 1*

Table 1S. Pseudo-first order rate constants (k_{obs}) for establishment of equilibrium and the conditional equilibrium constants (K')[a] of formation and hydrolysis of formanilide at 98 ± 2 °C and various pHs in aqueous formate buffer. $[buffer]_{total}$ = 0.10 M. μ = 1.0 (KCl).

pH	Rate constant (k_{obs}) for appearance or disappearance of aniline (s^{-1})	Rate constant (k_{obs}) for appearance or disappearance of formanilide (s^{-1})	[formanilide]/ [aniline] at equilibrium[c] (K')	Formation or Hydrolysis
4.17± 0.03	$(1.47\pm 0.05)*10^{-5}$ [b, c]	$(1.43\pm 0.18)*10^{-5}$ [d]	0.19	Hydrolysis
4.17± 0.03	$(1.50\pm 0.07)*10^{-5}$ [b, c]	$(1.53\pm 0.15)*10^{-5}$ [d]	0.20	Hydrolysis
4.17± 0.03	$(1.46\pm 0.17)*10^{-5}$ [d, c]	$(1.39\pm 0.05)*10^{-5}$ [b]	0.19	Formation
4.17± 0.03	$(1.49\pm 0.16)*10^{-5}$ [d, c]	$(1.42\pm 0.09)*10^{-5}$ [b]	0.19	Formation
3.60± 0.03	$(5.43\pm 0.06)*10^{-5}$ [b]	$(5.18\pm 0.09)*10^{-5}$ [d]	0.28	Hydrolysis
3.60± 0.03	$(5.35\pm 0.27)*10^{-5}$ [d]	$(5.14\pm 0.25)*10^{-5}$ [b]	0.26	Formation
3.18± 0.03	$(1.65\pm 0.07)*10^{-4}$ [b]	$(1.59\pm 0.05)*10^{-4}$ [d]	0.20	Hydrolysis
3.18± 0.03	$(1.49\pm 0.12)*10^{-4}$ [b]	$(1.48\pm 0.05)*10^{-4}$ [d]	0.20	Formation
3.18± 0.03	$(1.56\pm 0.03)*10^{-4}$ [b]	$(1.50\pm 0.07)*10^{-4}$ [d]	0.20	Hydrolysis

[a]Ratio of the concentrations at equilibrium.

[b]Appearance.

[c]Corrected for decomposition of aniline by calculating the final concentration of aniline and setting it as constant. At higher pH decomposition of aniline was observed for longer runs. The rate of decomposition of aniline was determined by heating aniline without formate buffer for 48 hour.

[d]Disappearance.

[e]Starting concentration of aniline or formanilide was (5.0 – 5.3) x 10^{-3} M. Error in K' is less than 7%.

*References for this appendix are in Part 1 (page 77-81)

Table 2S. Pseudo-first order rate constants (k_{obs}) for establishment of equilibrium and the conditional equilibrium constants (K') of formation and hydrolysis of formanilide at 98 ± 2 °C, pH = 3.60, μ = 1.0 (KCl) in aqueous formate buffer, at various buffer concentrations.

$[buffer]_{total}$ (M)	Rate Constant (k_{obs}) for appearance or disappearance of aniline (s^{-1})	Rate constant (k_{obs}) for appearance or disappearance of formanilide (s^{-1})	[formanilide] / [aniline] at equilibrium[c] (K')	Formation or Hydrolysis
0.10	$(5.43\pm 0.06)*10^{-5}$ [a]	$(5.18\pm 0.09)*10^{-5}$ [b]	0.28	Hydrolysis
0.10	$(5.35\pm 0.27)*10^{-5}$ [b]	$(5.14\pm 0.25)*10^{-5}$ [a]	0.26	Formation
0.50	$(2.12\pm 0.12)*10^{-4}$ [a]	$(2.16\pm 0.23)*10^{-4}$ [b]	1.25	Hydrolysis
0.50	$(2.16\pm 0.01)*10^{-4}$ [b]	$(2.07\pm 0.01)*10^{-4}$ [a]	1.26	Formation
0.50	$(2.33\pm 0.16)*10^{-4}$ [b]	$(2.18\pm 0.20)*10^{-4}$ [a]	1.20	Formation
1.00	$(4.55\pm 0.50)*10^{-4}$ [a]	$(4.48\pm 0.45)*10^{-4}$ [b]	2.62	Hydrolysis
1.00	$(4.75\pm 0.45)*10^{-4}$ [b]	$(4.73\pm 0.63)*10^{-4}$ [a]	2.66	Formation

[a]Appearance.

[b]Disappearance.

[c]Starting concentration of aniline or formanilide was $(5.2 - 5.4) \times 10^{-3}$ M.

Table 3S. Pseudo-first order rate constants (k_{obs}) for establishment of equilibrium and the conditional equilibrium constants (K') of formation and hydrolysis of acetanilide at 98 ± 2 ^{o}C in aqueous buffer at various pH, $[acetate]_{total}$ = 1.0 M, μ = 1.0 (KCl).

pH	Buffer	Rate constant (k_{obs}) for appearance or disappearance of aniline (s^{-1})	Rate constant (k_{obs}) for appearance or disappearance of acetanilide (s^{-1})	[acetanilide] / [aniline] at equilibrium[c] (K')	Formation or Hydrolysis
1.95± 0.05	HCl	$(3.74\pm 0.23)*10^{-5}$ [a]	$(3.62\pm 0.39*10)^{-5}$ [b]	0.06	Hydrolysis
1.95± 0.03	HCl	$(3.69\pm 0.57)*10^{-5}$ [b]	$(3.70\pm 0.42)*10^{-5}$ [a]	0.06	Formation
1.98± 0.04	HCl	$(3.45\pm 0.58)*10^{-5}$ [b]	$(3.80\pm 0.30)*10^{-5}$ [a]	0.05	Formation
1.95± 0.04	HCl	$(3.82\pm 0.15)*10^{-5}$ [b]	$(3.47\pm 0.18)*10^{-5}$ [a]	0.05	Hydrolysis
3.75± 0.03	Acetate	$(1.96\pm 0.06)*10^{-6}$ [a]	$(1.92\pm 0.27)*10^{-6}$ [b]	1.38	Hydrolysis
3.75± 0.03	Acetate	$(1.80\pm 0.27)*10^{-6}$ [b]	$(1.96\pm 0.07)*10^{-6}$ [a]	1.35	Formation
3.72± 0.04	Acetate	$(1.80\pm 0.11)*10^{-6}$ [a]	$(1.98\pm 0.38)*10^{-6}$ [b]	1.32	Hydrolysis

[a]Appearance.

[b]Disappearance.

[c]Starting concentration of aniline or acetanilide was $(5.2 - 5.4) \times 10^{-3}$ M.

Table 4S. Pseudo-first order rate constants (k_{obs}) for establishment of equilibrium and the conditional equilibrium constants (K') of formation and hydrolysis of formanilide at 79 ± 1 °C, pH = 2.80, μ = 1.0 (KCl) in aqueous formate buffer, at various buffer concentrations.

pH	Formation[a] or Hydrolysis[a]	$[buffer]_{total}$ (M)	Rate constant (k_{obs}) for appearance or disappearance of formanilide (s^{-1})	[formanilide]/ [aniline] at equilibrium. ($\Delta A_f/\Delta A_r = K'$)
2.80± 0.03	Hydrolysis	0.10	$(7.74\pm 0.03)*10^{-5}$	0.11
2.80± 0.03	Formation	0.10	$(7.82\pm 0.12)*10^{-5}$	
2.79± 0.03	Hydrolysis	0.50	$(1.18\pm 0.02)*10^{-4}$	0.57
2.79± 0.03	Formation	0.50	$(1.21\pm 0.01)*10^{-4}$	
2.81± 0.03	Hydrolysis	0.90	$(1.59\pm 0.02)*10^{-4}$	1.07
2.81± 0.03	Formation	0.90	$(1.59\pm 0.01)*10^{-4}$	

[a]The runs were done in duplicates (or triplicates). Starting concentration of aniline (for formation) or formanilide (for hydrolysis) was 8.4×10^{-5} M

Table 5S. Pseudo-first order rate constants (k_{obs}) for establishment of equilibrium and the conditional equilibrium constants (K') of formation and hydrolysis of formanilide at 79 ± 1 °C, pH = 3.20, μ = 1.0 (KCl) in aqueous formate buffer, at various buffer concentrations.

pH	Formation[a] or Hydrolysis[a]	$[buffer]_{total}$ (M)	Rate constant (k_{obs}) for appearance or disappearance of formanilide (s^{-1})	[formanilide]/[aniline] at equilibrium, ($\Delta A_f/\Delta A_r = K'$)
3.18± 0.03	Hydrolysis	0.10	$(3.86\pm 0.16)*10^{-5}$	0.21
3.18± 0.03	Formation	0.10	$(3.96\pm 0.09)*10^{-5}$	
3.20± 0.03	Hydrolysis	0.50	$(7.28\pm 0.07)*10^{-5}$	1.00
3.20± 0.03	Formation	0.50	$(7.23\pm 0.09)*10^{-5}$	
3.20± 0.03	Hydrolysis	1.00	$(1.24\pm 0.02)*10^{-4}$	2.05
3.20± 0.03	Formation	1.00	$(1.23\pm 0.01)*10^{-4}$	

[a]The runs were done in duplicates (or triplicates). Starting concentration of aniline (for formation) or formanilide (for hydrolysis) was 8.4×10^{-5} M

Table 6S. Pseudo-first order rate constants (k_{obs}) for establishment of equilibrium and the conditional equilibrium constants (K') of formation and hydrolysis of formanilide at 79 ± 1 °C, pH = 3.60, μ = 1.0 (KCl) in aqueous formate buffer, at various buffer concentrations.

pH	Formation[a] or Hydrolysis[a]	$[buffer]_{total}$ (M)	Rate constant (k_{obs}) for appearance or disappearance of formanilide (s^{-1})	[formanilide]/ [aniline] at equilibrium. ($\Delta A_f/\Delta A_r = K'$)
3.56± 0.03	Hydrolysis	0.001[b]	$(1.36\pm 0.02)*10^{-5}$	-
3.60± 0.03	Hydrolysis	0.10	$(1.83\pm 0.01)*10^{-5}$	0.29
3.60± 0.03	Formation	0.10	$(1.83\pm 0.03)*10^{-5}$	
3.61± 0.03	Hydrolysis	0.50	$(4.40\pm 0.02)*10^{-5}$	1.49
3.61± 0.03	Formation	0.50	$(4.39\pm 0.05)*10^{-5}$	
3.59± 0.03	Hydrolysis	1.00	$(8.01\pm 0.07)*10^{-5}$	2.77
3.59± 0.03	Formation	1.00	$(8.20\pm 0.15)*10^{-5}$	

[a]The runs were done in duplicates (or triplicates). Starting concentration of aniline (for formation) or formanilide (for hydrolysis) was 8.4×10^{-5} M

[b]Formation could not be observed

Table 7S. Pseudo-first order rate constants (k_{obs}) for establishment of equilibrium and the conditional equilibrium constants (K') of formation and hydrolysis of formanilide at 79 ± 1 °C, pH = 4.00, μ = 1.0 (KCl) in aqueous formate buffer, at various buffer concentration.

pH	Formation[a] or Hydrolysis[a]	$[buffer]_{total}$ (M)	Rate constant (k_{obs}) for appearance or disappearance of formanilide (s^{-1})	[formanilide]/ [aniline] at equilibrium. ($\Delta A_f/\Delta A_r = K'$)
4.01± 0.03	Hydrolysis	0.10	$(7.76\pm 0.01)*10^{-6}$	0.30
4.01± 0.03	Formation	0.10	$(7.75\pm 0.11)*10^{-6}$	
4.02± 0.03	Hydrolysis	0.50	$(2.02\pm 0.01)*10^{-5}$	1.58
4.02± 0.03	Formation	0.50	$(2.05\pm 0.04)*10^{-5}$	
4.03± 0.03	Hydrolysis	1.00	$(4.01\pm 0.02)*10^{-5}$	2.78
4.03± 0.03	Formation	1.00	$(4.00\pm 0.04)*10^{-5}$	

[a]The runs were done in duplicates (or triplicates). Starting concentration of aniline (for formation) or formanilide (for hydrolysis) was 8.4×10^{-5} M.

Table 8S. Pseudo-first order rate constants (k_{obs}) for establishment of equilibrium and the conditional equilibrium constants (K' of formation and hydrolysis of formanilide at 79 ± 1 °C, pD^a = 3.60, μ = 1.0 (KCl) in aqueous formate buffer, at various buffer concentration.

pD^a	Formation[b] or Hydrolysis[b]	$[buffer]_{total}$ (M)	Rate constant (k_{obs}) for appearance or disappearance of formanilide (s^{-1})	[formanilide]/ [aniline] at equilibrium, ($\Delta A_f/\Delta A_r = K'$)
3.60± 0.03	Hydrolysis	0.001[c]	$(1.34\pm 0.03)*10^{-5}$	-
3.58± 0.03	Formation	0.50	$(3.91\pm 0.05)*10^{-5}$	0.93
3.58± 0.03	Hydrolysis	0.50	$(3.54\pm 0.03)*10^{-5}$	
3.61± 0.03	Hydrolysis	0.75	$(5.07\pm 0.08)*10^{-5}$	1.37
3.61± 0.03	Formation	0.75	$(4.48\pm 0.05)*10^{-5}$	
3.60± 0.03	Hydrolysis	1.00	$(6.05\pm 0.05)*10^{-5}$	1.80
3.60± 0.03	Formation	1.00	$(6.20\pm 0.03)*10^{-5}$	

[a] $pD = pH_{measured} + 0.40$.[46]

[b] The runs were done in duplicate or triplicate. Starting concentration of aniline (for formation) or formanilide (for hydrolysis) was 8.4×10^{-5} M

[c] Formation could not be observed

Table 9S. Pseudo-first order rate constants (k_{obs}) for establishment of equilibrium and the conditional equilibrium constants (K') of formation and hydrolysis of *p*-nitroformanilide at 79 ± 1 °C, pH = 2.80 to 3.60, μ = 1.0 (KCl) in aqueous formate buffer, at various buffer concentration.

pH	Formation[a] or Hydrolysis[a]	$[buffer]_{total}$ (M)	Rate constant (k_{obs}) for appearance or disappearance of *p*-nitroaniline (s^{-1})	[*p*-NO_2-formanilide]/ [*p*-NO_2-aniline] at equilibrium. ($\Delta A_f/\Delta A_r = K'$)
2.82± 0.03	Formation	1.00	$(2.89\pm 0.01)*10^{-4}$	0.23
2.82± 0.03	Hydrolysis	1.00	$(2.85\pm 0.03)*10^{-4}$	
3.20± 0.03	Formation	0.10	$(1.02\pm 0.05)*10^{-4}$	0.02
3.20± 0.03	Hydrolysis	0.10	$(0.99\pm 0.02)*10^{-4}$	
3.20± 0.03	Formation	0.50	$(1.21\pm 0.02)*10^{-4}$	0.10
3.20± 0.03	Hydrolysis	0.50	$(1.27\pm 0.03)*10^{-4}$	
3.21± 0.03	Formation	1.00	$(1.55\pm 0.03)*10^{-4}$	0.19
3.21± 0.03	Hydrolysis	1.00	$(1.47\pm 0.02)*10^{-4}$	
3.60± 0.03	Formation	1.00	$(8.27\pm 0.05)*10^{-5}$	0.13
3.60± 0.03	Hydrolysis	1.00	$(7.98\pm 0.03)*10^{-5}$	

[a]The runs were done in duplicates (or triplicates). Starting concentration of *p*-NO_2-formanilide (for hydrolysis) or *p*-NO_2-aniline (for formation) was 1.85×10^{-4} M.

Table 10S. Pseudo-first order rate constants (k_{obs}) for establishment of equilibrium and the conditional equilibrium constants (K') of formation and hydrolysis of *p*-methoxyformanilide at 79 ± 1 °C, pH = 2.80 and 3.20. μ = 1.0 (KCl) in aqueous formate buffer. $[formate]_{total}$ = 1.00 M.

pH	Formation[a] or Hydrolysis[a]	Rate constant (k_{obs}) for appearance or disappearance of *p*-methoxyformanilide (s^{-1})	[*p*-OCH_3-formanilide]/ [*p*-OCH_3-aniline] at equilibrium. ($\Delta A_f/\Delta A_r$= K')
2.82± 0.03	Hydrolysis	$(7.95\pm 0.05)*10^{-5}$	0.98
2.82± 0.03	Formation	$(8.22\pm 0.15)*10^{-5}$	
3.18± 0.03	Hydrolysis	$(6.19\pm 0.10)*10^{-5}$	1.92
3.18± 0.03	Formation	$(6.30\pm 0.06)*10^{-5}$	

[a]The runs were done in duplicates (or triplicates). Starting concentration of *p*-OCH_3-aniline (for formation) or *p*-OCH_3-formanilide (for hydrolysis) was 1.14×10^{-4} M.

Table 11S. Pseudo-first order rate constants (k_{obs}) for establishment of equilibrium and the conditional equilibrium constants (K') of formation and hydrolysis of formanilide in the presence of phosphate (0.10 to 0.50 M). At 79 ± 1 °C, pH = 3.60 and 3.60, $[buffer]_{total}$ = 1.0 M, μ = 1.0 (KCl) in aqueous formate buffer.

pH	Formation[a] or Hydrolysis[a]	[Phosphate][b] (M)	Rate constant (k_{obs}) for appearance or disappearance of formanilide (s^{-1})	[formanilide]/ [aniline] at equilibrium. ($\Delta A_f/\Delta A_r$= K')
3.21± 0.03	Formation	0.10	$(1.41\pm 0.02)*10^{-4}$	2.04
3.21± 0.03	Hydrolysis	0.10	$(1.42\pm 0.02)*10^{-4}$	
3.21± 0.03	Formation	0.30	$(1.82\pm 0.03)*10^{-4}$	2.04
3.21± 0.03	Hydrolysis	0.30	$(1.80\pm 0.01)*10^{-4}$	
3.58± 0.03	Formation	0.10	$(9.41\pm 0.03)*10^{-5}$	2.72
3.58± 0.03	Hydrolysis	0.10	$(8.88\pm 0.04)*10^{-5}$	
3.60± 0.03	Formation	0.50	$(1.31\pm 0.02)*10^{-4}$	2.70
3.60± 0.03	Hydrolysis	0.50	$(1.28\pm 0.04)*10^{-4}$	

[a]The runs were done in duplicate or triplicate. Starting concentration of aniline (for formation) or formanilide (for hydrolysis) was 8.4×10^{-5} M.

[b]As KH_2PO_4

Table 12S. Pseudo-first order rate constants (k_{obs}) for establishment of equilibrium and the conditional equilibrium constants (K') of formation and hydrolysis of formanilide in aqueous ethanolic formate buffer, [formate] = 1.0 M, at 60.0 ± 0.3 °C and at various pH[a].

pH[a]	Formation[b] or Hydrolysis[b]	% (v/v) ethanol	Rate constant (k_{obs}) for appearance or disappearance of formanilide (s^{-1})	[formanilide]/ [aniline] at equilibrium. ($\Delta A_f/\Delta A_r = K'$)
3.59[c]± 0.06	Hydrolysis	20	$(4.20\pm 0.15)*10^{-5}$	6.21
3.59[c]± 0.03	Formation	20	$(3.47\pm 0.03)*10^{-5}$	
4.92± 0.04	Hydrolysis	80	$(2.12\pm 0.02)*10^{-5}$	6.54
4.92± 0.05	Formation	80	$(2.14\pm 0.03)*10^{-5}$	
3.60± 0.05	Hydrolysis	80	$(7.79\pm 0.05)*10^{-5}$	10.19
3.60± 0.05	Formation	80	$(7.88\pm 0.02)*10^{-5}$	
3.60[c]± 0.03	Hydrolysis	0	$(2.24\pm 0.03)*10^{-5}$	2.82
3.60[c]± 0.03	Formation	0	$(2.24\pm 0.01)*10^{-5}$	

[a]Measured before and after the runs.

[b]The runs were done in duplicates (or triplicates). Starting concentration of aniline (for formation) or formanilide (for hydrolysis) was 8.4×10^{-5} M

[c]The ionic strength was kept constant at 1.0 M with added KCl

Table 13S. Computed pK_as of anilines and acids at various temperature and at $\mu = 1.0$.

Temperature	pK_a in water	pK_a in 20 % (v/v) ethanol	pK_a in 80 % (v/v) ethanol
	Aniline		
25° C	4.89 ± 0.05[a]	4.42[g]	3.86[g, k]
60° C	4.30[b]	3.89[h]	3.33[h, k]
80° C	4.02[b]		
100° C	3.78[b]		
	Formic acid		
25° C	3.63 ± 0.03[a]	3.97[i]	4.88[i, k]
60° C	3.63[b]	3.97[j]	4.88[j, k]
80° C	3.63[b]		
100° C	3.64[b]		
	Acetic acid		
25° C	4.60[c]		
100° C	4.62[b]		
	p-NO_2-aniline		
25° C	1.00[d]		
80° C	0.65[d]		
	p-OCH_3-aniline		
25° C	5.34[e]		
80° C	4.35[e, f]		

[a]Measured at $\mu = 1.0$ (KCl).

[b]Calculated using $\Delta H_{ionization}$ and $\Delta S_{ionization}$ values.[48]

[c]Assumed from available data[49] at $\mu = 0$ to $\mu = 0.2$ (*vide infra*).

[d]Reference 52.

[e]Reference 51 at $\mu = 0.10$ M.

[f]Extrapolated value using data from Reference 51 (from 20° C to 40° C).

[g]Calculated using data from Reference 53.

[h]Assuming effect of temperature same as aqueous media.

[i]Calculated using data from Reference 54.

[j]Assuming no effect of temperature change.

[k]μ not corrected.

pK_a calculation for anilinium ion:

Isaacs has listed[48] the activation parameters for dissociation of various acids and ammonium ions: for anilinium ion $\Delta H_{ionization}$ = 7.38 kcal /mol. and $\Delta S_{ionization}$ = 3.7 cal/mol./deg. at μ = 0. By titration, the pK_a of anilinium ion was determined to be 4.89 ± 0.05 at 24 ± 1 °C and μ = 1.0 (KCl). Using the expression $-\Delta G = RT \ln K_a$. ΔG of anilinium dissociation is calculated to be 6.67 kcal/mol. ($K_a = 1.29 \times 10^{-5}$) at μ = 1.0, T = 24 ± 1 °C.

Since $\Delta G = \Delta H - T\Delta S$ and assuming the ΔH is unaffected by ionic strength, ΔS can be calculated as 2.39 cal/mol./deg. at μ = 1.0 (KCl). Thus the ΔG at 100 °C and μ = 1.0 becomes 6.49 kcal/mol. Hence, the pK_a of aniline under these conditions is 3.80.

Now, if it is assumed that ΔS is insensitive to ionic strength, ΔH at μ = 1.0 (KCl) becomes 7.77 kcal/mol. Therefore, the pK_a of anilinium ion at 100 °C becomes 3.75. An average pK_a of 3.78 was used for further calculations. Similar calculations were done at 80 °C (pK_a = 4.02) and at 60° C (pK_a = 4.30).

pK_a calculation for formic acid

The pK_a of formic acid, 3.63 ± 0.03, was obtained at 24 ± 1 °C and μ = 1.0 (KCl). It is reported[48] that, $\Delta H_{ionization}$ = -0.04 kcal /mol. and $\Delta S_{ionization}$ = -17 cal/mol./deg for formic acid at μ = 0. From calculations similar to those above, the pK_a at 100 °C is 3.63. Therefore, although the change in ionic strength (from 0 to 1.0 M) alters the pK_a of formic acid by 0.12 unit, there is no effect due to the change in temperature.[49]

pK_a calculation for *p*-methoxyanilinium ion

Biggs has shown that the pK_a of *p*-methoxyanilinium ion decreases with increasing temperature.[51b] The authors have obtained pK_as of *p*-methoxyanilinium ion at μ = 0.10 M (KCl) and at five deferent temperatures ranging from 20° C to 40° C. The pK_a vs temperature plot follows a linear equation, $pK_a = a + bT$, where T is temperature in °C. a = 0.018 and b = 5.79. Using these data pK_a of *p*-methoxyanilinium was calculated to be 4.35 at 80° C.

APPENDIX 2

Table 1S. Pseudo-first order rate constants for the reaction of thioglycolic acid (**29**) with the strained amide **1** obtained at various pH and various $[thiol]_{total}$, T = 25 °C, μ = 1.0 (KCl).

pH	$[thiol]_{total}$ (M)	$k_{obs} \times 10$ (s^{-1})
2.00	0.05	8.00 ± 0.30
2.01	0.10	8.70 ± 0.50
2.01	0.15	9.20 ± 0.30
2.01	0.20	10.30 ± 0.40
2.20	0.05	5.60 ± 0.20
2.18	0.10	6.30 ± 0.20
2.17	0.15	7.20 ± 0.30
2.19	0.20	7.60 ± 0.20
3.41	0.05	1.20 ± 0.10
3.43	0.15	2.30 ± 0.10
3.43	0.20	3.80 ± 0.30
9.75	0.05	0.50 ± 0.05
9.75	0.10	0.90 ± 0.06
9.74	0.15	1.30 ± 0.05
9.75	0.20	1.8 ± 0.10
10.06	0.05	0.40 ± 0.03
10.07	0.10	0.70 ± 0.05
10.06	0.15	1.20 ± 0.08
10.08	0.20	1.60 ± 0.06
10.46	0.05	0.40 ± 0.02
10.47	0.10	0.60 ± 0.04
10.46	0.15	0.70 ± 0.03
10.47	0.20	0.80 ± 0.05

Table 2S. Pseudo-first Order Rate Constant (k_{obs}) Measured at Various pH in Different Buffers (μ = 0.10 M (KCl)) for Thiol Esters **34-37** at 50 °C [a].

pH[b]	Buffer [Buffer]	**34**	**35**	**36**	
		k_{obs} x 10^{5} s^{-1}	k_{obs} x 10^{5} s^{-1}	k_{obs} x 10^{5} s^{-1}	k_{obs} x 10^{4} s^{-1}
1.98	HCl 0.01		0.46±0.10		
2.33	HCl .005		0.57±0.10		
3.85	Acetate 0.05		1.60±0.08		
3.83	Acetate 0.10		1.75±0.03		
4.75	Acetate 0.05		2.23±0.07		
4.77	Acetate 0.10		2.73±0.02		
6.58	MES 0.05	0.29±0.02	2.53±0.10	0.61±0.02	0.11±0.02
6.61	MES 0.10	0.42±0.03	2.78±0.13	0.82±0.01	0.15±0.01
7.62	MOPS 0.05	3.95±0.07	3.33±0.08	4.05±0.10	
7.59	MOPS 0.10	4.08±0.03	3.57±0.08	4.68±0.02	
7.71	MOPS 0.05				0.67±0.01
7.74	MOPS 0.10				0.72±0.01
8.06	MOPS 0.05	8.72±0.07		7.46±0.08	1.38±0.02
8.04	MOPS 0.10	9.02±0.11		8.12±0.07	1.45±0.02
8.55	EPPS 0.05				5.06±0.04
8.57	EPPS 0.10				5.18±0.03
8.70	EPPS	26.0±0.50	6.83±0.07	15.3±1.30	6.38±0.11

	0.05				
8.68	EPPS	34.7±0.02	7.77±0.03	16.3±0.30	6.63±0.10
	0.10				
9.72	Et_3N				31.8±0.30
	0.05				
9.70	Et_3N				33.6±1.00
	0.10				
9.80	Et_3N	243±2.00	54.8±0.50	18.0±0.30	
	0.05				
9.77	Et_3N	260±5.00	59.8±0.50	19.2±0.30	
	0.10				
11.46	NaOH	8300±230[c]	1370±30.0	30.5±0.50	
	0.003				

[a]Errors are standard errors of means of at least 2-4 replicates

[b]The error in the pH readings is ±0.04 for replicates

[c]46 °C by stopped flow kinetics.

Table 3S. Second order rate constants[a] for buffer catalysis for ester **34-37** at different pH. T = 50 °C, μ = 0.10 (KCl).

pH[a]	Buffer	**34**	**35**	**36**	**37**
		k_{2buf} x 10^5 (M^{-1} s^{-1})	k_{2buf} x 10^5 (M^{-1} s^{-1})	k_{2buf} x 10^3 (M^{-1} s^{-1})	k_{2buf} x 10^5 (M^{-1} s^{-1})
3.83	Acetate		3.34±0.09		
4.77	Acetate		9.98±0.07		
6.60	MES	2.77±0.04	6.67±0.16	4.05±0.02	8.60±0.02
7.61	MOPS	2.51±0.08	4.97±0.11	15.3±1.00	
7.72	MOPS				9.80±0.01
8.04	MOPS	7.33±0.13		11.4±1.10	13.3±0.20
8.55	EPPS				24.0±0.50
8.70	EPPS	175±5.00	19.2±0.80	37.4±1.30	50.0±1.00
9.70	Et_3N				447±11.0
9.78	Et_3N	367±5.00	100±5.00	38.1±0.30	

[a]Determined from the slope of k_{obs} vs [buffer] plots. Errors are standard deviations.